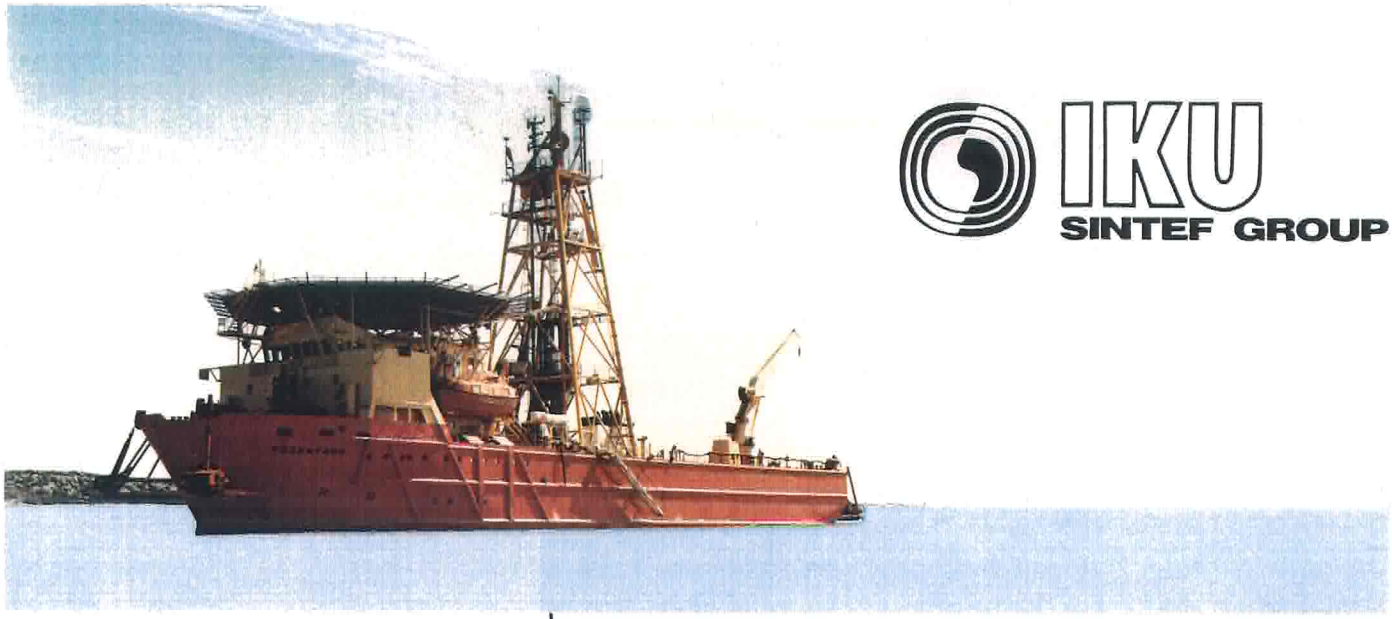
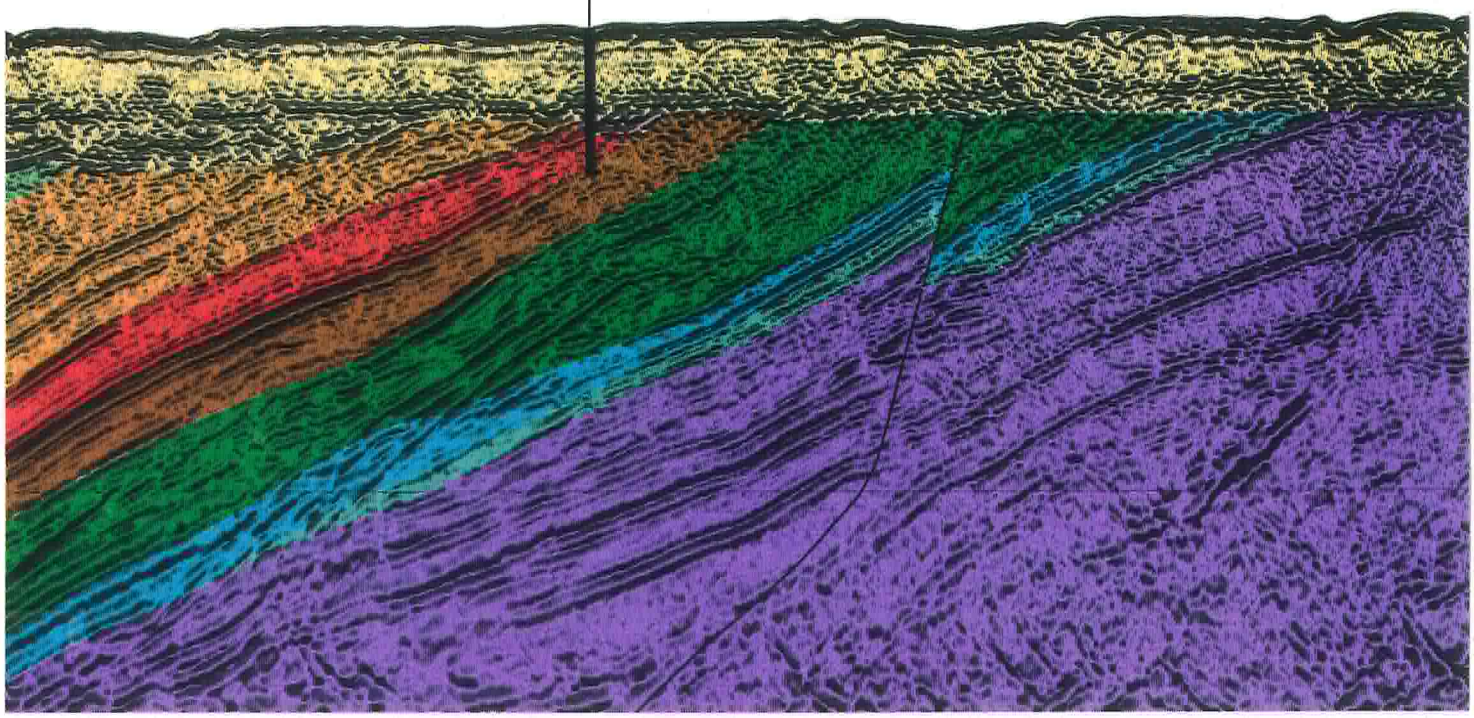


IKU
SINTEF GROUP

Shallow Drilling Bjørnøya West 1989

Appendix volume 1

Field work
Analyses
Consultant reports
Core logs (1:100)



IKU
SINTEF GROUP

Institutt for kontinentalsokkelundersøkelser og petroleumsteknologi A/S
Continental Shelf and Petroleum Technology Research Institute

S.P. Andersen veg 15 b * N-7034 Trondheim, Norway
Tel.: + 47 7 591100 * Telex: 55 434 iku n * Telefax: + 47 7 591102 (aut.)

REPORT

REG. NO.:	ACCESSIBILITY:
90.020	Restricted

REPORT TITLE:

SHALLOW DRILLING BJØRNØYA WEST 1989
Appendix volume 1: Field work, analyses, consultant reports, core logs.

REPORT NO.: 21.3465.00/02/90

AUTHORS:

Tom Bugge (ed)

DATE:	NO. OF PAGES:	NO. OF APPENDICES:	PROJECT MANAGER:	SIGN.:
20-FEB-90	108	10	Tom Bugge	Tom Bugge

CLIENT:	APPROVED	SIGN.:
Amoco Norway Oil Company, A/S Norske Shell, Conoco Norway Inc., Elf Aquitaine Norge A.S., Mobil Exploration Norway Inc., Norsk Hydro a.s, Oljedirektoratet, Total Marine Norsk A/S, Statoil, Saga Petroleum a.s	Martin Hamborg	Martin Hamborg

SUMMARY:

This is Appendix volume 1 to the Main Report "Shallow drilling Bjørnøya West 1989" and has the following content:

A.3 Field work - seismic survey and drilling operation
A.4 Navigation
A.5 Analytical methods
A.6 Oedometer tests
A.7 Trace fossils
A.8 Apatite fission track analysis
A.9 Thermal conductivity
A.10 Discussion of petrophysical core measurements and wireline logs
A.11 Range charts cores 7316/06-U-02 and 7316/03-U-01
A.12 Core logs (scale 1:100)

KEY WORDS:	
Shallow drilling	Trace fossil
Barents Sea	Thermal conductivity
Oedometer test	Apatite fission track

PREFACE

This is Appendix volume 1 to the Main Report of the project "Shallow drilling Bjørnøya West 1989" containing the following contributions:

Appendix A.3 Field work - seismic survey and drilling operation
by Tom Bugge

Appendix A.4 Navigation
by Tom Bugge

Appendix A.5 Analytical methods
by Geir Elvebakk

Appendix A.6 Oedometer tests
by Stein Christensen

Appendix A.7 Trace fossils
by Richard G. Bromley

Appendix A.8 Apatite fission track analysis
by P.F. Green and S.J. Marshallsea

Appendix A.9 Thermal conductivity
by Niels Balling

Appendix A.10 Discussion of petrophysical core measurements and wireline logs
by Stig Bakke

Appendix A.11 Range charts cores 7316/06-U-02 and 7316/03-U-01
coordinated by Jacob G. Verdenius

Appendix A.12 Core logs (scale 1:100)
Geir Elvebakk cores 7317/10-U-01 and 7316/06-U-02
Atle Mørk cores 7316/06-U-01 and 7316/03-U-01

IKU SINTEF-GRUPPEN

APPENDIX A.3

FIELD WORK - SEISMIC SURVEY AND DRILLING OPERATION

A.3 FIELD WORK - SEISMIC SURVEY AND DRILLING OPERATION

A.3.1 Seismic survey

The collection and processing of seismic data was subcontracted to A/S Geoteam in Oslo.

The vessel M/S "Geo Scanner" was used for the field work, and mobilization started 23 May in Hammerfest. After testing and acceptance test the vessel sailed to the survey area southwest of Bjørnøya. The survey lasted until 3 June with demobilization in Tromsø. During this period about 550 km of seismic data was obtained (Figure A.3.1).

The Geoteam personnel took care of the navigation, which was based on Geoloc as primary system and Navstar GPS as secondary system. More details about navigation are given below in Appendix A.4.

As in previous years multichannel digital data and analog single channel data were collected, in addition to side-scan sonar and deep towed sparker data. Based on the good experience from 1988 all this was recorded simultaneously. This means that both analog and digital data were collected in one pass. Exceptions were line IKU-7325-89 and parts of lines 170730, 7325 and 7335 that were run only with the digital equipment. More details are given in Geoteams field report (see reference in Appendix A.4).

The analog airgun was fired 3 - 4 times between each "digital" shot. Because the weather conditions were marginal during much of the survey, the quality of the analog mini-airgun data was not as good as it could have been. We mention that far better quality was obtained during the following survey in the Troms III area, which was run in generally fair weather conditions. The relatively rough weather influenced the quality of the analog data, but had apparently no significant influence on the quality of the digital, multichannel data. Except for two days waiting before the survey could start, there was nearly no other weather downtime (Figure A.3.2).

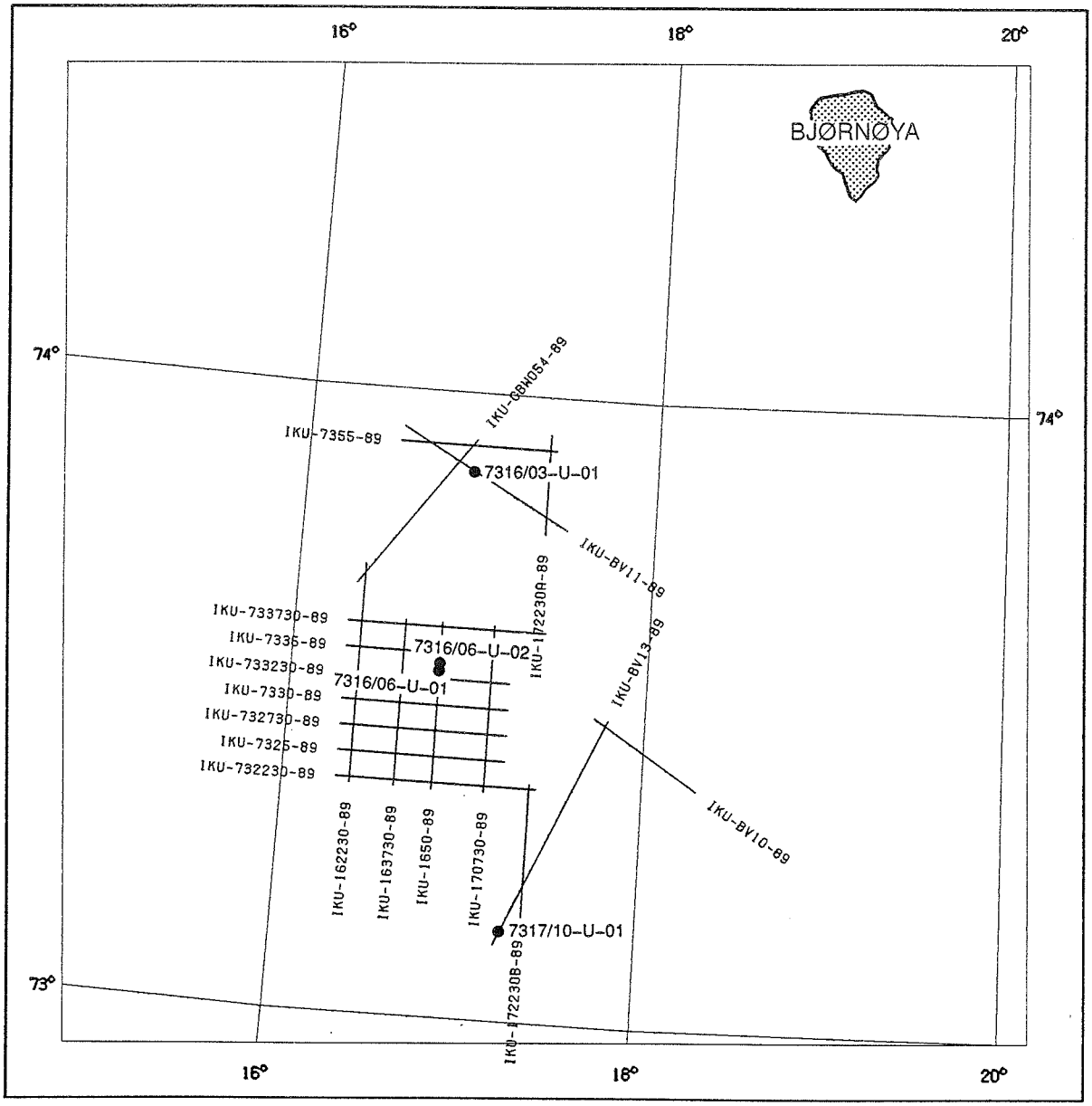


Figure A.3.1 *Seismic lines shot in 1989. About 550 km of seismic data was obtained. On most of the lines both digital multichannel data and analog single channel data were collected simultaneously. The four drill sites are also shown.*

A system for on-line processing of the multichannel data was also used. This system, called "Ramesses" has been developed by the Danish consultant engineering company Ødegaard & Danneskiold-Samsøe APS. The system was originally designed as a QC system, and has been developed further also to provide fully stacked sections in real time. The processing sequence is shown below. The hardware consists of a µ-VAX and a processing unit connected to a printer for the processing and display of the stacked

sections, and a PC with hard-disc for editing of new processing parameters and various displays for QC purposes. The system is connected to the DFS V recording system through a tape adapter. The system worked satisfactorily during the survey and all lines were available in this processed version by the end of the survey. The quality could be deemed to be better than an average brute stack section.

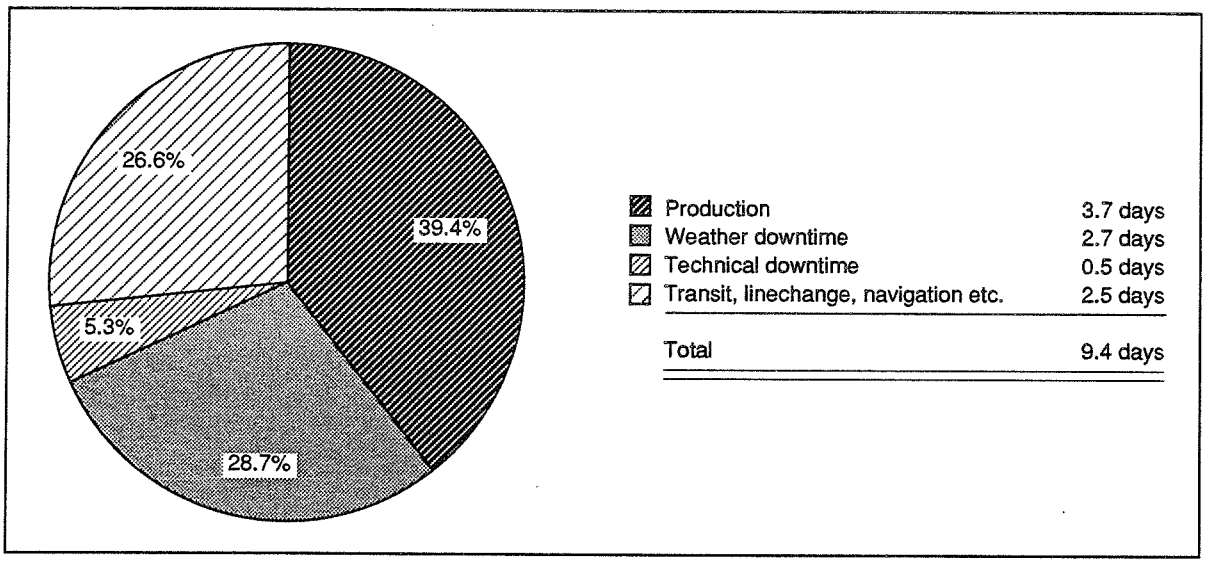


Figure A.3.2 *Duration of field work activities for the seismic survey (totally 9.4 days).*

In total the following amount of data was collected:

- Digital seismic 551.4 km
- Analog mini-airgun 464.9 km
- Side-scan sonar 397.1 km
- Deep towed sparker 355.8 km
- Echo sounder 551.4 km

IKU SINTEF-GRUPPEN

Main technical specifications

Analog data

Mini air-gun:

- Single air-gun, Bolt 600 B, 30 cu inch (10 cu inch effective)
- Shot interval 1 sec
- Recording time 0.5. sec and 1.0 sec
- Streamer length 15 m
- Filtering 70-500 Hz

Deep towed sparker:

- Huntec, multielectrode
- 240 joule output energy
- Shot interval 0.5 sec
- Recording time 0.125 sec
- Filtering internal hydrophone 0.5-7.5 kHz
- Filtering external hydrophone 0.6-3.0 kHz

Side-scan sonar:

- EG&G 990 SMS
- Shot interval 0.75 sec
- Frequency 59 kHz
- Scale corrected, range 500 m

IKU SINTEF-GRUPPEN

Digital data

- Single air-gun, Bolt par 1500 C, 550 cu inch, Geoteam design wave shape kit (1/3 primary chamber)
- 12.5 m shot point interval
- Teledyne T2, 1500 m streamer
- Streamer offset 115 m
- 120 channels
- Towing depth streamer 2-4 m
- Towing depth air-gun 3 m
- 12.5 m group interval
- 11.25 m group length
- 2.5 sec recording time
- 2 msec sampling rate
- Filter 8-180 Hz

Processing flow for "Ramesses" real time processing system:

- Demultiplexing
- Gain: Time Variant
  RMS
  AGC
- Filtering
- Trace Quality Check
- Sort
- Mute
- Filtering
- Deconvolution
- Filtering
- NMO-Correction
- Mute
- Stacking
- Deconvolution on Stack
- Filtering on Stack

A.3.2 Drilling

General

Main contractor for the drilling operation was A/S K/S Farmand Survey in Oslo, using the Norwegian built drill ship M/S "Bucentaur" (Figure A.3.3). The bedrock coring was based on the piggyback coring concept as described below. Farmand Survey had subcontracted Dia-Team in Trondheim for diamond coring staff and Fugro-McClelland BV in Holland to operate the seabed template with the pipe clam. IKU had subcontracted A/S Geoteam in Oslo for the positioning (see Appendix A.4 below) and British Plaster Board Instruments (BPB) Ltd in U.K. to carry out downhole logging.

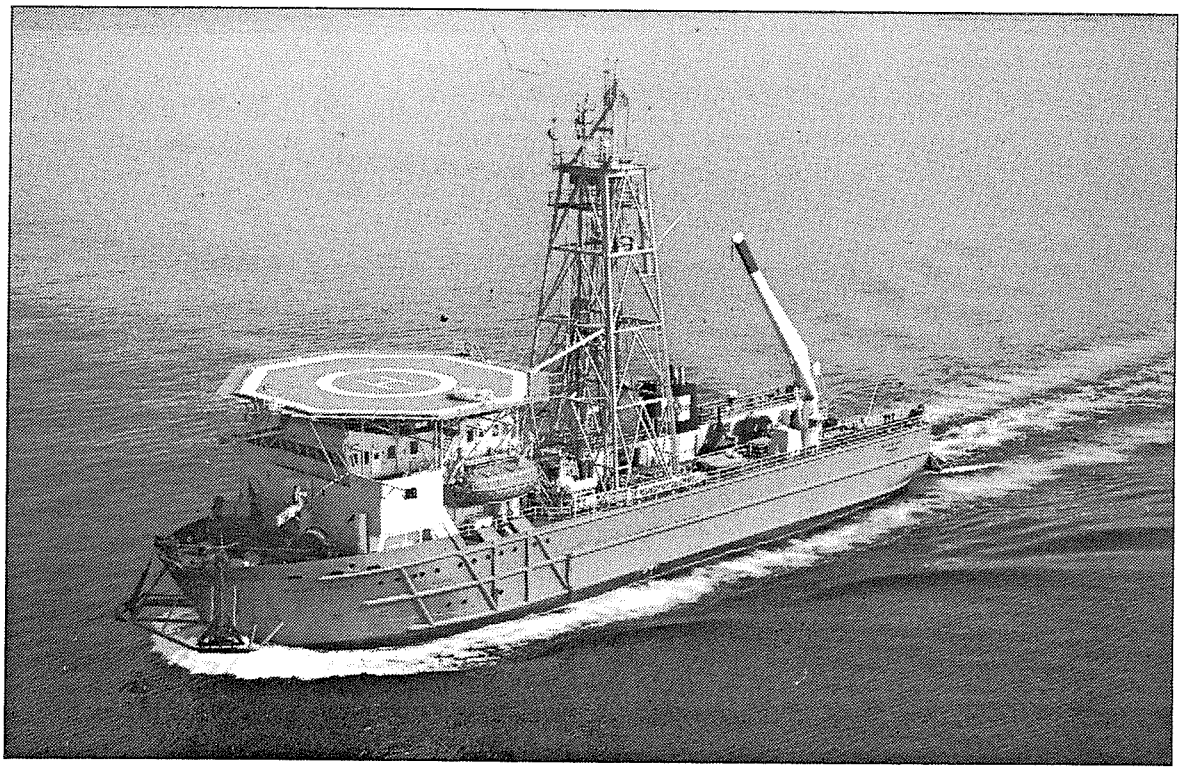


Figure A.3.3 *The drilling vessel M/S "Bucentaur".*

IKU SINTEF-GRUPPEN

Technical data

M/S Bucentaur

Length over all	78.07 m
Breadth moulded	16.00 m
Draft fully loaded	5.55 m
Displacement	4.470 tons
Gross register tonnage, international	2.768 tons

Dynamic positioning system:	One GEC simplex system with GEC-Elliot 2050 computer, video display and joystick. Positioning reference by deep water tautwire system and by Simrad HPR T209 hydro-acoustic system.
Derrick:	26 m high from deck to water table, base 7.40 x 11.55 m, water table 4.50 x 4.50 m, max. 40 tons dynamic hookload, 80 tons static hookload.
Drillstring Heave Motion Compensator:	One Fugro/Hydraudyne type CSC 90.23, max. 40 tons dynamic load, 80 tons load in locked position, accomodates for max. heave of 7 m. With piggyback platform frame installed the max. heave is about 4.5 m.
Mud system:	Complete dry mud system, mud mixing equipment, mud storage and mud pumps (three X: WIRTH TPK 5½" x 5½", 84 HP hydraulic motor, capacity 1600 l/min at 20 bar). No mud resirculation.

Main drill string

Drill pipe:	2000 m of API-5" Grade E, range II, 32 kg/m in air, 28 kg/m in water with 5½" tool joints, 4" ID.

Drill collars:	5 m long, 7" OD and 4" ID with 5½" tool joints. Weight 0.1 tons/m.
Coring and sampling devices:	Christensen rotary coring: (Core diameter 3" (76 mm) or push/hammersampling (Max. sample diameter 3").

Piggyback coring system (diamond core drill system)

Drilling machine:	DBH 1500S electro/hydraulic drill.
Spindle opening:	127 mm.
Rotating speed:	max. 900 rpm.
Drill string:	Wireline HR heavy duty rods OD 88.9 mm, ID 77.8 mm, 70.8 mm at internal joint upset, length 10 ft, weight 12.5 kg/m in air, 10.9 kg/m in water. Back-up NR heavy duty wire line drill rods, OD 69.9 mm, ID 60.3 mm, 54.8 mm at internal joint upset.
Core barrels:	Triple tube, 10 ft with steel split tube liner or double tube 10 ft without liner.
Core diameters:	HR triple tube 54.5 mm, NR triple tube 38.1 mm. HR double tube 57.6 mm, NR double tube 41.6 mm.

Brief description of the piggyback coring operation

The bedrock coring is carried out by an approx. 9 cm OD drillstring with a 3.05 m long retrievable wireline operated corebarrel. Normally a surface set of impregnated diamond bit is used, and the diameter of the core is about 5.5 cm.

The drilling method is often referred to as Piggyback drilling. This is because the diamond coring drillstring is operated by a coring machine resting on top of the powerswivel of the main drilling system (Figure A.3.4), and is run inside the 5"OD (4"ID) string. The benefits of the Piggyback method and the use of a diamond drilling machine are several:

- high core recovery
- fast production
- good core quality
- ability to core fractured and poorly consolidated sediments (even in clays of shear strength down to 100 kPa)

The piggyback concept was used for the first time by Encore (UK) in 1975 and by IKU in 1982. The British vessel M/V "Pholas" was used by IKU in 1982 and 1984. Since then M/S "Bucentaur" has been used in all IKU shallow drilling programs.

Much experience has been gained during this period, and with the equipment presently available the concept offers an efficient method for high recovery core drilling in offshore conditions.

With reference to the sketch in Figure A.3.4 a summary description of the piggyback drilling operation is given below:

- The vessel moves onto position and sets the dynamic positioning system (D.P.) in operation.
- Seabed re-entry template is lowered to the seabed, and constant tension is applied to the template wires via the template heave compensation system.
- The 5" drill pipe with open centre bit (4"ID) is lowered on guided template rider through the re-entry frame at the seabed.

- The Quaternary overburden is penetrated until the drillbit is drilled into rockhead. Hammer samples of main Quaternary units are recovered during drilling.

- The powerswivel heave compensator is then set to give a main bit weight sligthly in excess of the maximum weight that may be required by the diamond core bit used for the coring, and the 5" drill string is clamped to the seabed template.

- The coring string and wireline core barrel (4"OD) is then lowered inside the 5" drill string.

- The diamond coring commences, with length of each run being determined by the length of the inner tube (3.05 m), or by the drilling conditions. Coring normally continues for 1-2 days. Typical production rates are 2.5 - 4.5 m/h.

- The coring string and subsequently the 5" drill string are pulled and stored on the deck.

- Before the drill string is pulled entirely out of the seabed, downhole logging is carried out.

- The seabed template is hoisted into the moonpool, D.P. is disengaged and the vessel proceeds to the next location.

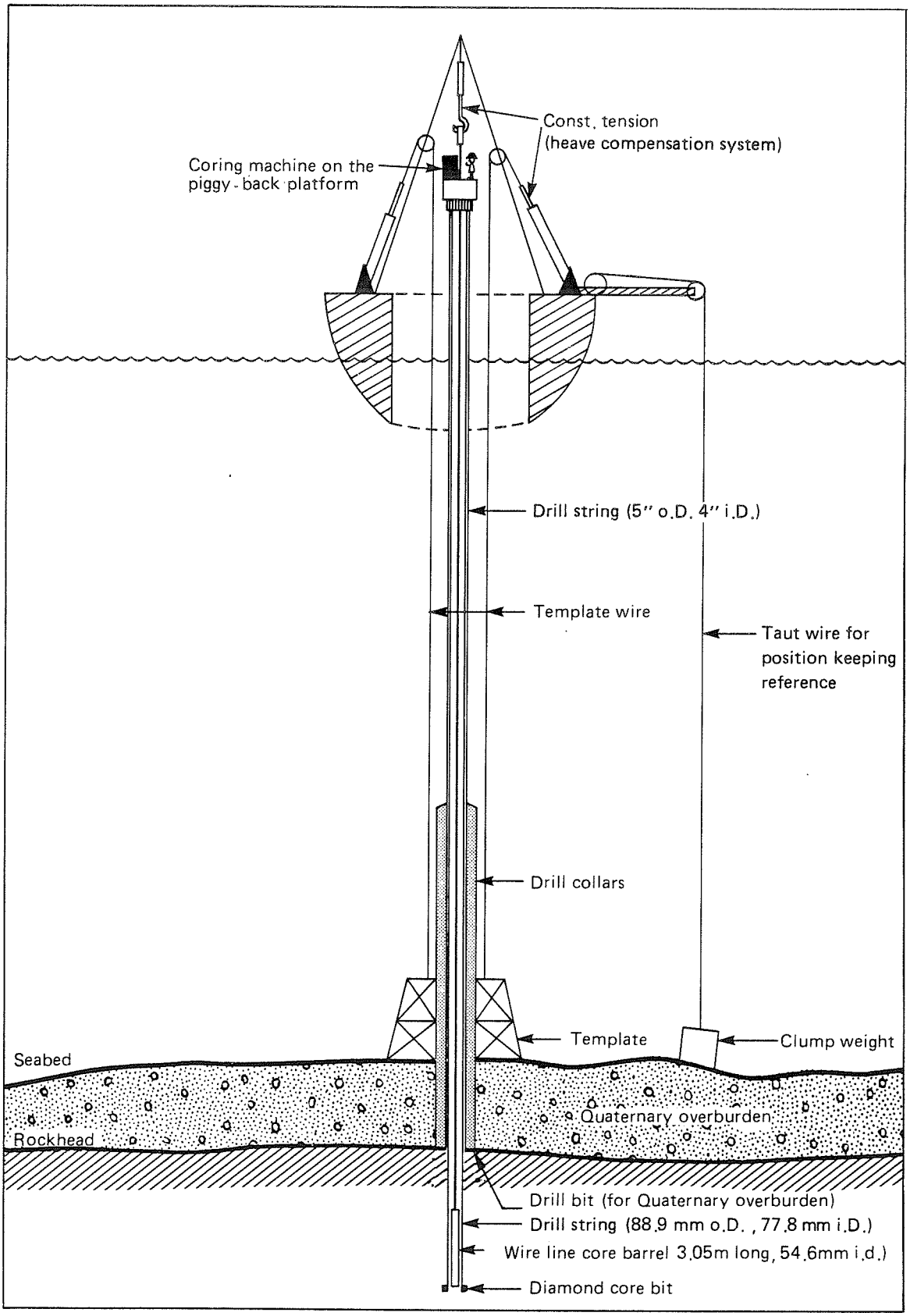


Figure A.3.4 *Sketch showing the piggyback coring operation on board M/S "Bucentaur".*

The coring operation

The field operations started with mobilization at the Coast Center Base outside Bergen 31 July 1989. Here all the equipment was mobilized before the vessel sailed to Tromsø where all the IKU personnel and personnel subcontracted by IKU embarked 4 August. The survey lasted for 24 days, until 28 August when the vessel demobilised in Tromsø.

There were no particular technical problems with the vessel or the drilling equipment, although drilling was impaired by the condition of the sediments. Loose and poorly lithified strata were anticipated, and we used drilling muds formulated specifically for unstable formations. Because of the risk of getting stuck in the hole, the drilling crew included personnel qualified for cutting the drill string by use of dynamite, in order to avoid the expensive of awaiting the arrival of experts from the mainland. The mud quality obviously improved drilling performance, and the blasting capability was a good investment because the drill string became stuck in hole 7316/06-U-01.

In chronological order the operation hole by hole can summed up as below.

- Hole 7316/03-U-01 was drilled nearly to the maximum allowed depth of 200 m below seabed without any problems.

- Hole 7316/06-U-01 appeared to be problematic because of extremely loose formation. At 108 m (43 m in bedrock) the hole suddenly collapsed and the drill string became stuck. As mentioned above, dynamite was used to separate the drill string.

- Hole 7316/06-U-02 was drilled to the allowed limit of 200 m below seabed, with very high core recovery (98 %) and with no significant problems.

- Hole 7317/10-U-01 was the last hole drilled. Because it was foreseen that we could reach the 200 m limit and still have some operation time left, a dispensation application was sent to the NPD, who extended the maximum depth to 300 m. With as much as 143 m of overburden this was of great value, and we managed to drill to 225 m before our drilling budget was exhausted.

With no weather downtime and only 19 hours of technical standby, the operation was very efficient. Sailing time consumed 24 hours each way, and we spent 87 % of the total time on-site, as shown in the Figure A.3.5. With an average of 180 m penetration per hole and a total of 355 m of sediment cored, we concluded that the results are better than anticipated (Table A.3.1).

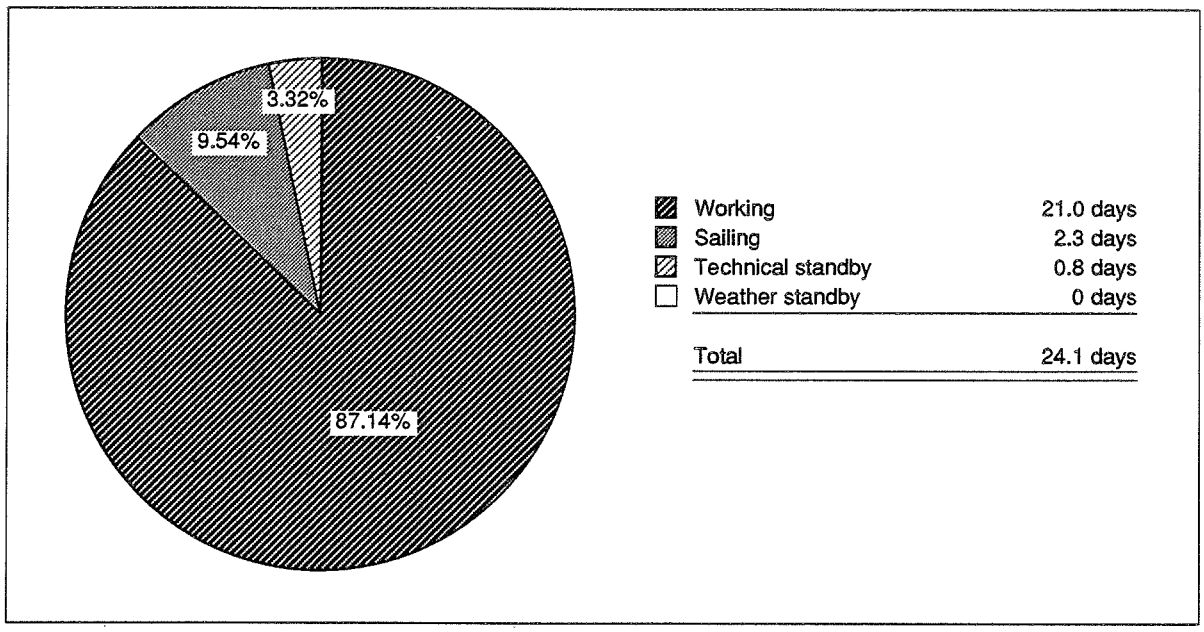


Figure A.3.5 *Statistical field data of the drilling operation.*

Table A.3.1 *Key data of the core holes.*

Core no	Seismic line	Shotpoint	Water depth	Overburden (Top of core)	Penetration in bedrock	Core length	Core recovery	Tot.penetr. below seabed (Base of core)
7316/03-U-01	IKU-BV11-89	~1077	297 m	31.9 m	160.8 m	137.7 m	85.6%	192.7 m
7316/06-U-01	IKU-1650-89	~1688	328 m	65.0 m	43.0 m	9.8 m	22.7%	108.0 m
7316/06-U-02	IKU-1650-89	~1814	421 m	68.5 m	131.0 m	128.8 m	98.0%	199.5 m
7317/10-U-01	IKU-BV13-89	~3344	465 m	143.2 m	81.4 m	78.4 m	96.3%	224.6 m
			Av. 378 m	308.6 m	416.2 m	354.7 m	85.2%	Av.181.2 m
				Av.77.1 m	Av. 104.0 m			

Logging

All holes were logged with downhole petrophysical logging tools, but due to the loose formations, only site 7317/10-U-01 could be logged in open hole. The other three holes were logged inside the HR drill string. For the same reason, sonic log was run only in hole 7317/10-U-01. Table A.3.2 shows the logging program.

Table A.3.2 *Downhole logging program.*

CORE NO	GAMMA	DENSITY	NEUTRON POROSITY	SONIC
7316/03-U-01	X*	X*	X*	
7316/06-U-01	X*	X*	X*	
7316/06-U-02	X*		X*	
7317/10-U-01	X	X	X	X

* Logged inside HR-string.

IKU SINTEF-GRUPPEN

APPENDIX A.4

NAVIGATION

A.4 NAVIGATION

A.4.1 General

The navigation services during the seismic survey and the drilling operation were undertaken by A/S Geoteam, Oslo. Two field reports have been compiled:

- "Field report shallow seismic survey, Bjørnøya West 1989 for IKU A/S", Geoteam Report No. 32036.4, June 1989.

and

- "Navigation and positioning of M/V Bucentaur Bear Island West for IKU", Geoteam Report No. 32117.8.

Both reports have been submitted to the participants, and below we present some key data from the reports.

A.4.2 Seismic survey

The following navigation equipment was used for the seismic survey:

- Geoloc, primary system
- Navstar GPS with post-processed differential corrections, secondary system
- HPR for positioning of towed instrument fishes

Navstar GPS was used as a control system, and in order to improve the accuracy of the system, simultaneous logging was done at a monitoring station in Tromsø. This made it possible to calculate the required east and north corrections for each fix of GPS data after the survey. Compared with the Diffstar system used during the drilling, this could be called an off-line differential system.

The following base stations were used for Geoloc:

- Kongsfjordfjellet
- Sennaland
- Ringvassøy
- Bjørnøya

The typical Geoloc quality control parameters during the survey were (as compared to corrected GPS):

ELMP (Sigma)	0-15 m
ST.dev Lat.	Approx. 5 m
St.dev Long.	Approx. 10 m
DRMS (clock error ellipse)	Approx. 10 m (5-14 m)

During the survey there was very high atmospheric noise in the area, with the highest values north and west in the area. The high overall signal to noise ratio combined with weak signals from the Kongsfjordfjellet station caused severe navigation problems for three of the profiles, in part also caused by extra radio noise as a result of use of the radiotelephone.

The three profiles were: IKU-7330-89, whole line
IKU-1650-89, shot points 1940-2451
IKU-170730-89, whole line

The Geoloc positions for these profiles have been corrected by help of the calculated difference between Geoloc and GPS. The GPS positions used for this purpose have been corrected with the data from the onshore GPS receiver. The difference between GPS and Geoloc is assumed to be constant for the periods where navigation problems occurred.

The positional accuracy of these three profiles is estimated to be within 20 metres.

A.4.3 Drilling operation

In general the same navigation systems were used for the drilling as for the seismic survey.

GEOLOC navigation combined with the vessels HPR System were used to position the drill ship M/S Bucentaur at the four boreholes. Kongsberg Navigation's (KN's) Diffstar (differential GPS) was used as backup navigation system.

Diffstar which is a differential GPS system, received correction values from KN's transmitter on Bjørnøya.

GEOLOC and Diffstar were interfaced to a HP90000 Series 310 computer with graphic display of position information, logging on disc and hard copy printout of data.

The vessel's HPR and gyro were also interfaced to the computer system.

Four GEOLOC stations were used in the calculation of positions: Kongsfjordfjellet, Sennaland, Ringvassøy and Bjørnøya.

Final positions were computed by taking an average of GEOLOC and HPR readings. First logging started when the seacalf was on bottom, and lasted for about 20 minutes. Applied data sets were selected from periods with stable GEOLOC and HPR.

The overall navigation performance was satisfactory. It was although periods when no Diffstar correction values could be received from Bjørnøya, and the Andøya Diffstar transmitter had to be used instead. During the last part of the survey no Diffstar signals could be received at all.

Regarding the repeatability, stability and comparison of the two systems we quote from Geoteams report:

Comparison of Geoloc and Diffstar:

To compare the performance of the two systems during this survey, the recorded navigation data at each site is used to study three different

aspects of the systems:

1) Comparison of absolute positions obtained with the two systems

2) The repeatability of each system

3) The stability of the position fixes obtained with each system.

All the Diffstar absolute positions are based on loggings from periods with PDOP less than 7.0, i.e. periods with a good satellite geometry. As the Diffstar system applies differential corrections for each satellite, any systematic error in a satellite will be removed.

Comparison of absolute positions:

To compare the absolute positions obtained with the two systems, positions based on each systems are presented in Table A.4.1. The GEOLOC positions are computed from a data logging period lasting 20 minutes. Diffstar positions are based on loggings from a period (typically 15 minutes long) with good satellite geometry (PDOP less than 7.0).

The table shows the distance between the two fixes and the direction from the GEOLOC position to the Diffstar position:

Table A.4.1 Comparison of absolute positions from Geoloc and Diffstar.

Site	GEOLOC	DIFFSTAR	Distance (m)	Direction (degrees grid)
7316/03-U-01	N 8 203 472 m E 373 285 m	8 203 456 m 373 293 m	17.9	153.4
7316/06-U-01	N 8 167 166 m E 368 422 m	8 167 177 m 368 418 m	11.7	340.0
7316/03-U-02	N 8 168 746 m E 368 544 m	8 168 741 m 368 551 m	8.6	125.5
7317/10-U-01	N 8 121 151 m E 379 389 m	8 121 155 m 379 359 m	30.3	277.6

From the comparison of the absolute positions above, no systematic shift between the two systems is revealed.

Comparison of repeatability:

During the day of each site, several independent logging periods (control loggings) were recorded in order to control the positions being obtained with the two different systems. To study the repeatability of each of the systems, comparisons of results from each independent control logging are made. Table A.4.2 shows for each site the number of independent control loggings performed, and the standard deviation on these logging periods for each system.

Table A.4.2 Repeatability of Geoloc and Diffstar.

Site	Number of control loggings		Standard deviation of control loggings (m)	
			GEOLOC	DIFFSTAR
7316/03-U-01	7	N	9.0	14.1
		E	8.2	15.5
7316/06-U-01	10	N	7.6	8.8
		E	10.0	18.3
7316/06-U-01	5	N	9.9	6.9
		E	3.7	8.2
7317/10-U-01	6	N	4.7	5.0
		E	12.0	2.7

Table A.4.2 shows that the independent fixes obtained with GEOLOC at one site has a relatively stable repeatability. Diffstar has in periods a significantly more unstable repeatability than GEOLOC which can be seen for the two first locations in the table above.

Comparison of stability:

To compare the stability of the two systems, the position standard deviation for each control logging for one site has been computed for each system. Table A.4.3 presents the mean of all these standard deviations

computed for each system at each site. The total number of loggings on one site is the number of navigation data samples made for a system with an interval of 60 seconds.

Table A.4.3 Stability comparison of Geoloc and Diffstar.

Site	Total number of loggings on one site		Mean standard deviation (m)		
	GEOLOC	DIFFSTAR		GEOLOC	DIFFSTAR
7316/03-U-01	86	64	N E	0.8 1.3	3.5 4.1
7316/06-U-01	116	74	N E	1.1 1.5	2.5 3.7
7316/06-U-02	112	112	N E	2.0 2.0	2.2 3.0
7317/10-U-01	110	110	N E	1.5 2.1	3.5 4.5

The figures above show that the GEOLOC system gives a more stable position fix than the Diffstar system during a logging period.

Final positions:

The final site positions are shown in Table A.4.4. All the final positions are based on loggings from the GEOLOC system.

Table A.4.4 Final co-ordinates of the drill sites. Geographical co-ordinates.

Core no.	Latitude	Longitude	Easting	Northing
7316/03-U-01	73°52'55.8"N	16°54'28.9"E	373285	8203472
7316/06-U-01	73°33'16.5"N	16°49'59.6"E	368422	8167166
7316/06-U-02	73°34' 7.7"N	16°50' 0.9"E	368544	8168746
7317/10/U-01	73° 8'58.5"N	17°16'13.0"E	379389	8121151

The co-ordinates above are referenced to European Datum 1950, UTM projection, zone 34 with central meridian 21 degrees east.

IKU SINTEF-GRUPPEN

APPENDIX A.5

ANALYTICAL METHODS

A.5 ANALYTICAL METHODS

A.5.1 Core description and sampling

Detailed core description was undertaken on board the ship (as time permitted) as well as all subsampling for the screening analyses. Both core description and sampling were completed at IKU laboratories in Trondheim. The legend of the sedimentological columns is given below in Figure A.5.1.

A.5.2 X-ray diffraction analysis

Samples for X-ray diffraction analysis were ground in ethanol to a fine powder dried and pressed in sample holders for whole rock analysis.

Radiation:	monochromatic CuKα
Voltage:	40 kV
Current:	30 mA
Speed:	2°/minute, 2Θ = 2°-35°

The quantification is based on the peak height multiplied by the width of the peak at half maximum and by a weighted factor relative to quartz of the following reflections

Smectite	(Smec):	(14Å - 4.7Å) x 0.35
Mixed layer minerals	(Mix) :	10 to 14Å x 0.55
Muscovite/Illite	(Mic/Ill):	10Å x 1.0 or 10Å x 1.4 (illite)
Chlorite	(Chl) :	4.74Å x 3 x 0.7
Kaolinite	(Kaol):	7Å x 0.7 - Chl
Quartz	(Qtz) :	4.26Å x 1
Opal C-T	(Op C-T):	4.05Å x 1
Goethite	(Goet):	4.18Å x 1
K-feldspar	(KFsp):	3.24Å x 0.5
Plagioclase	(Plag):	3.19Å x 0.5
Calcite	(Calc):	3.04Å x 0.25
Dolomite/Ankerite	(Dol/Ank):	2.89Å x 0.20
Siderite	(Sidr):	2.79Å x 0.25
Gypsum	(Gyps) :	7.56Å x 1
Pyrite	(Pyr) :	2.71Å x 0.7
Zeolite	(Zeol):	9.00Å x 0.5
Marcasite	(Marc):	2.71Å x 0.7
Melankrite	(Mela):	4.90Å x 1
Bassanite	(Bass):	3.00Å x 1

A.5.3 Thin section microscopy

The studies were undertaken on a Leitz ortholux polarizing microscope. Due to the friable nature of some samples and to avoid destruction of pore filling minerals, most samples had to be impregnated by epoxy resin prior to preparation. Scanning electron microscope studies and electron microprobe analyses were carried out on an Jeol 733 Superprobe with a Tracor Northern EDS System on polished carbon coated thin sections.

A.5.4 Sound velocity measurements

Sound velocity measurements, mainly horizontal and a few vertical, were carried out on board on wet, consolidated core pieces, using a portable ultrasonic (100 kHz) non destructive digital indicating tester (PUNDIT).

The pulse velocity (v) was calculated using $v = \frac{L}{T}$

where L is the path length and T is the transit time. Sound velocity measurements are discussed in Appendix A.10.

A.5.5 Natural gamma-radiation

The measurements were carried out on board using a 5" x 5" NaI-detector connected to a 4048 channel analyser of the Canberra 40 series. The core was placed below the detector with its long axis parallel to the detector window. In that position a spectrum was accumulated for 600 sec (10 minutes). To reduce the background radiation, the detector and the samples were shielded by lead. The method requires a minimum sample length which is equal to the detector diameter if the collimation is 100% effective. To avoid this problem, only core pieces longer than twice the detector diameter (= 26 cm) were analysed.

The measured peaks are:

1) K-40: 1.460 MeV
2) U-238 via Bi-214: 1.764 Mev
3) Th-232 via Tl-208: 2.615 Mev

The results are presented as counts per 10 minutes. The logs show the relative amount of radition and not the absolute abundance of K, Th and U. The laboratory measurements are discussed further and compared with the downhole gamma logs in Appendix A.10.

A.5.6 Thermal conductivity

Thermal conductivity has been measured on core samples from all the eight three cores (7317/10-U-01, 7316/06-U-02, 7316/03-U-01). A total of 41 samples has been measured. The measurements are carried out at the University of Aarhus under supervision of Niels Balling. A complete report by Balling is included in Appendix A.9.

The conductivity is measured by the needle probe method. The measurements are undertaken with the probe vertically in the cores (yielding horizontal thermal conductivity, k_h) and with the probe horizontally in the cores (yielding a weigthed mean of vertical and horizontal thermal conductivity, k_m).

A.5.7 Palynology

The standard processing for palynology included hot hydrochloric and hydrofluoric acids with continuous stirring. In most cases the organic residues were oxidized by the use of nitric acid (app. 3 minutes) followed by KOH. If necessary this process was repeated.

Samples from the cores were prepared at 1 - 10 m intervals mainly dependent on lithology, leaving reference material at all levels.

Slides were prepared of: the total residues, unoxidized sieved residues, and oxidized residues at various stages.

A.5.8 Microfauna

Samples were prepared at approximately 3 m intervals, adjusted for lithological units. The samples were soaked in water for some days after being dried. Problematic samples were treated by diluted H_2O_2, and pH

conditions were checked during oxidation. The fraction >125 µm was analysed with respect to foraminifera, ostracods and macrofossil debris. The fraction 63 - 125 µm was examined for siliceous microfossils.

The microfaunas were counted, and the legend in the range charts show the figures corresponding to approximately 10 g of sediment.

A.5.9 Other analyses

The technical part of the oedometer (compressional) tests are presented in Appendix A.6 and the organic geochemical analytical methods are presented in Appendix volume 3.

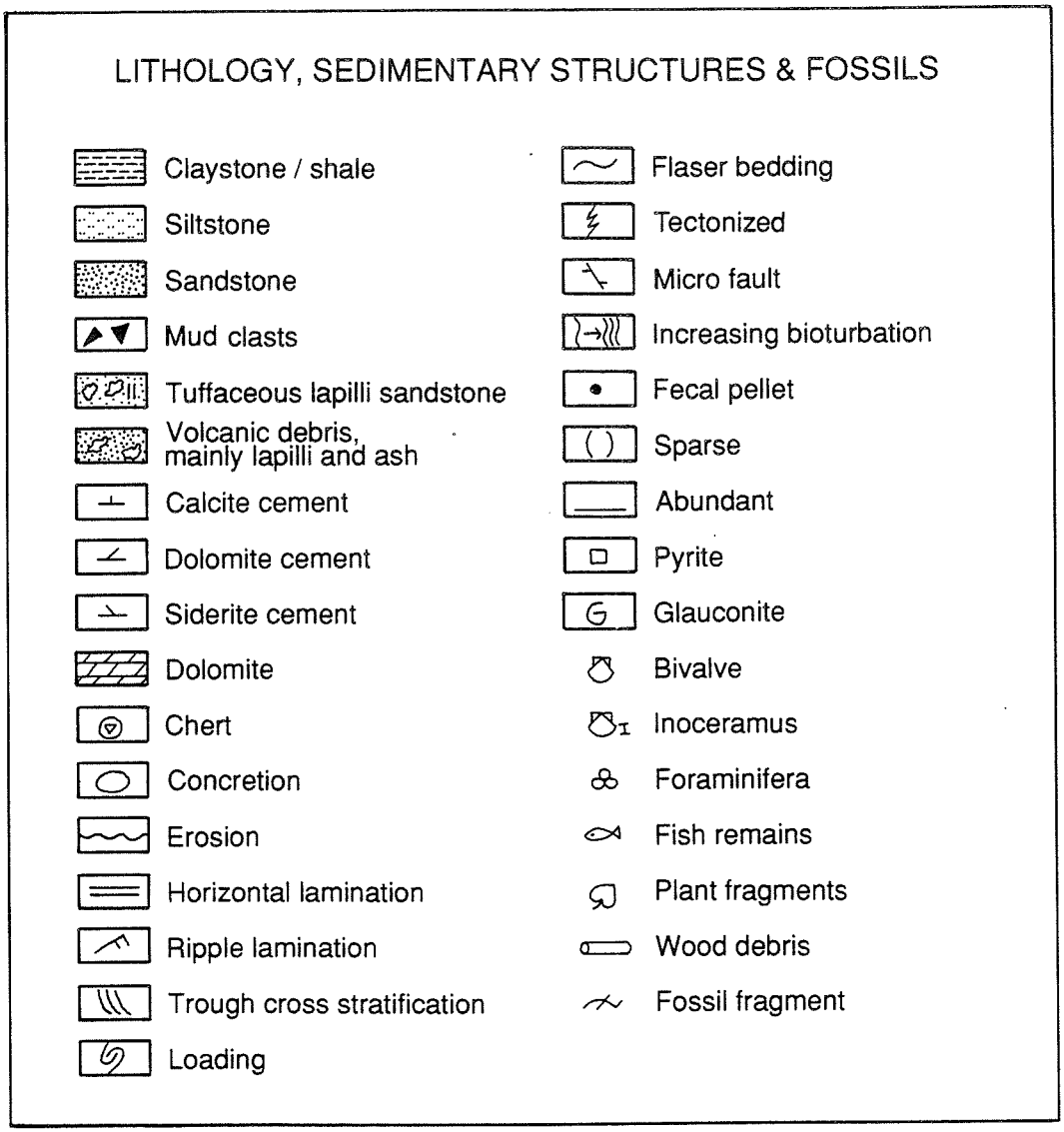


Figure A.5.1 Legend to lithological logs.

IKU SINTEF-GRUPPEN

APPENDIX A.6

OEDOMETER TESTS

by

S. Christensen

Sintef Division of Geotechnical Engineering

SINTEF REPORT -A.6.2-

The Foundation for Scientific and Industrial
Research at the Norwegian Institute of Technology

N-7034 Trondheim-NTH Norway

Telephone: (+ 47 7) 59 30 00
Telex: 55 620 SINTF N
Telefax: (+ 47 7) 59 24 80

Report no. STF69 F89033

Classification
Restricted

Title of report	Date
SHALLOW DRILLING BJØRNØYA WEST 1989 - OEDOMETER TESTS ON SEDIMENTARY ROCKS	1989-12-22
	No. of pages/appendices 24/0
Author(s) Stein Christensen	Divisional responsibility (sign.) G.J. Westerlund
Division Geotechnical Engineering	Project no. 690175
ISBN no.	Price group

Client/sponsor of project	Clients' ref.
IKU (The Continental Shelf and Petroleum Technology Research Institute A/S)	21.3465.00 T. Bugge

Abstract SINTEF Geotechnical Engineering has performed a total of 5 oedometer tests on sedimentary rocks from wells 7316/06-U-02, 7317/10-U-01 and 7316/03-U-01 S-W of Bjørnøya in the Barents Sea. The main findings are:

- The material from well 7316/06-U-02 from depths 138 m and 181 m shows from odeometer tests a preconsolidation stress level $\sigma_c' \approx 14\text{-}20$ MPa, indicating a previous sediment overburden for ice thickness of 1.4-2.0 km ($\bar{\gamma}' = 10$ kN/m³).
- The material from well 7316/03-U-01 shows a σ_c'-value only slightly in excess of the present effective stress
- The material from well 7317/10-U-01 from depths 147 and 207 m show preconsolidation stresses $\sigma_c' \approx 35\text{-}40$ MPa. The deformation behaviour indicates that possible grain bonding or cementation together with secondary minerals in the pores could have been important, and may have contributed considerably to these values for σ_c'.

	Indexing terms: English	Norwegian
Group 1	Geotechnics	Geoteknikk
Group 2	Testing	Prøving
Key terms selected by author(s)	Sedimentary rocks	Sedimentære bergarter
	Preconsolidation	Prekonsolidering

TABLE OF CONTENTS

		Page
1	INTRODUCTION	3
2	GEOTECHNICAL TESTS TO AID GEOLOGY	3
3	TEST FACILITIES	4
4	METHODS OF INTERPRETATION	5
5	LABORATORY TEST	6
	5.1 Test material	6
	5.2 Test results	6
6	EVALUATION OF TEST RESULTS	12
	6.1 General	12
	6.2 Evaluation	12
	6.3 Comments	14
7	REFERENCES	15

FIGURES

1 INTRODUCTION

At the request of IKU (The Continental Shelf and Petroleum Technology Research Institute A/S) SINTEF Geotechnical Engineering has in November 1989 carried out five oedometer tests on samples of sedimentary rock from the western part of the Barents Sea.

The material was cored from M/S Bucentauer during the summer 1989 in the Barents Sea at 73° - 74° N and 16-17°E. The results from the test will be included in IKU's multiclient project called "Shallow Drilling Bjørnøya West 1989.

2 GEOTECHNICAL TESTS TO AID GEOLOGY

During several decades geotechnical engineers have used oedometer tests to determine the preconsolidation pressure of various sediments, primarily clay and clayey silts. Information about the preconsolidation pressure, σ_c', as compared to present overburden, p_0', has been of considerable help in clarifying the past geological history of these sediments.

For instance, when $\sigma_c' >> p_0'$ it indicates that the sediment has previously been subjected to effective (granular) stresses much larger than todays stress level, leading to the following question to geology: Have the soil been loaded by ice, or with sediments now eroded, or subjected to other actions? Another example; when $\sigma_c' << p_0'$ the question can be whether or not artesian pressure with upwards gradients has caused the state of underconsolidation.

Over the last 3 to 4 years our Division has used these same principles to interpret compression tests on sedimentary rocks, and it has been verified that these rocks in principle behave in exactly the same way as samples from Quaternary soil layers. This analogy applies whether the interpretation is based on strain-stress, modulus-stress, or creep-stress relationship. Even semi-empirical rules established in soil mechanics appear to be helpful in interpreting sedimentary rock behaviour. The absolute resistance values of sedimentary rocks are of course much larger than for soils in general.

In our opinion oedometer tests on sedimentary rocks /1/, carried out and interpreted in the same way as in geotechnics, will become an important tool in aiding the geologists in their identification of the geological history.

3 TEST FACILITIES

The rig for performing oedometer tests on sedimentary rocks consists of three main units

- An hydraulic jack, providing up to 600 kN (60 tons) force, with oil pressure of 30 MPa.

- Measuring devices consisting of three excentrically positioned LVDT's (Linear Variable Differential Transducers) for axial strain measurements, a load cell with a nominal capacity of 200 kN, and a recorder for axial strain, force and time.

- An oedometer cell, made of high-quality, acid-resistant steel.

Each sample is being machine-levelled prepared to a height of approximately 20 mm. The net sample area can be varied, by trimming the samples in a lathe, between 20 and 23 cm^2.

The oedometer ring with the sample is placed in the rig in a water bath. An initial stress of 200-400 kN/m² is applied. Then the sample is loaded stepwise up to a stress level of 100 to 130 MPa, depending on the sample area. The axial strain, the load and the time are recorded automatically with connection to our HP1000 computer. A key sketch of the oedometer rig is shown in Fig. 3.1.

4 METHODS OF INTERPRETATION

The modulus concept was first introduced by Janbu /2/ in 1963. The definitions of the modulus and the time resistance /3/ are shown in Fig. 4.1. The axial strain (ϵ) at the end of each loadstep is plotted versus effective stress (σ'), and the tangent modulus to this curve (M) can be plotted versus average effective stress (σ'). For a low stress on the loading branch the resistance (M) against deformation is large. While the stress increases this high resistance eventually decreases appreciably, owing to partial collapse of the grain skeleton. This breakdown of the resistance occurs around the preconsolidation stress level σ_c'. When the effective stress is increased beyond σ_c' the resistance increases with increasing effective stress. The behaviour in the normally consolidated stress range can be approximated by a linear oedometer modulus as shown in Fig. 4.1.

The tangent to the strain-time curve of each load step is defined as the time resistance (R). Irrespective of whether $\sigma' \gtrless \sigma_c'$ a linear dependency of the time resistance is found after some elapsed time for each load level. The time resistance number (r_s) can be found as a straight line fit to the R-t-curve. The inclination of a line drawn from zero to the point where the time resistance becomes linear represents the primary time resistance number (r_c). The time resistance found

at the intersection point of the r_s- and r_c-lines is called the reference time resistance (R_c). When plotting the time resistance numbers versus effective stress the preconsolidation stress (σ_c') can be interpreted from the lowest point of the r-σ'-curves. This method of interpreting the preconsolidation stress can often be more precise than interpretation of σ_c' from either the ϵ-σ' of the M-$\bar{\sigma}'$-curves.

A linear time resistance indicates a creep behaviour. Therefore, the term creep resistance is also used more frequently. As a consequence r_s is also called the creep number.

5 LABORATORY TEST

5.1 Test material

A total number of 5 oedometer tests have been performed on cores drilled from the sedimentary rock west of Bjørnøya in the Barents Sea. Two cores are tested from well 7316/06-U-02, two cores are tested from well 7317/10-U-01, and one core is tested from well 7316/03-U-01. The cores are taken from depths 54 m to 207 m below the seabed. For a detailed geological description of the material reference is made to the main report.

5.2 Test results

The laboratory index parameters are tabulated in Table 5.1. The total unit weight ranges from γ = 18.2-21.5 kN/m³ and the water content lies in the range w = 15.1-27.8%. The specific unit weight has been found to be γ_s = 25.8-27.6 kN/m³ and the initial porosity has been calculated to n_0 = 28.5-48.5%. All the tests except for one have been performed on fully saturated samples (S_w = 100%). Table 5.1 also includes the stress determined parameters modulus (M_{oc}), modulus number (m) and the preconsolidation stress (σ_c').

The creep determined parameters primary creep number (r_c), reference time resistance (R_c) and secondary creep number (r_s) for each load level in each test are tabulated in Table 5.2. The main test results are visualized in Figs. 5.1 to 5.4.

Test 7316/06-U-02, E8292, D = 138.2 m

The sample was mounted in a steel ring with an area of 23.3 cm² and machine levelled to a height of 2 cm. The load was applied in steps with time intervals in the range of 2-10 hours up to a maximum stress of σ_v' = 73.5 MPa. The sample had an initial porosity of n_0 = 38.6% and a water content of w = 23.4%. The modulus in the OC-range was interpreted to M_{OC} = 150 MPa, and a modulus number in the NC-range of m = 8.6 was interpreted. The material was a clayey siltstone showing an overconsolidated clay-type deformation behaviour. Both the stress- and time-dependent parameters pointed to a preconsolidation stress level around
σ_c' ≈ 14-16 MPa. The primary creep number r_c ≈ 50 and the secondary creep number r_s ≈ 250 were interpreted at σ_c'.

Test 7316/06-U-02, E8363, D = 181.05 m

The sample was fit to a steel ring with an area of 23.3 cm² and machine levelled to a height of 2 cm. The load was applied in steps with time intervals in the range of 6-14 hours up to a maximum stress of σ_v' = 100 MPa. The sample had an initial porosity of n_0 = 37.5% and a water content of w = 22.8%. The modulus in the OC-range was found as M_{OC} = 180 MPa and in the NC-range a modulus number of m = 8.9 was interpreted. The material was a silty claystone showing an overconsolidated clay-type deformation behaviour. Both the stress- and time-dependent parameters pointed to a preconsolidation stress level around
σ_c' ≈ 18-20 MPa. Interpretation of the creep numbers showed r_c ≈ 70 and r_s ≈ 210 at σ_c'.

Test 7317/10-U-01, E8414, D = 147.8 m

The sample was machine levelled to an area of 20 cm² and a height of 2 cm, and loaded in steps with time intervals in the range of 2.5-14 hours up to a maximum vertical stress of σ_v' = 130 MPa. An initial porosity of n_0 = 31.2% and a water content of w = 16.6% could be calculated. The modulus in the OC-range was found as M_{OC} = 450 MPa, and the modulus number in the NC-range was found to be m = 9.5. The material was a silty claystone showing a clay-type deformation behaviour with a typical decrease in the modulus when approaching σ_c'. Interpretation of the stress-strain-time behaviour pointed to a preconsolidation stress level of σ_c' ≈ 35-40 MPa. The primary creep number r_c ≈ 100 and the secondary creep number r_s ≈ 350 were interpreted at σ_c'.

Test 7317/10-U-01, E8502, D = 207.5 m

The sample was fit to a steel ring with an area of 23.3 cm² and machine levelled to a height of 2 cm. The load was applied in steps with time intervals in the range of 4-13 hours up to a maximum stress of σ_v' = 100 MPa. The sample had an initial porosity of n_0 = 28.5 % and a water content of w = 15.1 %. The modulus in the OC-range was found as M_{OC} = 575 MPa and the modulus number in the NC-range was found to be m = 10. The material was a sandy siltstone showing a clay-type deformation behaviour with a typical decrease in the modulus when approaching the preconsolidation stress level. Interpretation of the stress-strain-time behaviour pointed to preconsolidation stress level around σ_c' ≈ 35-40 MPa. The primary creep number r_c ≅ 150 and the secondary creep number r_s ≈ 500 were interpreted at σ_c'.

Test 7316/03-U-01, E26, D = 53.9 m

The sample was tested with an area of 20 cm² and a height of 2 cm in our ordinary oedometer rig with measurement of pore pressure in the bottom. The load was applied in steps with time

intervals sufficient to interprete secondary creep numbers. The maximum stress applied to the sample was σ_v' = 4600 kPa = 4.6 MPa. The sample had an initial porosity of n_o = 48.5 % and a water content of w = 27.8 %. The modulus in the OC-range was found as M_{OC} = 40 MPa and the modulus number in the NC-range was found to be m = 23.8. The material was a sandy siltstone probably suffering from some sample disturbance. This can be vizualized by the smooth transition in the ϵ-σ' and the M-σ' curves when approaching σ_c'. The preconsolidation stress σ_c' = 1.6-1.8 MPa could best be determined from the interpretation of the creep numbers r_c and r_s, which showed values of 800 and 900 around σ_c', respectively.

TABLE 5.1 Laboratory index parameters and interpreted deformation parameters from oedometer tests on cores from the Barents Sea.

Parameter	Index	Unit	7316/06-U-02 E8292	7316/06-U-02 E8363	7317/10-U-01 E8414	7317/10-U-01 E8502	7316/03-U-01 E26
Lithology			Clayey Siltstone	Silty Claystone	Silty Claystone	Sandy Siltstone	Sandy Siltstone
Depth from seafloor	D	m	138.2	181.05	141.85	207.53	53.90
Total unit weight	γ	kN/m³	20.02	19.81	21.46	21.36	18.19
Specific unit weight	γ_s	kN/m³	26.31	25.80	26.75	25.97	27.60
Water content	w	%	23.43	22.80	16.63	15.06	27.82
Porosity	n_0	%	38.58	37.49	31.20	28.50	48.45
Void ratio	e_0		0.628	0.600	0.454	0.399	0.940
Water saturation	S_w	%	100	100	100	100	83.3
Modulus	M_{OC}	MPa	150	180	450	575	40
Stress exponent	a		0	0	0	0	0
Modulus number	m		8.6	8.9	9.5	10.0	23.8
Preconsolidation stress	σ_c'	MPa	14-16	18-20	35-40	35-40	1.6-1.8

			Modulus	Strain
General			$M = m\sigma_a(\frac{\sigma}{\sigma_a})^{1-a}$	$\epsilon = \frac{1}{ma}[(\frac{\sigma'}{\sigma_a})^a - (\frac{\sigma_0'}{\sigma_a})^a]$
Special	a = 1	→	$M = \text{const}$	$\epsilon = \frac{\Delta\sigma}{M}$
	a = 0.5	→	$M = m\sqrt{\sigma' \cdot \sigma_a}$	$\epsilon = \frac{2}{m}[\sqrt{\frac{\sigma}{\sigma_a}} - \sqrt{\frac{\sigma_0'}{\sigma_a}}$
	a = 0	→	$M = m\sigma'$	$\epsilon = \frac{1}{m} \ln \frac{\sigma' - \sigma_r'}{\sigma_0' - \sigma_r'}$

TABLE 5.2 Creep determined parameters of each load level from oedometer tests on cores from the Barents Sea drilling project.

7316/06-U-02, E8292 D = 138.2 m				7316/06-U-02, E8363 D = 181.1 m				7317/10-U-01, E8414 D = 147.8 m				7317/10-U-01, E8502 D = 207.5 m				7316/03-U-01, E26 D = 53.9 m			
Stress	r_c	R_c	r_s	Stress	r_c	R_c	r_s	Stress	r_c	R_c	r_s	Stress	r_c	R_c	r_s	Stress	r_c	R_c	r_s
MPa		yr		MPa		yr		MPa		yr		MPa		yr		MPa		yr	
1.0	317	0.0045	3605	1.0	250	0.0106	5000	1.2	2143	0.0245	5084	1.3	2200	0.0021	4166	196.2	1578	0.0051	2069
2.3	384	0.0066	2920	2.5	214	0.0204	1540	3.5	1705	0.0195	4687	2.9	2222	0.0169	10126	392.4	1111	0.0076	1887
4.7	282	0.0056	1905	4.6	200	0.020	1290	6.0	1570	0.0194	4000	5.3	2000	0.0228	20000	686.7	1026	0.0020	1818
9.4	100	0.0126	816	9.9	131	0.0287	555	10.3	1176	0.0161	3848	10.0	1470	0.0224	13158	1177.2	822	0.0021	1000
18.9	54	0.0139	250	18.5	81	0.0339	214	19.9	408	0.0078	1428	19.7	714	0.0217	2898	2158.2	789	0.0039	909
32.5	56	0.0224	214	32.2	65	0.0445	203	33.0	175	0.0097	571	33.5	284	0.0211	1224	3139.2	833	0.0042	926
50.1	62	0.0265	200	51.0	63	0.0443	208	52.4	93	0.0168	305	51.7	143	0.0215	392	4610.7	870	0.0043	1143
73.5	83	0.0387	285	71.9	69	0.0538	205	75.3	133	0.0164	326	75.0	135	0.0216	333				
				100.0	95	0.0687	203	95.5	219	0.0188	335	100.0	147	0.0210	339				
								130.0	222	0.0139	440								

Legend: (see also Fig. 4.1)

r_c = primary creep number
R_c = reference time resistance
r_s = secondary creep number

6 EVALUATION OF TEST RESULTS

6.1 General

All oedometer test results except for the test from 7316/03-U-01 at depth D = 53.91 m, show clearly an appreciable preconsolidation stress level as compared to the present effective stress which is in the range of σ_v' = 1.4-2.1 MPa for depth intervals D = 140-210 m (γ = 20 kN/m³). The interpretation of the preconsolidation stress was based on the curves of ϵ-σ', M-σ' and r-σ'. The clearest σ_c'-indication was found from the r-σ' plots, which agrees with experience from soils and other sedimentary rocks.

6.2 Evaluation

The oedometer tests have been performed on cores of varying porosity (n_o) and water content (w). In addition, different types of material have been tested. However, we observe that there is an increasing preconsolidation stress (σ_c') with decreasing porosity. This finding is in agreement with the theory of idealized soil profiles developed by Janbu in /4/. The calculated porosity values from the tests deviate more and more from the theoretical porosity-depth profile in Fig. 6.1 as the depth of burial increases. (The depth of burial is found as $D_b = \sigma_c'/\bar{\gamma}'$, $\bar{\gamma}'$ = 10 kN/m³).

The porosity values on the tested material revealing the highest σ_c' values should indicate an even deeper burial during geological history. The mismatch between the measured porosity and the theoretical values is probably due to infill of secondary materials in the pores. It is also possible that cementation and bonding of grains become important factors and may have impact on the preconsolidation stress as the depth of burial and the temperature increase.

However, assuming that the values found for the preconsolidation stress are solely due to previous load, one may conclude the following:

The findings from hole 7316/06-U-02 show that approximately 1.4- 2.0 km of sediments or net ice thickness could have overlain the material at present depths 138-181 m below seafloor.

The material tested from hole 7316/03-U-01 at depth 54 m below seafloor, shows a preconsolidation value slightly in excess of the present effective overburden stress. This material could therefore not have been subjected to significant overburden load in the past geological history. The material behaviour in stress-strain-time for the above mentioned tests indicates only minor influence of diagenesis on σ_c' and the values of σ_c' may therefore be considered to give a good indication of previous overburden.

The results from samples at 147 m and 207 m in hole 7317/10-U-01 resemble collapse of an unstable grain structure. This indicates that cementation between grains could be important and that the values found are maximum values. In addition, these tests show values of porosity and water content below a theoretical basis, and could have caused calculation of too high values of previous depth of burial.

All oedometer tests showed creep numbers at stresses $\sigma' \geq \sigma_c'$ similar to those one can obtain from tests on Quaternary materials with similar mineral composition except for the order of stress magnitude. This implies that creep is a fundamental behaviour for any sediment, and that creep may be a key concept applied on decompaction evaluation of a sediment back to its origin.

6.3 Comments

It must be emphasized that these interpretations are entirely based on findings from the oedometer test only, and that no effects of grain bonding or cementation have been considered. Scanning electrone microscope (SEM) applied to prepared samples may give information of the degree of cementation or secondary porosity which may have affected the oedometer test results. However, apart from the above mentioned effects, the laboratory methods and interpretation techniques applied on the tested material herein have resulted in well defined values of the preconsolidation stress.

The effect of diagenesis on σ_c' is believed to be most pronounced for the materials with low porosity and less pronounced for the materials with high porosity.

7 REFERENCES

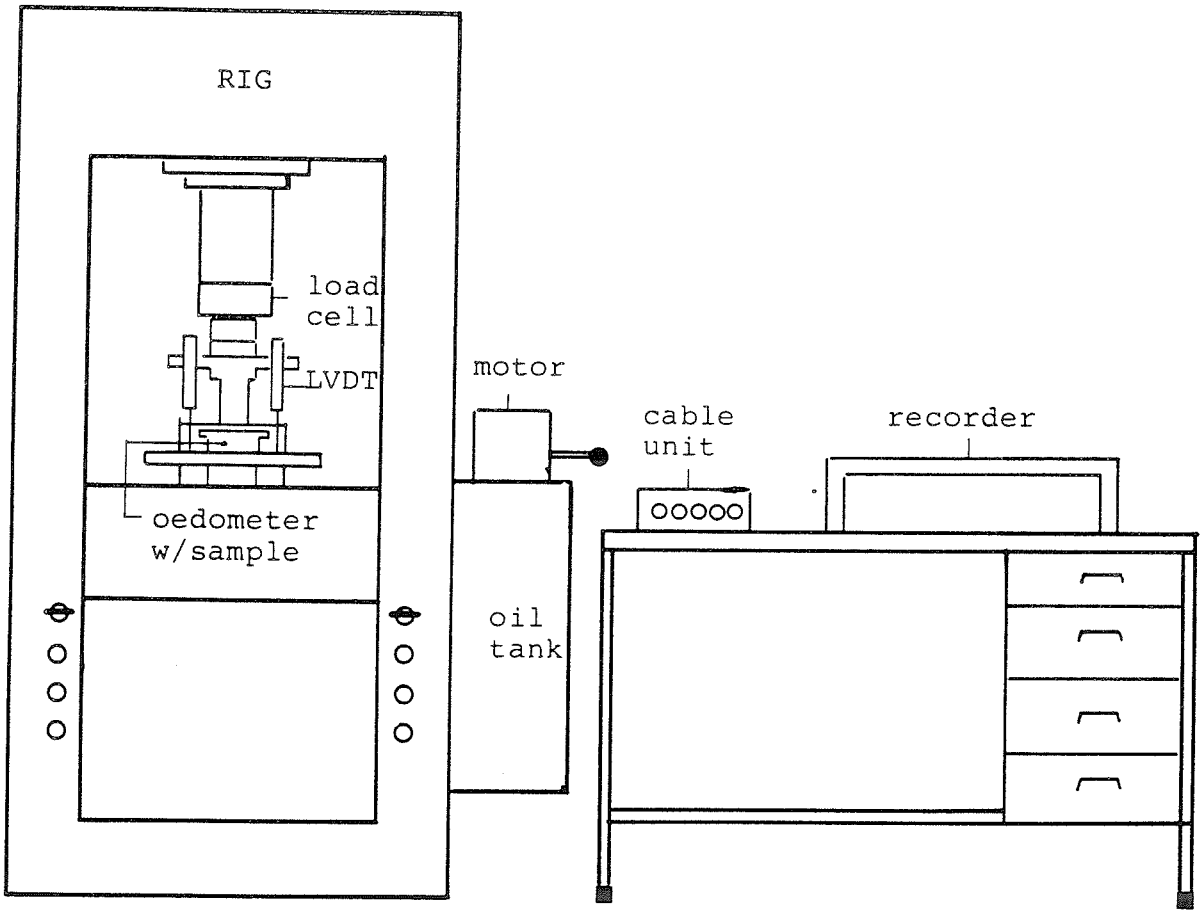
/1/ JONES, M. (1986): "The mechanical behaviour of reservoir chalks and overburden shales". NIF-course: "Application of rock mechanics to petroleum reservoir problems".

/2/ JANBU, N. (1963): "Soil compressibility as determined by oedometer and triaxial tests". Proc. 3rd Eur. Conf. Soil Mech. Wiesbaden 1, 19-25.

/3/ JANBU, N. (1985): "Soil models in offshore engineering". 25-Rankine Lecture, Geotechnique 35, No. 3, pp 241-281.

/4/ JANBU, N., EMDAL, A. (1987): "Soil profile idealizations - A theoretical method to predict soil parameters". SINTEF Report STF69 F87004.

F I G U R E S



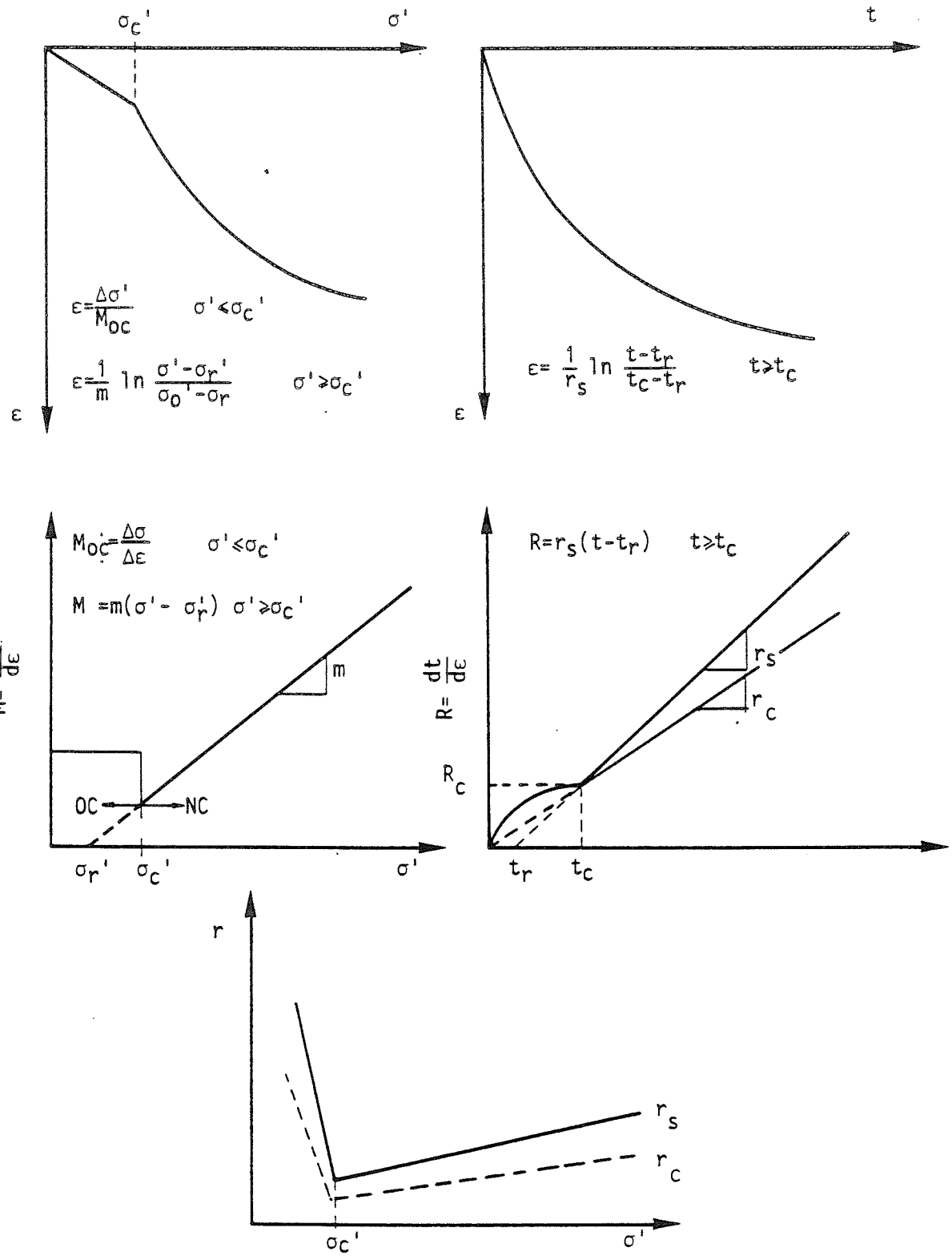
Principal sketch of hydraulic rig with oedometer and equipment.

PROJECT 690175.00

DATE 1989.12.27

FIG. 3.1

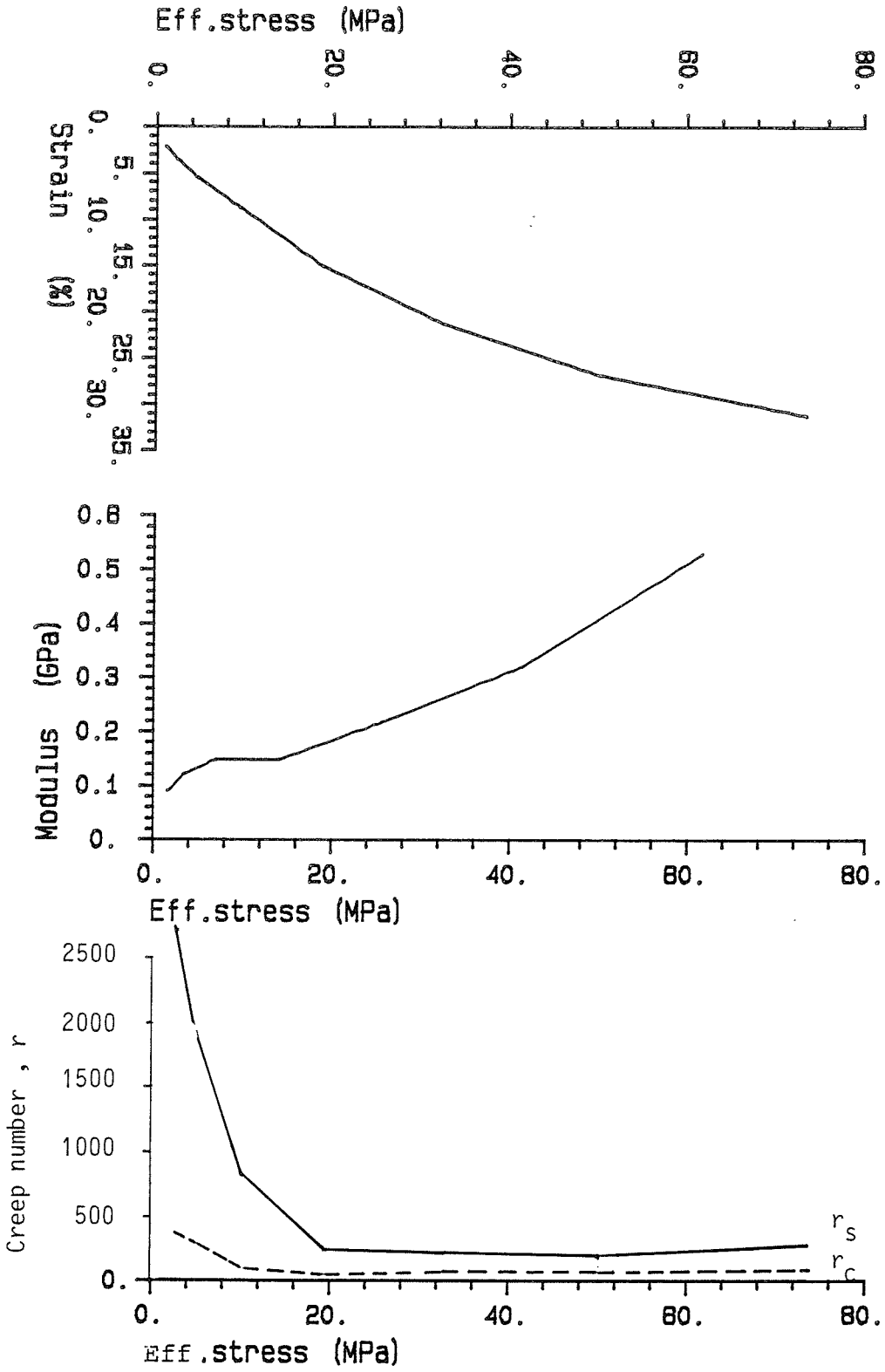
SINTEF DIVISION OF GEOTECHNICAL ENGINEERING



Definition of modulus and time resistance.
Principal sketches.

PROJECT	690175.00
DATE	1989.12.29
FIG.	4.1

SINTEF DIVISION OF GEOTECHNICAL ENGINEERING



IL - oedometer.

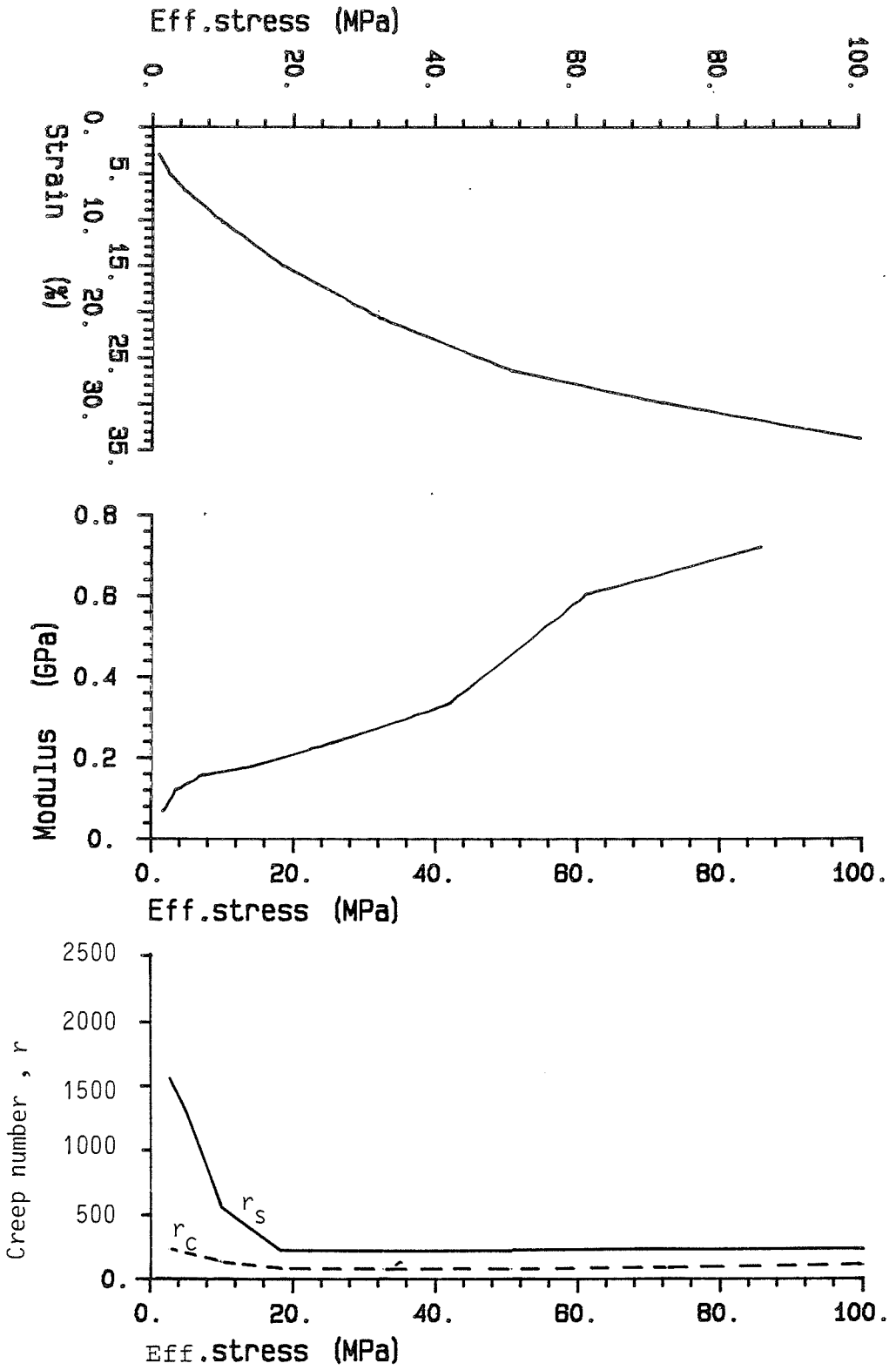
**BARENTSHAVET, 7316/06-U02, E8292, D=138.2m

SINTEF DIVISION OF GEOTECHNICAL ENGINEERING

PROJECT 690175.00

DATE 8 NOV., 1989

FIG. 5.1



IL - oedometer.

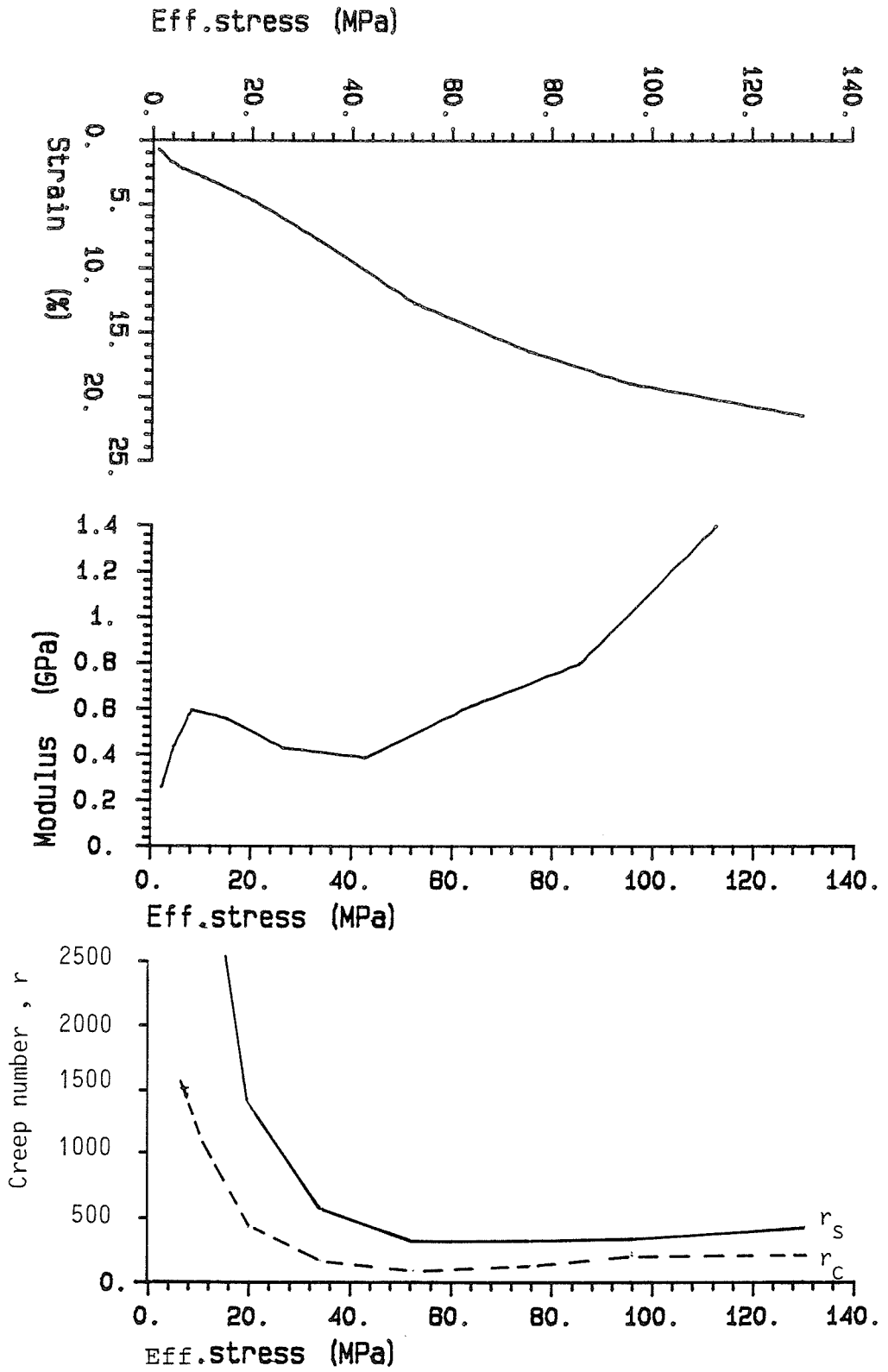
**BARENTSHAVET, 7316/06-U02, EB363, D=181.0 m

SINTEF DIVISION OF GEOTECHNICAL ENGINEERING

PROJECT 690175.00

DATE 26 NOV., 1989

FIG. 5.2



IL - oedometer.

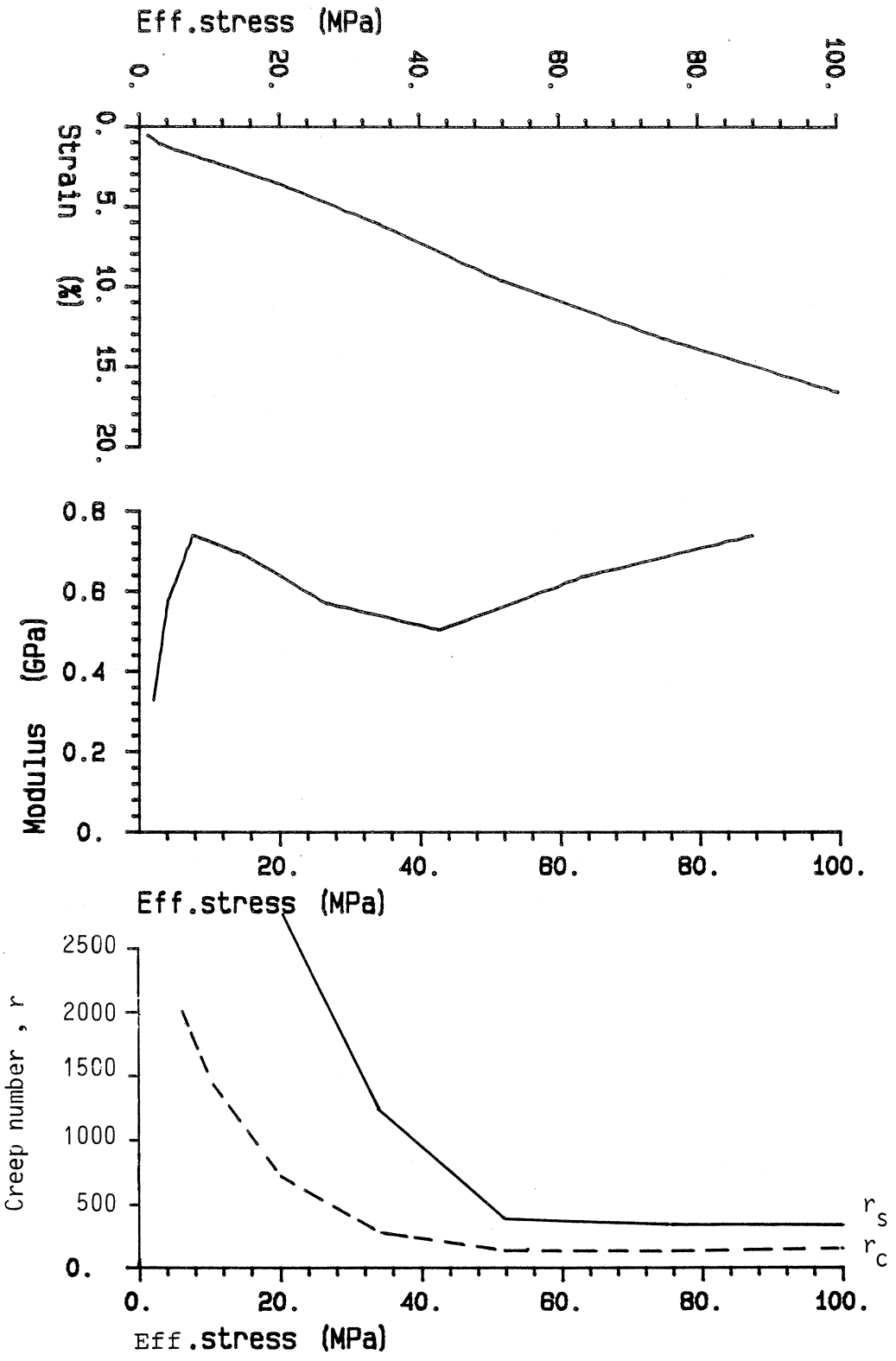
**BARENTSHAVET, 7317/10-U01, EB414, D=147.8 m

SINTEF DIVISION OF GEOTECHNICAL ENGINEERING

PROJECT 690175.00

DATE 16 NOV., 1989

FIG. 5.3



IL - oedometer.

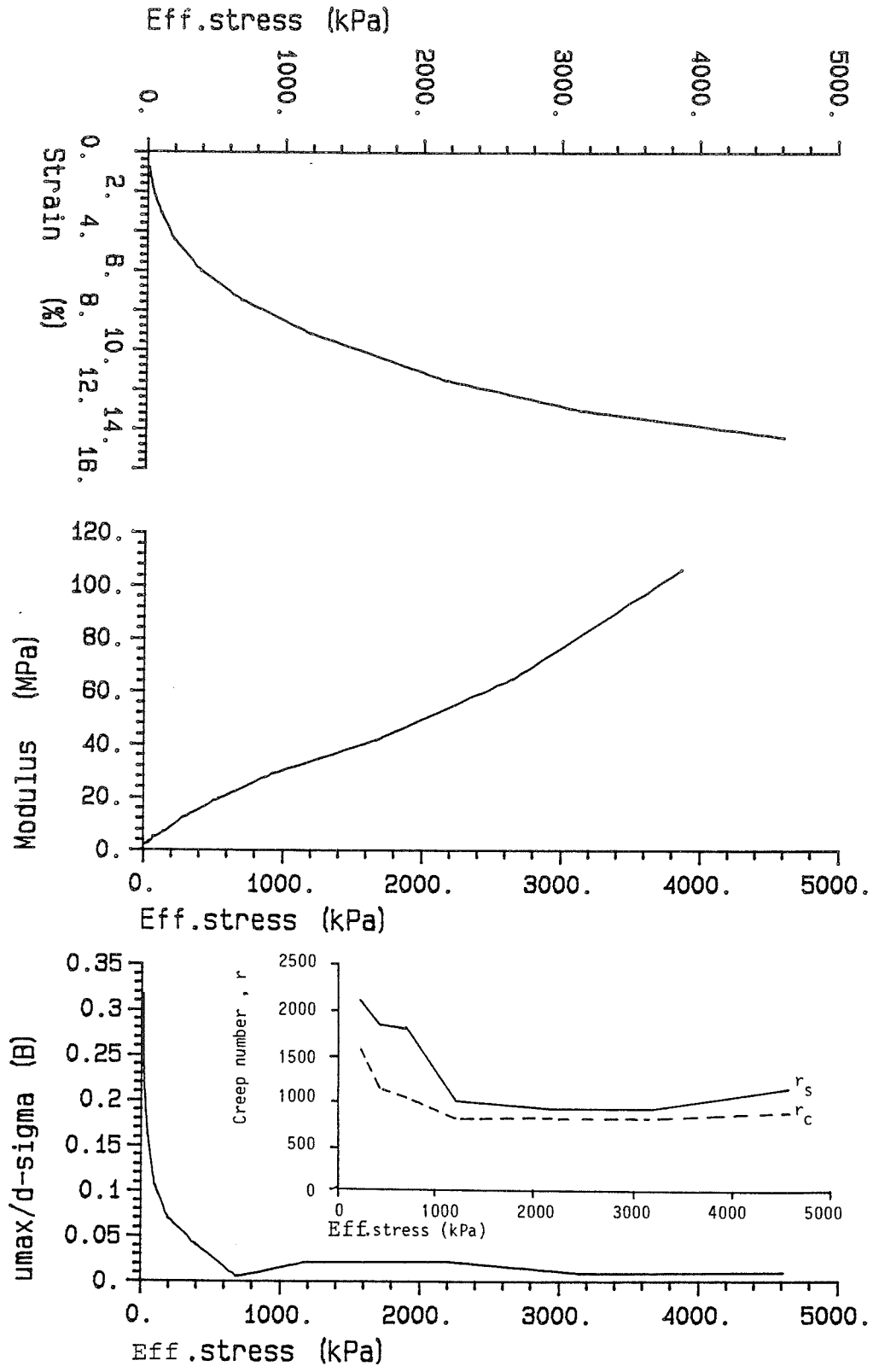
**BARENTSHAVET, 7317/10-U01, E8502, D=207.5 m

SINTEF DIVISION OF GEOTECHNICAL ENGINEERING

PROJECT 690175.00

DATE 10 NOV., 1989

FIG. 5.4



IL - oedometer.

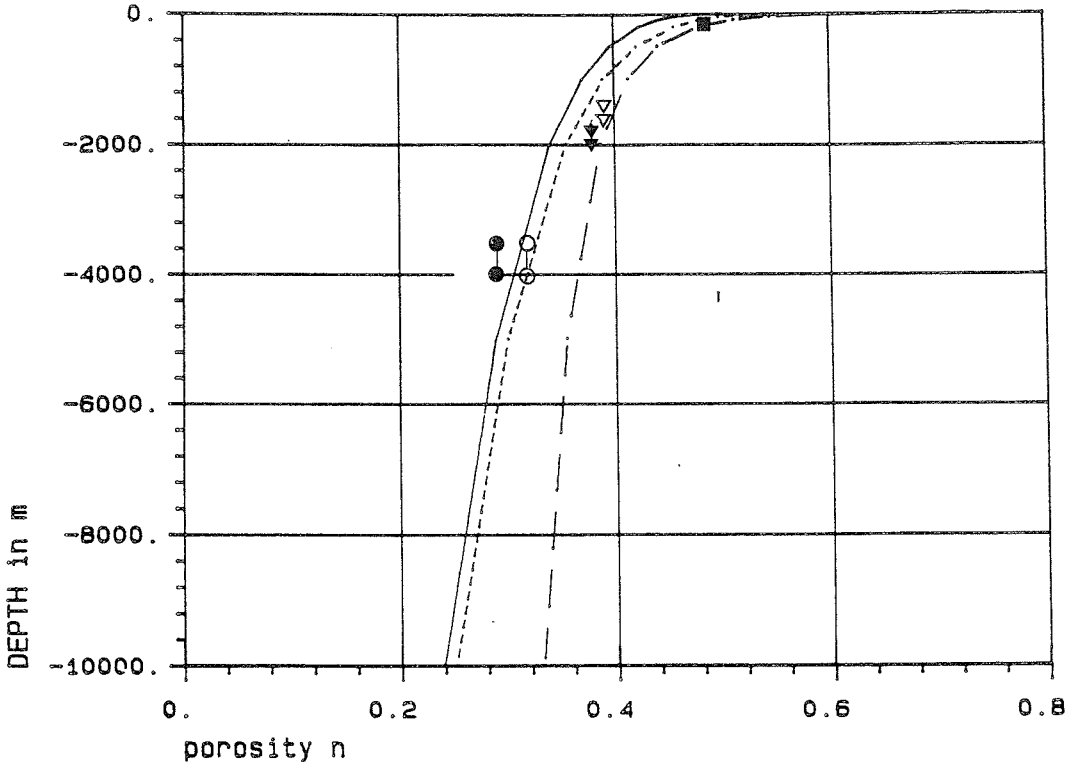
**BARENTSHAVET, 7316/03-U01, E26, D=53.90 M

SINTEF DIVISION OF GEOTECHNICAL ENGINEERING

PROJECT 690175.00

DATE 6 NOV., 1989

FIG. 5.5



Legend :

———— sand a=0.5

------- silt a=0.35

– – – – clay a=0.0

See Tab.5.1

■ 7316/03-U-01,E26 ,D= 53.91m

▽ 7316/06-U-02,E8292,D=138.20m

▼ 7316/06-U-02,E8363,D=181.05m

○ 7317/10-U-01,E8414,D=147.85m

● 7317/10-U-01,E8502,D=207.53m

Depth of previous burial : $D_b=\sigma_c'/\bar{\gamma}'$ $(\bar{\gamma}'=10\ kN/m^3)$

RESULTS: Porosity vs depth. (From /4/)

PROJECT 690175.00

DATE 1989.12.27

FIG. 6.1

SINTEF DIVISION OF GEOTECHNICAL ENGINEERING

IKU SINTEF-GRUPPEN

APPENDIX A.7

TRACE FOSSILS

by

Richard G. Bromley

Ichnos, Copenhagen, Denmark

ICHNOLOGICAL STUDY OF WELL 7316/06-U-02, BARENTS SEA

Monotonous claystone and siltstone. The clay has responded badly to wetting during previous study, and surfaces are not in good condition. Biogenic structures are poorly visible.

199.45 - 143.34 m

Biogenic structures are poorly visible at several horizons, e.g., 199.15 m, 190.15 m, 187.00 m, 177.41 m, 164.90 m, 150.10 m and 144.00 m. Structures are horizontal, small and generally represent slightly darker, possibly more coarse-grained fills than the surrounding rock. On horizontal surfaces, mica grain orientation shows biogenic disturbance.

Lamination is present at all levels and has been enhanced by compaction. It is possible that lamination enhancement has tended to downgrade bioturbation visibility and that bioturbation is more generally present than is immediately apparent.

At several horizons, lamination seems to be perfect, indicating a complete lack of bioturbation. Undisturbed mica grains on lamina surfaces support this. E.g., at 177.93 m, 163.00 m and 151.20 m. However, in general, incomplete bioturbation by low diversity deposit-feeder communities is indicated. The stress factor may be rapidity of fine grain deposition, causing turbid bottom water and very soft to soupy substrates.

The chevron structure at 165.10 m may be a backfill.

143.34 - c.143.00 m

Above a sandy, laminated intercalation, the ichnofabric becomes more clearly visible. Diversity and burrow size increase, possibly in response to an increase in silt content and a firming up of substrate consistency. Backfill structures of 1 cm diameter are visible together with smaller fills. Zoned fills suggestive of *Helminthopsis* are present at 143.5 m, pale outside dark centres. A fairly well established deposit-feeder community is indicated. Visibility fades upwards.

c.143.00 - c.140.90 m

Very poor visibility. Apparently similar ichnological data as below 143.34 m.

c.140.90 - 137.30 m

Helminthopsis is visible and well developed throughout this interval. Bioturbation levels approach 100%. *Planolites* of several size classes, 5 mm to 10 mm, occurs at several levels. Other forms are also present, particularly clearly visible at 138.00 m, where diversity appears to be 5 - 6.

137.30 - 136.00 m

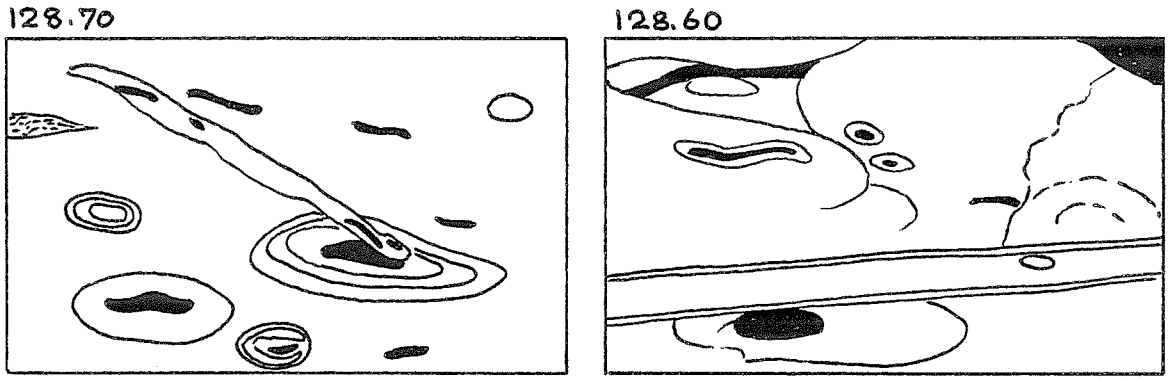
Very clear ichnofabric, 100% bioturbation, diversity high and probably 6 - 8. *Helminthopsis* is sparse but distinct, 1 - 2 mm in diameter, dominantly horizontal. A 1 cm diameter meniscus backfill structure is seen at 136.36 m. These forms cut several larger, indistinct structures that in longitudinal section imitate bedding, and which represent shallow-tier activity.

136.00 - 132.65 m

Reduction in visibility with a few "windows" that indicate similar bioturbation level and degree as below.

132.65 - 124.60 m

Very clearly visible ichnofabric. Complete bioturbation almost throughout. A diverse ichnoassemblage. *Helminthopsis* is minute to 1 mm in diameter and cuts all other forms. At 128.70 m, a meniscus backfill structure 1 cm in diameter is cut by an oblique backfilled structure 5 mm in diameter that is in turn cut by minute *Helminthopsis*. The miniscus structure itself truncates a background mottling characterized by *Planolites* in several sizes but poorly defined (see fig.). Thus a four- to five-tier structure is indicated; deposit feeders dominated a mature endobenthic community.



Immediately above that, at 128.60 m, a *Palaeophycus* is sectioned longitudinally, and large scale disturbance suggests the presence of *Thallassinoides* (see fig.).

124.60 - c.116.95 m

Increase in clay content obscures visibility but apparently the assemblage remains little changed.

c.116.95 - 100.76 m

Gradual change between two alternating fabrics. In the one, *Helminthopsis* runs freely and dominates; in the other, *Thallassinoides* dominates and *Helminthopsis* is largely restricted to reworking *Thalassinoides* fills (Figs next page). In the later case, locally *Helminthopsis* is absent (e.g., 111.50 m).

100.76 - 72.25 m

Visibility drops as clay content increases. Through this unit there is a decrease in ichnodiversity. *Helminthopsis* can only be demonstrated at a few levels (e.g. 97.50 m, 96.64 m, 95.15 m and 81.60 m). *Thalassinoides* also is only indicated at a few horizons. Several *Planolites* are seen, e.g. a dark fill at 88.60 m that resembles *Helminthopsis* without the mantle.

At the top of the unit, large burrows return - large *Planolites* and possible *Thalassinoides* -from 73.55 m to 72.25 m. These are accompanied by a high

diversity of very small structures and a possible retrusive spreite form at 73.40 m.

At several levels, primary lamination is preserved in the fabric, e.g. at 97.40 m, 96.70 m, 86.10 m, 85.55 m, 85.00 m and 82.40 m.

72.25 - 71.05 m

Highly contorted fabric, structures at a 10 cm scale. Darker organic-rich clumps are involved in swirl structures.

71.05 - 65.91 m (top)

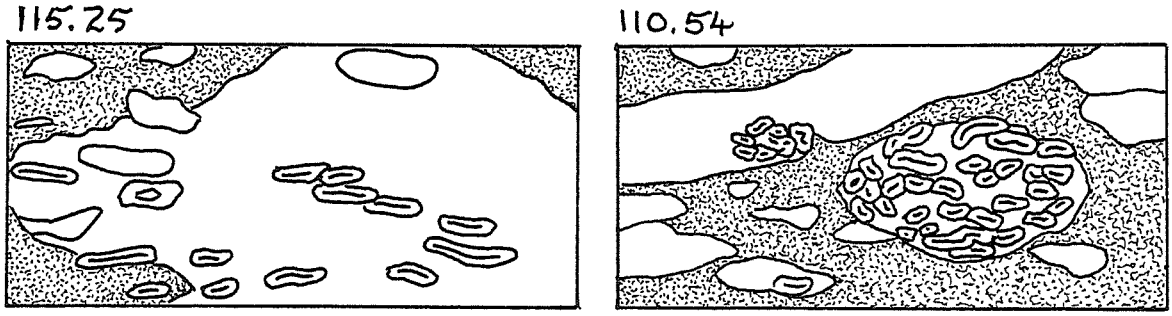
Mudstone containing much mudclast material, some contorted bedding and few biogenic structures (simple *Planolites* at e.g. 69.00 m).

Interpretation

The ichnological data support an interpretation as a regressional sequence. The lower part to about 143 m is little bioturbated and the ichnodiversity low. Substrate consistency and reduced water circulation may control this.

Thereafter a trend is seen toward high ichnodiversity assemblages dominated by *Helminthopsis* to 125 m; a mud-bottom deposit feeder community suggesting marine shelf conditions. The absence of *Zoophycos* and *Chondrites* may indicate relatively rapid deposition, allowing the dominance of mobile deposit feeders instead of stationary ones.

The change to dominance by *Thallassinoides* from 117 m to 100 m may indicate greater proximity of the shore, slightly higher energy of the bottom water.



There follows a reduction in ichnodiversity owing possibly to restricted coastal conditions. The larger structures at 75 m - 73 m are certainly shallow water indicative. The remainder of the core is apparently marginal marine to backshore, containing abundant signs of massive disturbance and little or no ichnological structure.

COMMENTS ON TRACE FOSSILS IN WELL 7316/03-U-01

54.58 m and 54.70 m

White-walled trace fossils of this sort have chaotic nomenclature. Individual pale- and thick-walled tubes like this normally are referred to as *Terebellina* isp. or *Palaeophycus heberti*. I would favour the last, as the precise nature of *Terebellina* (originally described as a foraminifer) is uncertain.

54.78 m and 55.00 m

Same again, here in cross section. These obvious, pale-walled structures appear to be domichnia of stationary animals, probably suspension feeders. The sediment appears to be totally bioturbated and glimpses are seen of many different structures indicating a considerable ichnodiversity. This indicates a marine, dominantly deposit-feeding community, well oxygenated seafloor, and not excessive depositional rate; i.e. an environment of reasonable predictability.

113.75 m - 125.40 m

Seeing is difficult. I have not tried to improve surfaces with water for fear of further destroying them.

The sediment is more or less fully bioturbated throughout this interval. The dominant trace fossil is *Helminthopsis* - dark-centred and pale mantled, maximum diameter 3 mm (unusually large). Smaller *Helminthopsis* and other smaller structures are glimpsed at several levels, so ichnodiversity is not negligible. I would guess at open marine shelf.

171.30 m- 187.40 m

Most of this interval is bioturbated in a style similar to 54.58 m - 55.00 m. *Helminthopsis* is not visible. White-walled burrows here occur at 172.58 m, 172.76 m, 173.45 m, 174.56 m and 175.37 m. The last occurrence is clearly clustered, with overlap of neighbouring tubes. This form is called *Shaubcylindrichnus coronus* by Frey & Howard (1981) and Howard & Frey (1984). These authors do not explain where the boundary lies between clusters of many individuals, three, two and isolated tubes. The latter we called before *Palaeophycus heberti*. That is the older name and I would refer to groups as "clustered *P. heberti*" for simplicity.

Other biogenic structures here are hard to see. Pale burrow fills lacking a wall, 1 - 2 mm in diameter, may be *Chondrites*. Some have a distinct dark wall and are another ichnospecies of *Palaeophycus*. Above and below 176.00 m, *Helminthopsis* is visible, rather small here. A good marine assemblage possibly representing open shelf.

REFERENCES

FREY, R.W. & HOWARD, J.D., 1981: *Conichnus* and *Shaubcylindrichnus*: redefined trace fossils from the Upper Cretaceous of the Western Interior. Jour. Paleontol. 55: 800-804.

HOWARD, J.D. & FREY, R.W., 1984: Characteristic trace fossils in nearshore and offshore sequences, Upper Cretaceous of east-central Utah. Canadian Jour. Earth Sci. 21: 200-219.

IKU
SINTEF-GRUPPEN

APPENDIX A.8

APATITE FISSION TRACK ANALYSIS

by

P.F. Green and S.J. Marshallsea

Geotrack International, Melbourne, Australia

IKU SINTEF-GRUPPEN

Preface and erratum

Please, note that the stratigraphic ages given in Tables 1 and 2 in this appendix are incorrect (based on the earliest biostratigraphic data and caused by reworked fossils). Corrected stratigraphic ages are therefore given below (Table 1). The new age data give younger deposition ages for cores 7316/03-U-01 and 7316/06-U-01, while the other two cores are unchanged. This does not influence the main conclusions of the enclosed report from Geotrack International, since the apatite fission track ages are older than the deposition ages for the sediments.

Table 1 Supplement to Tables 1 and 2 (Appendix A.8) with revised age data.

Geotrack number	Core number	Depth (m)	Series/ Subseries	Age	Age of reworked fossils
GC204-1	7316/03-U-01	53.15-53.60	Late Miocene	~11-5 Ma	(?)Late Oligocene-Early Miocene Mid Eocene
GC204-2	7316/03-U-01	78.8-79.5	Late Miocene		Aptian - Cenomanian
GC204-3	7316/06-U-02	70.6-75.5	Early-Middle Eocene	~52-40 Ma	Aptian-Cenomanian
GC204-4	7316/06-U-01	70.40	Late Oligocene-Early Miocene	~30-16 Ma	?Late Oligocene-?Early Miocene Aptian-Cenomanian
GC204-5	7317/10-U-01	146.40-148.15	Late Paleocene-Early Eocene	~63-52 Ma	Aptian-Cenomanian

GEOTRACK™
INTERNATIONAL

APATITE FISSION TRACK ANALYSIS OF FIVE SAMPLES FROM FOUR SHALLOW CORES FROM BJØRNØYA WEST

A report prepared for
IKU, Trondheim, Norway

Report prepared by:	P F Green & S J Marshallsea
Fission track age determinations by:	S J Marshallsea
Track length measurements by:	S J Marshallsea

December 1989

GEOTRACK REPORT #204

Geotrack International p/l, PO Box 4120, Melbourne University, Victoria 3052, AUSTRALIA
Telephone: National (03) 344 7214; International +61 3 344 7214; Facsimile +61 3 347 5938

GEOTRACK™
INTERNATIONAL

APATITE FISSION TRACK ANALYSIS OF FIVE SAMPLES FROM FOUR SHALLOW CORES FROM BJØRNØYA WEST

CONTENTS

		Page
Executive Summary		i
Paleotemperature Analysis - Table 1		ii
1.	Introduction	1
2.	Thermal History Interpretation	1
3.	Provenance Information	2
4.	Zircon Separates	3
Appendix A - Sample Details		A1-A2
Appendix B - Sample Preparation and Experimental Details		B1-B2
Appendix C - AFTA Data Tables and Figures		C1-C13
Appendix D - Principles of Interpretation of AFTA Data		D1-D6

GEOTRACK REPORT #204

Geotrack International p/l, PO Box 4120, Melbourne University, Victoria 3052, AUSTRALIA
Telephone: National (03) 344 7214; International +61 3 344 7214; Facsimile +61 3 347 5938

GEOTRACK™
INTERNATIONAL

APATITE FISSION TRACK ANALYSIS OF FIVE SAMPLES FROM FOUR SHALLOW CORES FROM BYØRNØYA WEST

EXECUTIVE SUMMARY

1. None of the samples analysed showed any signs of having been subjected to significantly elevated paleotemperatures at any time since deposition. The AFTA data suggest quite clearly that the samples have not been subjected to temperatures in excess of 50°C at any time since deposition.

2. AFTA parameters in all five samples are dominated by inheritance from source areas. The dominant pattern is of a younger group of ages around 80-100 Ma, and an older group of ages in the 200-400 Ma range. The older group of ages can be understood in terms of inheritance from Hercynian and/or Caledonian Basement. The younger groups of ages around 80-100 Ma may be due to Late Cretaceous or Early Tertiary uplift, which is widely recognised in the Svalbard/Barents Sea region. No apatite grains in any of the samples showed any evidence for derivation from Tertiary volcanism.

3. None of the samples showed any evidence for zircon grains of volcanic origin.

GEOTRACK REPORT #204

Geotrack International p/l, PO Box 4120, Melbourne University, Victoria 3052, AUSTRALIA
Telephone: National (03) 344 7214; International +61 3 344 7214; Facsimile +61 3 347 5938

Table 1: Paleotemperature analysis - Shallow cores from Byørnøya West (Geotrack Report #204)

Sample number	Core number	Fission track age (Ma)	Corrected age (Ma)	Stratigraphic age (Ma)	Mean track length µm)	l_p*1 (µm)	Present temperature (°C)	Estimated maximum paleotemperature*2 (°C)
GC204-1	7316/03-U-01	189.6 ± 13.1	209	33-42?	13.22 ± 0.24	15	4	<50
GC204-2	7316/03-U-01	192.0 ± 26.7	209	33-42?	13.30 ± 0.14	15	5	<50
GC204-3	7316/06-U-02	104.5 ± 17.7	127	38-45	12.06 ± 0.42	15	5	<50
GC204-4	7316/06-U-01	290.5 ± 28.4	313	33-55?	13.47 ± 0.92	15	5	<50
GC204-5	7317/10-U-01	135.1 ± 19.3	160	~55	12.22 ± 0.28	15	7	<50

*1 See Appendix D.
*2 No evidence of significantly elevated paleotemperatures since deposition.

NB! Note the revised stratigraphic ages given in the preface (Table 1).

1. Introduction

This report describes results of an AFTA™ study of five samples from four shallow cores from Byørnøya West submitted for analysis by the Continental Shelf and Petroleum Technology Research Institute A/S, Trondheim, Norway (IKU). The main aims of the study were:

a) to obtain any possible constraints on the thermal history of the samples; and

b) to investigate the provenance of these sediments, and in particular to constrain the age of any Tertiary volcanic material within the samples.

Sample details are summarised in Appendix A, while sample preparation and experimental details etc are described in Appendix B. The AFTA data obtained from the samples are presented in Appendix C, in the form of both Tables and Figures. Details of the data presentation are also discussed in Appendix C, while Appendix D outlines the principles employed in interpreting the AFTA data in terms of thermal histories.

None of the samples showed any signs of having been subjected to significantly elevated paleotemperatures at any time since deposition. In addition, none of the samples showed any firm evidence for the presence of apatites of volcanogenic origin. Some individual apatite grains gave Upper Cretaceous to Tertiary fission track ages, although these could be produced by uplift and erosion in Svalbard and surrounding areas. Zircon separates from the five samples were also inspected, but in none of the samples was there any evidence for zircons of likely volcanogenic origin.

In the following discussion, the interpretation of AFTA data from the five samples is discussed collectively, in terms of thermal history, and then in terms of provenance.

2. Thermal history interpretation

None of the samples analysed shows any signs of having been subjected to significantly elevated paleotemperatures at any time since deposition. The mean or pooled fission track age in each sample (as appropriate) is much older than the stratigraphic age (see Figure 2, Appendix C). Furthermore, in none of the samples do any individual grains give fission track ages significantly less than the stratigraphic age. Mean track lengths are all less than the value expected for tracks formed at the prevailing temperatures (~15 μm, see Table 1), but on the basis of the fission track age data, this can be interpreted in terms of a large number of shorter tracks having been inherited from source areas. Note that in the three samples in which over 50 confined track lengths were measured (GC204-1, 2 and 5), the

track length distributions all show a fair number of tracks in the 14-16 μm range, which would represent tracks formed after deposition, at low temperatures.

Because fission tracks are not particularly sensitive to temperature differences in the 10-50°C range, and also because these samples are dominated by tracks inherited from source areas, it is not possible to state with confidence that the samples have never been hotter than their present, low temperatures, and indeed this seems unlikely. However, the AFTA data from these samples do show quite clearly that they have never been subjected to temperatures in excess of 50°C at any time since deposition.

3. Provenance information

The AFTA parameters in the five samples analysed are essentially similar, with individual grains giving fission track ages generally between ~50 and ~450 Ma, and pooled or mean fission track ages (as appropriate) around the middle of this range. In three samples (GC204-1, 3 and 4), all grains are compatible with a single population of ages, while the other two (GC204-2 and 5) both show a significant spread of single grain ages. The radial plots of the single grain age data in these two samples suggest a distinct separation into two groups of ages around ~100 Ma and ~200-300 Ma. More rigorous analysis of these data using the techniques outlined by Galbraith (1988) confirm the division into two groups, with ages of 88±12 Ma and 284±16 Ma in GC204-2, and 82±8 and 223±17 Ma in GC204-5.

Although a number of grains give Tertiary fission track ages, particularly in GC204-2, 3 and 5, these are actually compatible with the (older) pooled ages of the younger groups in GC204-2 and 5, or the pooled age of the sample in GC204-3. Thus none of the samples shows any evidence, from AFTA parameters, of any contribution due to Tertiary volcanism. This is supported by evidence from grain morphologies, since no sample shows any dominance of euhedral forms which might be characteristic of a volcanogenic provenance. Only one sample (GC204-5) showed an appreciable number of euhedral grains, and several extra grains of this type were analysed in an attempt to identify a possible Tertiary volcanogenic component. However euhedral grains in this sample gave ages in both the age groups described above, and they are clearly not derived from Tertiary volcanism.

Looking at the data from all five samples collectively, the dominant pattern is of a younger group of ages around 80-100 Ma, and an older group of ages in the 200-400 Ma range. Note that although the data from GC204-1 are compatible with a pooled age of ~190 Ma, it is quite likely (on the basis of data from other samples) that there is actually an unresolvable spread of ages within this sample also. The older group of ages can be understood in terms of inheritance from Hercynian and/or Caledonian Basement. The younger group of ages

around 80-100 Ma is less easily understood, but may be due to Late Cretaceous or Early Tertiary uplift, which is widely recognised in the Svalbard/Barents Sea region. A contribution from Late Cretaceous and/or Early Tertiary volcanism is also possible.

4. Zircon separates

Zircon separates were obtained from each sample, although in most samples zircon yields were only fair. None of the samples showed any evidence for the presence of the sort of pale, euhedral zircon grains which might be expected to characterise a Tertiary volcanic origin, all grains being somewhat rounded to highly rounded and deeply coloured. Therefore none of the zircon separates were analysed.

APPENDIX A

Sample Details

Five samples from four shallow cores from Byørnøya West were submitted by IKU for apatite fission track analysis (AFTA). Sample details supplied by IKU are summarised in Table 2, together with the yields of detrital apatite obtained after mineral separation. Numerical values for stratigraphic ages have been assigned using the timescale of Harland et al. (1982). Present temperatures are based on a geothermal gradient of 37°C/km and surface temperatures of 1.7°C, as provided by IKU.

All five samples provided apatite suitable for analysis, with yields varying from poor to excellent. Most of the apatite grains analysed from each sample were rounded to sub-rounded or anhedral, with only a small number of euhedral or sub-euhedral grains in most sample. In GC204-5, a larger proportion of euhdral grains were present, although still in the minority. The quality of the apatites obtained was excellent in all samples, and the overall quality of the data is regarded as excellent.

References

Harland, W.B., Cox, A.V., Llewellyn, P.G., Pickton, C.A.G., Smith, A.G. and Walters, R. 1982, A geologic time scale. Cambridge University Press.

Table 2: Sample details and apatite yields - Bjørnøya West shallow cores (Geotrack Report #204)

Note the revised stratigraphic ages given in the preface (Table 1).

Geotrack number	Core number	Depth (m)	Stratigraphic sub-division	Stratigraphic age (Ma)	Present temperature (Ma)	Apatite yield*1 (g)
GC204-1	7316/03-U-01	53.15-53.60	Late Eocene-?Early Oligocene	33-42?	4	Excellent
GC204-2	7316/03-U-01	78.8-79.5	Late Eocene-?Early Oligocene	33-42?	5	Excellent
GC204-3	7316/06-U-02	70.6-75.5	Middle-Late Eocene	38-45	5	Fair
GC204-4	7316/06-U-01	70.40	?Eocene-?Early Oligocene	33-55?	5	Poor
GC204-5	7317/10-U-01	146.40-148.15	Late Paleocene- ?Early Eocene	~55?	7	Excellent

*1 Yield based on quantity of apatite suitable for age determination. Excellent: >20 grains; Very good: ~20 grains; Good: 15-20 grains; Fair: 10-15 grains; Poor: 5-10 grains; Very poor: <5 grains.

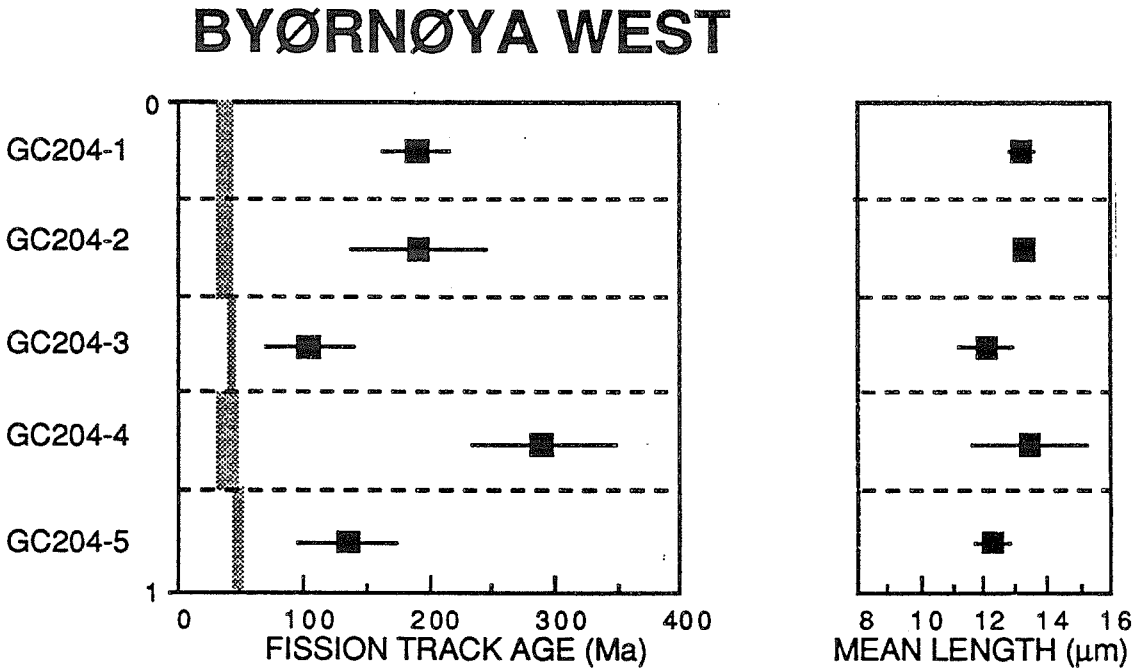


Figure 1: AFTA parameters plotted in relation to stratigraphic age for samples from **Byørnøya West shallow cores.** The range of possible stratigraphic age for each sample is shown by the dotted pattern.

APPENDIX B

Sample Preparation and Experimental Details

The core samples were reduced in size in a jaw crusher, and then ground to sand grade in a rotary disc mill. The ground material was then washed to remove dust, dried and processed by conventional heavy liquid and magnetic separation techniques to recover heavy minerals.

Fission track age and length measurements were made using techniques outlined by Green (1986). Apatites were mounted in epoxy resin on glass slides, polished and etched for 20 sec in 5M HNO_3 at 20°C to reveal the fossil fission tracks. Fission track ages were determined by the external detector method or EDM (Gleadow, 1981) using an Autoscan™ microcomputer controlled automatic stage (Smith and Leigh Jones, 1985). The EDM has the advantage of allowing fission track ages to be determined on single grains. Wherever possible, tracks were counted over 20 grains in each mount. In those samples where this number was not present, all available grains were counted, the actual number depending on the availability of suitably etched and oriented apatites. Only grains oriented with surfaces parallel to the crystallographic c-axis were analysed. Such grains can be identified on the basis of the etching characteristics, as well as from morphological evidence in euhedral grains. The grain mount was scanned sequentially, and the first 20 suitably oriented grains identified were analysed. Track counting was carried out using a Zeiss(R) Axioplan microscope, with an overall linear magnification of 1068 x using dry objectives.

Neutron irradiations were carried out in a well thermalised flux (X-7 facility) in the Australian Atomic Energy Commission's HIFAR research reactor. Total neutron fluence was monitored by counting tracks in mica external detectors attached to two pieces of the NBS standard glass SRM612 included in the irradiation canister at each end of the sample stack. No flux gradient is usually found in the irradiation facility used over the length of the sample package and this was confirmed by the track counts over the two dosimeter glasses. The two values have been pooled to give the single value quoted in Table 3.

For track length studies, the full lengths of 'confined' fission tracks were measured. Confined tracks are those which do not intersect the polished surface but have been etched from other tracks or fractures, so that the whole length of the track is etched. Confined track lengths were measured using a digitising tablet connected to a microcomputer, superimposed on the microscope field of view via a projection tube. With this system, calibrated against a stage graticule ruled in 2 μm divisions, individual tracks can be measured with a precision of ± 0.2

μm. Tracks were measured only in prismatic grains, characterised by sharp polishing scratches with well etched tracks of narrow cone angle in all orientations, because of the anisotropy of annealing of fission tracks in apatite (as discussed by Green et al., 1986). Tracks were also measured following the recommendations of Laslett et al. (1982), the most important of which is that only horizontal tracks should be measured. One hundred tracks were measured whenever possible. In apatite samples with low track density, or in those samples in which only a small number of apatite grains were obtained, fewer confined tracks may be available, and in such cases, the whole mount was scanned to measure as many confined tracks as possible.

References

Gleadow, A.J.W. 1981, Fission track dating methods; what are the real alternatives? *Nuclear Tracks*, 5, 3-14.

Green, P.F. 1986, On The thermo-tectonic evolution of Northern England: evidence from fission track analysis. *Geol. Mag.*, 123, 493 - 506.

Green, P.F., Duddy, I.R., Gleadow, A.J.W., Tingate, P.R. and Laslett, G.M. 1986, Thermal annealing of fission tracks in apatite 1. A qualitative description. *Chem. Geol. (Isot. Geosci. Sect)* , 59, 237-253.

Laslett, G.M., Green, P.F., Duddy, I.R. and Gleadow, A.J.W. 1987, Thermal annealing of fission tracks in apatite 2. A quantitative analysis. *Chem. Geol. (Isot. Geosci. Sect)*, 65, 1-13.

Smith, M.J. and Leigh-Jones, P. 1985, An automated microscope scanning stage for fission-track dating. *Nuclear Tracks*, 10, 395-400.

APPENDIX C

AFTA Data Tables and Figures

Full analytical data for the fission track age determinations are given in Table 3 together with the mean confined track length and the standard deviation of the distribution of confined track lengths in each sample. In Figure 2, the fission track age and mean track length of each sample are plotted as a function of depth and present temperature, (with errors plotted at $\pm 2\sigma$). The variation of stratigraphic age with depth is also shown as the solid line in the central panel.

Fission track ages were calculated using the standard fission track age equation (Hurford and Green, 1982) and errors are quoted at the level of one standard deviation throughout. All constants used in derivation of the results are shown at the bottom of Table 3 using the nomenclature of Hurford and Green (1982). The Zeta calibration factor has been determined empirically (Green, 1985) by direct comparison with K-Ar ages for a set of carefully chosen age standards, following the methods outlined by Hurford and Green (1983). The pooled or maximum probability age is determined from the ratio of the total spontaneous and induced track counts in all the analysed grains. Errors for the pooled age were calculated using the 'conventional' technique outlined by Green (1981), based on the total number of tracks counted for each track density measurement.

The variability of fission track ages between individual apatite grains within each sample can be assessed using a chi-squared (χ^2) statistic (Galbraith, 1981), the results of which are summarised for each sample in Table 3. The probability of obtaining the observed χ^2 value, for ν degrees of freedom (where ν = number of crystals -1), which can be obtained from standard tables, indicates the probability that all the grains counted belong to a single age population. A probability of less than 5% denotes a significant spread of single grain ages, and suggests that real differences exist between the fission track ages of individual apatite grains. A significant spread in grain ages can result either from inheritance of detrital grains from mixed source areas, or from differential annealing in apatite grains of different composition, within a narrow range of temperature (see Appendix D).

Calculation of the pooled age inherently assumes that only a single population of ages is present, and is thus not appropriate to samples containing a significant spread of fission track ages. In such cases the mean of the single grain fission track ages provides a useful measure and this parameter has been used for those samples in which $P(\chi^2)<5\%$. The error in the mean fission track age is taken as the standard deviation of the single grain ages.

Full details of the fission track age data for individual apatite grains in each sample are given, together with the primary counting results and statistical data, on pages C9-C13. Plots of the single grain age data in each sample are shown in Figure 3. The distributions of single grain ages are shown in histogram form and also as smoothed probability functions. In constructing these functions, each grain is represented by a normal probability curve with mean equal to the single grain age, standard deviation given by the error on the single grain age, and the contributions from all grains analysed in each sample are summed to produce the plotted curve.

Single grain age data are also plotted on radial plot diagrams (Galbraith, 1988) in Figure 3. These plots display the variation of individual grain ages as a plot of $y = (z_i - z) / \sigma_i^2$ against $x = 1/\sigma_i^2$ where z_i is the fission track age of each grain, z is the mean age, and σ_i is the error in each age. In this plot, the slope of a straight line from the origin is equivalent to fission track age, and the value of x is a measure of the precision of each individual grain age. Therefore, precise individual grain ages fall to the right of the plot (high x), enabling precise, young grains to be identified. The age scale is shown radially around the perimeter of the plot (in Ma). If all grains belong to a single age population, all data should scatter between $y = +2$ and $y = -2$, equivalent to scatter within $\pm 2\sigma$. Scatter outside these boundaries shows a significant spread of individual grain ages, as also reflected in the Chi-square statistic in Table 3.

Distributions of confined track lengths in each sample are shown in Figure 4, and have been normalised to 100 tracks for each sample to facilitate comparison. The number of tracks (N) measured for each sample is indicated in Table 3 and full details of the track length distributions are given in Table 4.

Finally, note that throughout this report, the term "fission track age" is understood to denote the parameter calculated from the fission track age equation, using the observed spontaneous and induced track counts (either pooled for all grains or for individual grains). The resulting number (with units of Ma) should not be taken as possessing any significance in terms of events taking place at the time indicated by the measured fission track age, but should rather be regarded as a measure of the integrated thermal history of the sample, and should be interpreted in that light using the principles outlined in Appendix D. Use of the term "apparent age" is not considered to be useful in this regard, as almost every fission track age should be regarded as an apparent age, in the classic sense, and repeated use becomes cumbersome.

References

Galbraith, R.F. 1988, Graphical display of estimates having differing standard errors. *Technometrics*, 30, 271-281.

Green, P.F. 1981, A new look at statistics in fission track dating. *Nuclear Tracks 5*, 77-86.

Green, P.F. 1985, A comparison of zeta calibration baselines in zircon, sphene and apatite. *Chem. Geol. (Isot. Geol. Sect.)*, 58, 1-22.

Hurford, A.J. and Green, P.F. 1982, A user's guide to fission track dating calibration. *Earth. Planet. Sci Lett.* 59, 343-354.

Hurford, A.J. and Green, P.F. 1983, The zeta age calibration of fission track dating. *Isotope Geoscience* 1, 285-317.

Table 3: Apatite fission track analytical results - Bjørnøya West shallow cores (Geotrack Report #204)

Geotrack number GC-	Average depth (m)	Number of grains	Standard track density ($x10^6 cm^{-2}$)	Fossil track density ($x10^6 cm^{-2}$)	Induced track density ($x10^6 cm^{-2}$)	Chi square probability (%)	Fission track age (Ma)	Uranium content (ppm)	Mean track length (µm)	Standard deviation (µm)
204-1	53.375	21	1.283 (4036)	0.629 (426)	0.736 (498)	13.7	189.6 ± 13.1	7.5	13.22 ± 0.24 (51)	1.71
204-2	78.875	23	1.283 (4036)	0.911 (910)	0.834 (833)	<1	241.1 ± 12.6 *192.0 ± 26.7**	8.5	13.30 ± 0.14 (71)	1.21
204-3	73.050	12	1.283 (4036)	0.305 (52)	0.651 (111)	83.5	104.5 ± 17.7	6.6	12.06 ± 0.42 (6)	1.02
204-4	70.400	4	1.283 (4036)	1.558 (255)	1.180 (193)	7.5	290.5 ± 28.4	12.0	13.47 ± 0.92 (4)	1.83
204-5	147.075	31	1.283 (4036)	0.465 (511)	0.700 (770)	<1	147.6 ± 9.0 *135.1 ± 19.3**	7.2	12.22 ± 0.28 (64)	2.27

Brackets show number of tracks counted.
Standard and induced track densities measured on mica external detectors (g=0.5), and fossil track densities on internal mineral surfaces.
* Mean age, used where pooled data fail χ^2 test at 5%. Errors quoted at ±1σ.
Ages for samples calculated using ζ=338.9 (Analyst: S J Marshallsea) for dosimeter glass SRM612 (Hurford and Green, 1983).
Track length measurements by S J Marshallsea.

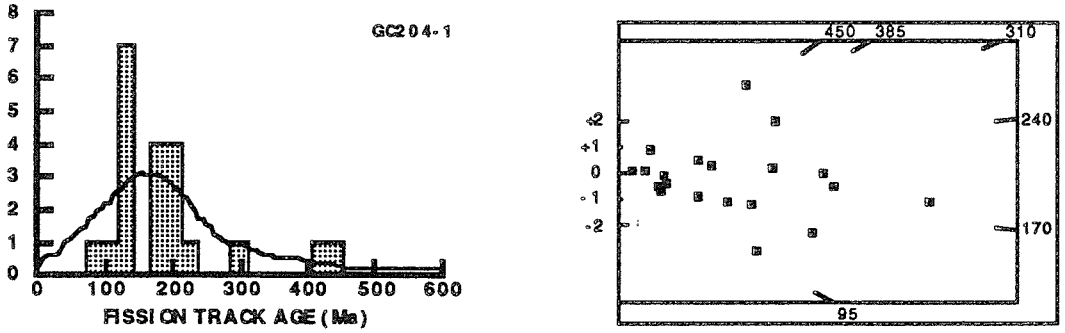
Table 4: Length distribution summary data - Bjørnøya West shallow cores (Geotrack Report #204)

Sample number GC-	Core number	Mean track length (µm)	Std dev (µm)	Number of tracks (N)	Number of tracks in length interval (µm) 1	2	3	4	5	6	7	8	9	10	11	12	13	14	15	16	17	18	19	20
204-1	7316/03-U-01	13.22 ± 0.24	1.71	51	-	-	-	-	1	-	-	-	-	-	1	2	17	17	9	4	-	-	-	-
204-2	7316/03-U-01	13.30 ± 0.14	1.21	71	-	-	-	-	-	-	-	-	-	-	1	9	18	22	15	6	-	-	-	-
204-3	7316/06-U-02	12.06 ± 0.42	1.02	6	-	-	-	-	-	-	-	-	-	-	1	2	2	1	-	-	-	-	-	-
204-4	7316/06-U-01	13.47 ± 0.92	1.83	4	-	-	-	-	-	-	-	-	-	-	-	1	1	1	-	-	1	-	-	-
204-5	7317/10-U-01	12.22 ± 0.28	2.27	64	-	-	1	-	-	1	-	-	1	4	9	7	17	9	11	4	-	-	-	-

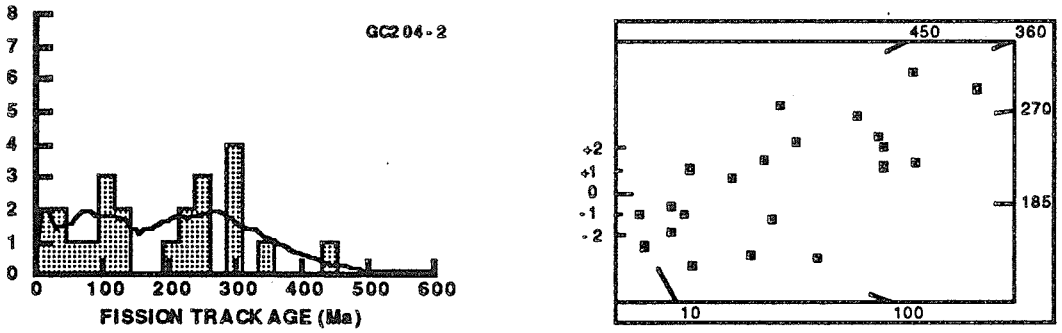
Length measurements by S J Marshallsea.

GEOTRACK™ INTERNATIONAL

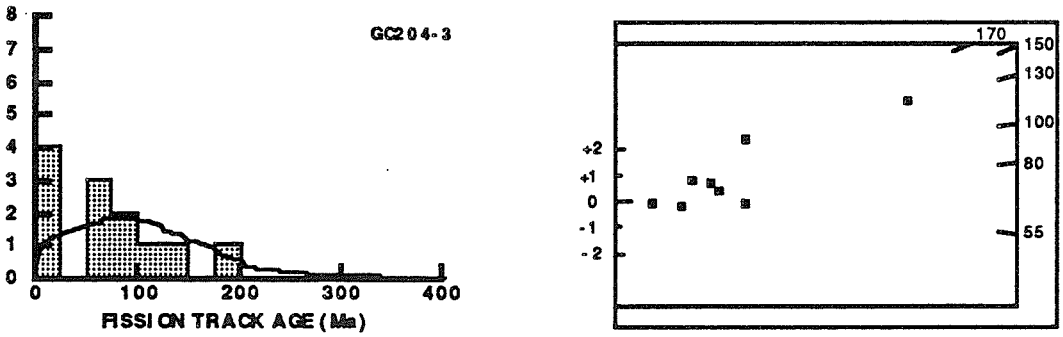
GC204-1



GC204-2



GC204-3



GC204-4

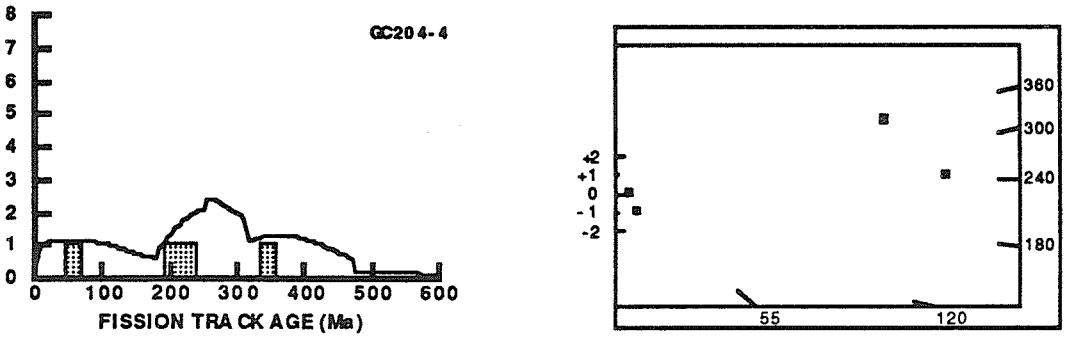


Figure 2: Single grain age distributions with smoothed cumulative age probability distributions (left) and radial plots of single grain age data (right) in apatites from **Bjørnøya West shallow cores.** See text for explanation of radial plots.

.../cont'd

GC204-5

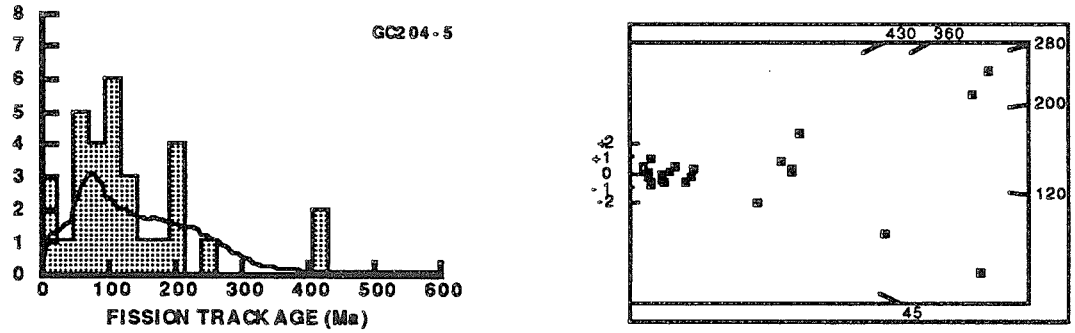
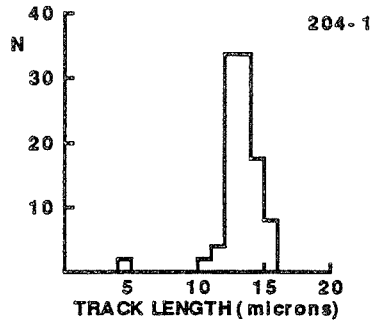
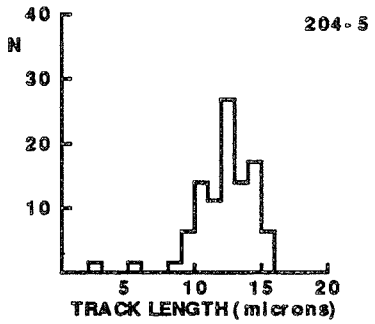


Figure 2: (cont'd)

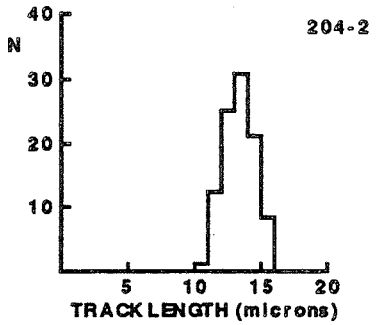
GC204-1



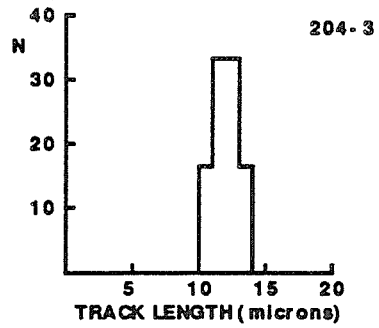
GC204-5



GC204-2



GC204-3



GC204-4

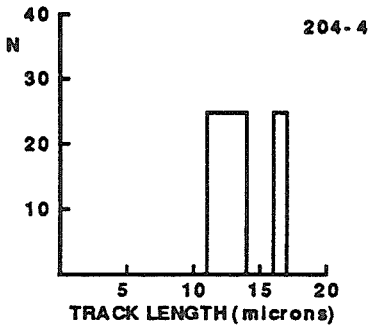


Figure 3: Distributions of confined track lengths in apatites from Byørnøya West shallow cores.

GC204-1 APATITE (7316/03-U-01)

IRRADIATION G080
SLIDE NUMBER 1
COUNTED BY: SJM

No.	N_s	N_i	Na	RATIO	U (ppm)	RHO_s	RHO_i	F.T. AGE (Ma)
1	48	57	49	0.842	18.9	1.557E+06	1.848E+06	186.7 ± 36.8
2	3	5	36	0.600	2.3	1.324E+05	2.207E+05	133.6 ± 97.6
3	11	10	100	1.100	1.6	1.748E+05	1.589E+05	242.8 ± 106.2
4	4	2	92	2.000	0.4	6.909E+04	3.454E+04	434.8 ± 376.7
5	13	20	57	0.650	5.7	3.624E+05	5.576E+05	144.6 ± 51.6
6	2	2	24	1.000	1.4	1.324E+05	1.324E+05	221.1 ± 221.1
7	4	6	56	0.667	1.7	1.135E+05	1.703E+05	148.2 ± 95.7
8	15	34	22	0.441	25.1	1.083E+06	2.456E+06	98.5 ± 30.6
9	29	31	96	0.935	5.2	4.800E+05	5.131E+05	207.0 ± 53.7
10	1	1	20	1.000	0.8	7.945E+04	7.945E+04	221.1 ± 312.7
11	32	52	40	0.615	21.1	1.271E+06	2.066E+06	136.9 ± 30.9
12	3	5	49	0.600	1.7	9.729E+04	1.621E+05	133.6 ± 97.6
13	40	19	35	2.105	8.8	1.816E+06	8.626E+05	456.9 ± 127.7
14	18	27	25	0.667	17.5	1.144E+06	1.716E+06	148.2 ± 45.2
15	4	5	20	0.800	4.1	3.178E+05	3.973E+05	177.5 ± 119.1
16	40	29	90	1.379	5.2	7.063E+05	5.120E+05	303.0 ± 74.2
17	13	13	30	1.000	7.0	6.886E+05	6.886E+05	221.1 ± 86.8
18	3	6	63	0.500	1.5	7.567E+04	1.513E+05	111.5 ± 78.9
19	8	13	22	0.615	9.6	5.778E+05	9.390E+05	136.9 ± 61.6
20	89	110	80	0.809	22.3	1.768E+06	2.185E+06	179.5 ± 25.9
21	46	51	70	0.902	11.8	1.044E+06	1.158E+06	199.7 ± 40.8
	426	498			7.5	6.291E+05	7.355E+05	

Area of basic unit = 6.293E-07 cm-2

CHI SQUARED = 26.923 WITH 20 DEGREES OF FREEDOM
P(chi squared) = 13.7 %
CORRELATION COEFFICIENT = 0.937
VARIANCE OF SQR(Ns) = 5.32
VARIANCE OF SQR(Ni) = 6.04

Ns/Ni = 0.855 ± 0.056
MEAN RATIO = 0.916 ± 0.096

Ages calculated using a zeta of 350.7 ± 5 for SRM612 glass
RHO D = 1.283E+06cm-2; ND = 4036

POOLED AGE = 189.6 ± 13.1 Ma
MEAN AGE = 202.7 ± 21.7 Ma

GC204-2 APATITE (7316/03-U-01)

IRRADIATION G080
SLIDE NUMBER 2
COUNTED BY: SJM

No.	N_s	N_i	Na	RATIO	U (ppm)	RHO_s	RHO_i	F.T. AGE (Ma)
1	17	16	50	1.062	5.2	5.403E+05	5.085E+05	234.7 ± 81.9
2	12	30	50	0.400	9.7	3.814E+05	9.534E+05	89.3 ± 30.6
3	4	7	60	0.571	1.9	1.059E+05	1.854E+05	127.3 ± 79.8
4	157	113	49	1.389	37.4	5.092E+06	3.665E+06	305.2 ± 38.2
5	3	11	56	0.273	3.2	8.513E+04	3.121E+05	61.1 ± 39.8
6	130	77	100	1.688	12.5	2.066E+06	1.224E+06	369.0 ± 53.6
7	26	51	48	0.510	17.2	8.607E+05	1.688E+06	113.7 ± 27.5
8	0	1	24	0.000	0.7	0.000E+00	6.621E+04	0.0 ± 0.0
9	28	23	100	1.217	3.7	4.449E+05	3.655E+05	268.2 ± 75.7
10	52	25	40	2.080	10.1	2.066E+06	9.932E+05	451.6 ± 110.3
11	1	23	72	0.043	5.2	2.207E+04	5.076E+05	9.8 ± 10.0
12	44	32	91	1.375	5.7	7.683E+05	5.588E+05	302.1 ± 70.5
13	10	7	47	1.429	2.4	3.381E+05	2.367E+05	313.6 ± 154.7
14	5	10	100	0.500	1.6	7.945E+04	1.589E+05	111.5 ± 61.1
15	4	22	100	0.182	3.6	6.356E+04	3.496E+05	40.8 ± 22.2
16	1	5	30	0.200	2.7	5.297E+04	2.648E+05	44.8 ± 49.1
17	79	64	61	1.234	17.0	2.058E+06	1.667E+06	271.8 ± 46.1
18	86	84	90	1.024	15.1	1.518E+06	1.483E+06	226.3 ± 35.0
19	78	54	70	1.444	12.5	1.771E+06	1.226E+06	317.0 ± 56.5
20	70	69	100	1.014	11.2	1.112E+06	1.096E+06	224.2 ± 38.3
21	78	68	100	1.147	11.0	1.239E+06	1.081E+06	253.0 ± 42.3
22	5	10	49	0.500	3.3	1.621E+05	3.243E+05	111.5 ± 61.1
23	20	31	100	0.645	5.0	3.178E+05	4.926E+05	143.5 ± 41.3
	910	833			8.5	9.112E+05	8.341E+05	

Area of basic unit = 6.293E-07 cm-2

CHI SQUARED = 99.820 WITH 22 DEGREES OF FREEDOM
P(chi squared) = 0.0 %
CORRELATION COEFFICIENT = 0.933
VARIANCE OF SQR(Ns) = 13.01
VARIANCE OF SQR(Ni) = 6.60

Ns/Ni = 1.092 ± 0.052
MEAN RATIO = 0.867 ± 0.119

Ages calculated using a zeta of 350.7 ± 5 for SRM612 glass
RHO D = 1.283E+06cm-2; ND = 4036

POOLED AGE = 241.1 ± 12.6 Ma
MEAN AGE = 192.0 ± 26.7 Ma

GEOTRACK™
INTERNATIONAL

GC204-3 APATITE (7316/06-U-02)

IRRADIATION G080
SLIDE NUMBER 3
COUNTED BY: SJM

No.	N_s	N_i	Na	RATIO	U (ppm)	RHO_s	RHO_i	F.T. AGE (Ma)
1	5	18	36	0.278	8.1	2.207E+05	7.945E+05	62.2 ± 31.5
2	4	11	25	0.364	7.1	2.542E+05	6.992E+05	81.3 ± 47.5
3	0	1	16	0.000	1.0	0.000E+00	9.932E+04	0.0 ± 0.0
4	4	9	10	0.444	14.6	6.356E+05	1.430E+06	99.2 ± 59.6
5	3	6	14	0.500	7.0	3.405E+05	6.810E+05	111.5 ± 78.9
6	0	1	30	0.000	0.5	0.000E+00	5.297E+04	0.0 ± 0.0
7	2	8	24	0.250	5.4	1.324E+05	5.297E+05	56.0 ± 44.3
8	25	41	25	0.610	26.6	1.589E+06	2.606E+06	135.7 ± 34.6
9	8	10	8	0.800	20.3	1.589E+06	1.986E+06	177.5 ± 84.3
10	0	1	18	0.000	0.9	0.000E+00	8.828E+04	0.0 ± 0.0
11	0	1	30	0.000	0.5	0.000E+00	5.297E+04	0.0 ± 0.0
12	1	4	35	0.250	1.9	4.540E+04	1.816E+05	56.0 ± 62.6
	52	111			6.6	3.049E+05	6.509E+05	

Area of basic unit = 6.293E-07 cm-2

CHI SQUARED = 6.540 WITH 11 DEGREES OF FREEDOM
P(chi squared) = 83.5 %
CORRELATION COEFFICIENT = 0.962
VARIANCE OF SQR(Ns) = 2.21
VARIANCE OF SQR(Ni) = 2.62

Ns/Ni = 0.468 ± 0.079
MEAN RATIO = 0.291 ± 0.077

Ages calculated using a zeta of 350.7 ± 5 for SRM612 glass
RHO D = 1.283E+06cm-2; ND = 4036

POOLED AGE = 104.5± 17.7 Ma
MEAN AGE = 65.2± 17.2 Ma

GEOTRACK™
INTERNATIONAL

GC204-4 APATITE (7316/06-U-01)

IRRADIATION G080
SLIDE NUMBER 4
COUNTED BY: SJM

No.	N_s	N_i	Na	RATIO	U (ppm)	RHO_s	RHO_i	F.T. AGE (Ma)
1	1	4	50	0.250	1.3	3.178E+04	1.271E+05	56.0 ± 62.6
2	124	74	50	1.676	24.0	3.941E+06	2.352E+06	366.3 ± 54.4
3	129	114	100	1.132	18.5	2.050E+06	1.812E+06	249.6 ± 32.5
4	1	1	60	1.000	0.3	2.648E+04	2.648E+04	221.1 ± 312.7
	255	193			12.0	1.558E+06	1.180E+06	

Area of basic unit = 6.293E-07 cm-2

CHI SQUARED = 6.904 WITH 3 DEGREES OF FREEDOM
P(chi squared) = 7.5 %
CORRELATION COEFFICIENT = 0.963
VARIANCE OF SQR(Ns) = 35.01
VARIANCE OF SQR(Ni) = 22.97

Ns/Ni = 1.321 ± 0.126
MEAN RATIO = 1.014 ± 0.294

Ages calculated using a zeta of 350.7 ± 5 for SRM612 glass
RHO D = 1.283E+06cm-2; ND = 4036

POOLED AGE = 290.5 ± 28.4 Ma
MEAN AGE = 224.2 ± 65.1 Ma

GEOTRACK™
INTERNATIONAL

GC204-5 APATITE (7317/10-U-01)
IRRADIATION G080
SLIDE NUMBER 5
COUNTED BY: SJM

No.	N_s	N_i	Na	RATIO	U (ppm)	RHO_s	RHO_i	F.T. AGE (Ma)
1	4	10	50	0.400	3.2	1.271E+05	3.178E+05	89.3 ± 52.9
2	1	2	49	0.500	0.7	3.243E+04	6.486E+04	111.5 ± 136.6
3	3	5	48	0.600	1.7	9.932E+04	1.655E+05	133.6 ± 97.6
4	2	1	56	2.000	0.3	5.675E+04	2.838E+04	434.8 ± 532.6
5	157	135	50	1.163	43.8	4.990E+06	4.290E+06	256.4 ± 30.6
6	24	39	48	0.615	13.2	7.945E+05	1.291E+06	136.9 ± 35.6
7	1	1	20	1.000	0.8	7.945E+04	7.945E+04	221.1 ± 312.7
8	0	7	70	0.000	1.6	0.000E+00	1.589E+05	0.0 ± 0.0
9	1	5	50	0.200	1.6	3.178E+04	1.589E+05	44.8 ± 49.1
10	23	33	60	0.697	8.9	6.091E+05	8.740E+05	154.9 ± 42.2
11	2	5	80	0.400	1.0	3.973E+04	9.932E+04	89.3 ± 74.8
12	2	6	100	0.333	1.0	3.178E+04	9.534E+04	74.5 ± 60.9
13	1	3	50	0.333	1.0	3.178E+04	9.534E+04	74.5 ± 86.1
14	4	5	42	0.800	1.9	1.513E+05	1.892E+05	177.5 ± 119.1
15	129	127	48	1.016	42.9	4.271E+06	4.204E+06	224.5 ± 28.5
16	1	2	60	0.500	0.5	2.648E+04	5.297E+04	111.5 ± 136.6
17	12	34	40	0.353	13.8	4.767E+05	1.351E+06	78.9 ± 26.5
18	34	98	60	0.347	26.5	9.005E+05	2.595E+06	77.6 ± 15.5
19	36	36	45	1.000	13.0	1.271E+06	1.271E+06	221.1 ± 52.3
20	1	3	40	0.333	1.2	3.973E+04	1.192E+05	74.5 ± 86.1
21	2	1	80	2.000	0.2	3.973E+04	1.986E+04	434.8 ± 532.6
22	0	3	60	0.000	0.8	0.000E+00	7.945E+04	0.0 ± 0.0
23	2	4	70	0.500	0.9	4.540E+04	9.080E+04	111.5 ± 96.6
24	6	9	72	0.667	2.0	1.324E+05	1.986E+05	148.2 ± 78.2
25	0	4	64	0.000	1.0	0.000E+00	9.932E+04	0.0 ± 0.0
26	5	10	50	0.500	3.2	1.589E+05	3.178E+05	111.5 ± 61.1
27	1	2	60	0.500	0.5	2.648E+04	5.297E+04	111.5 ± 136.6
28	54	173	70	0.312	40.1	1.226E+06	3.927E+06	69.8 ± 11.0
29	1	4	40	0.250	1.6	3.973E+04	1.589E+05	56.0 ± 62.6
30	1	2	70	0.500	0.5	2.270E+04	4.540E+04	111.5 ± 136.6
31	1	1	45	1.000	0.4	3.531E+04	3.531E+04	221.1 ± 312.7
	511	770			7.2	4.648E+05	7.004E+05	

Area of basic unit = 6.293E-07 cm-2

CHI SQUARED = 94.324 WITH 30 DEGREES OF FREEDOM
P(chi squared) = 0.0 %
CORRELATION COEFFICIENT = 0.842
VARIANCE OF SQR(Ns) = 9.50
VARIANCE OF SQR(Ni) = 11.70
Ns/Ni = 0.664 ± 0.038
MEAN RATIO = 0.607 ± 0.086
Ages calculated using a zeta of 350.7 ± 5 for SRM612 glass
RHO D = 1.283E+06cm-2; ND = 4036

POOLED AGE = 147.6 ± 9.0 Ma
MEAN AGE = 135.1 ± 19.3 Ma

APPENDIX D

Principles of Interpretation of AFTA Data in Sedimentary Basins

Detrital apatite grains are incorporated into sedimentary rocks from three dominant sources - crystalline basement rocks, older sediments and from contemporaneous volcanism. Apatites derived from the first two sources will, in general, contain fission tracks when they are deposited, with AFTA parameters characteristic of the source regions. However apatites derived from contemporaneous volcanism, or from rapidly uplifted basement, will contain no tracks when they are deposited. For now, we will restrict discussion to this situation, and generalise at a later point to cover the case of apatites which contain tracks that have been inherited from source regions.

Fission tracks are trails of radiation damage, which are produced within apatite grains at a more or less constant rate through geological time, as a result of the spontaneous fission of ^{238}U impurity atoms. Therefore the number of fission events which occur within an apatite grain during a fixed time interval depends on the magnitude of the time interval and the uranium content of the grain. Each fission event leads to the formation of a single fission track and the proportion of tracks which can intersect a polished surface of an apatite grain depends on the length of the tracks. Therefore, the number of tracks that are etched in unit area of the surface of an apatite grain (the "spontaneous track density") depends on three factors - (i) the time over which tracks have been accumulating, (ii) the uranium content of the apatite grain, and (iii) the distribution of track lengths in the grain. In sedimentary rocks which have not been subjected to temperatures greater than ~50°C since deposition, spontaneous fission tracks have a characteristic distribution of confined track lengths, with a mean length in the range 14-15 μm, and a standard deviation of ~1 μm. In such samples, by measuring the spontaneous track density and the uranium content of a collection of apatite grains, a "fission track age" can be calculated which will be equal to the time over which tracks have been accumulating. The technique is calibrated against other isotopic systems using age standards which also have this type of length distribution (see Appendices B and C).

In samples which have been subject to temperatures greater than ~50°C after deposition, fission tracks are shortened because of the gradual repair of the radiation damage which constitutes the unetched tracks. In effect, the tracks shrink from each end, in a process which is known as fission track "annealing". The final length of each individual track is essentially determined by the maximum temperature that track has experienced. Time differences of orders of magnitude produce changes in fission track parameters that are equivalent to temperature changes of only

~10°C, so temperature is by far the dominant factor in determining the final fission track parameters. As temperature increases, all existing tracks rapidly shorten to a length determined by the prevailing temperature, regardless of when they were formed. After the temperature has subsequently cooled, all tracks formed prior to the thermal maximum are "frozen" at the degree of length reduction they attained at that time. Thus, the length of each track can be thought of as a maximum-reading thermometer, recording the maximum temperature to which it has been subjected.

In samples for which the present temperature is maximum, all tracks therefore have much the same length resulting in a narrow, symmetric distribution. The degree of shortening will depend on the temperature, with the mean track length falling progressively from ~14 μm at 50°C, to zero at around 110°-120°C, the actual value depending on the timescale of heating and the composition of the apatites present in the sample (see below). Values quoted here relate to times of the order of 10^7-10^8 years, and average apatite composition. If the effective timescale of heating is shorter than 10^7-10^8 years, then the temperature responsible for a given degree of track shortening will be higher, depending in detail on the kinetics of the annealing process (Green et al., 1986; Laslett et al., 1987; Duddy et al., 1988; Green et al., 1989b). Shortening of tracks produces an accompanying reduction in the fission track age, because of the reduced proportion of tracks which can intersect the polished surface. Therefore, the fission track age is also highly temperature dependent, falling to zero at around 120°C, due to total erasure of all tracks.

Complex thermal histories produce correspondingly complex length distributions and ages. Samples which have cooled from a thermal maximum (with peak temperature between ~50° and 120°C) at some time in the past will contain two populations of tracks. Those formed prior to the thermal maximum will all be shortened to more or less the same degree (the precise value depending on the peak temperature) while those formed during and after cooling will be longer due to the lower prevailing temperatures. The length distribution in such samples will be broader than in the simple case, and the fission track age will be a reflection of the amount of length reduction which has occurred. In some cases this kind of history produces a characteristic bimodal distribution of confined track lengths. If cooling is sufficiently rapid, and the final temperature is low enough (<~50°C), tracks formed subsequently will have lengths of 14-15 μm, and will contribute a fission track age component corresponding to the age of the cooling "event". If maximum temperatures exceed ~120°C, all pre-existing tracks will be erased, and all tracks now present will have formed during and subsequent to cooling. The fission track age in such samples therefore relates directly to the time of cooling.

Because temperature dominates the thermal response of tracks in apatite, no information is preserved on the approach to maximum temperature, and the only information available is the

magnitude of the maximum temperature, the timing of cooling from that maximum, and some indication of the thermal history since cooling. Note that if temperature increases again, subsequent to the initial cooling, those tracks formed during this second heating phase will undergo greater shortening. If the temperature in the second heating phase reaches similar values to that reached in the original heating, the two generations of tracks will be identical and all information on the original heating phase will be lost. If the temperature during the second heating phase increases beyond that reached in the original heating phase, all tracks are shortened further.

Our understanding of the behaviour of the AFTA system during geological thermal histories is based on study of the response of fission tracks to elevated temperatures in the laboratory (Green et al., 1986; Laslett et al., 1987; Duddy et al., 1988; Green et al., 1989b) and in geological situations (Green et al., 1989a), observations of the lengths of spontaneous tracks in apatites from a wide variety of geological environments (Gleadow et al., 1986), and the relationship between track length reduction and reduction in fission track age observed in controlled laboratory experiments (Green, 1988).

Final interpretation is based on computer modelling of track shortening through likely thermal histories for an apatite of average composition (Green et al., 1989b). As explained by Green et al. (1989b), the uncertainty in estimates of maximum paleotemperature derived using this approach is thought to be ~10°C. Predictions from these modelling procedures agree well with observed AFTA parameters in apatites of the appropriate composition in samples from the Otway Basin reference wells (Gleadow and Duddy, 1981; Gleadow et al., 1983; Green et al., 1989a), providing support for the validity of extrapolation from laboratory to geological timescales.

The ratio of chlorine to fluorine in the apatite lattice exerts a compositional control on the degree of annealing, with apatites richer in fluorine being more easily annealed than those richer in chlorine. Our understanding of the kinetics of fission track annealing relates to apatite with Cl/Cl+F of ~0.1 (Durango apatite) on which most of our original experimental studies were carried out. Unpublished laboratory annealing studies on a range of different apatites, together with observations of annealing in apatites from the Otway Basin reference wells, which show a wide spread of compositions, afford a means of extending the model predictions to apatites of other compositions. Since the apatite grains analysed in this study are likely to have been originally derived predominantly from basement rocks, a restricted compositional range would be expected in all samples, with Cl/(Cl+F) varying from zero (pure fluorapatite) to around 0.1, the value in Durango apatite. Therefore, in the following discussion, paleotemperature estimates are based on this assumption. Experience with sedimentary rocks derived from a variety of different source terrains suggests that this assumption should be valid.

The basic principle involved in the interpretation of AFTA data in sedimentary basins is to ask whether the degree of annealing shown by tracks in apatite from a particular sample could have been produced by the thermal history suggested by the preserved sedimentary section and the prevailing geothermal gradient.

The degree of annealing is assessed in two ways - (i) from fission track age, and (ii) track length data. The stratigraphic age provides a basic reference point for the interpretation of fission track age, because reduction of the fission track age below the stratigraphic age unequivocally reveals that appreciable annealing has taken place after deposition of the host sediment. Large degrees of fission track age reduction, with the mean or pooled fission track age very much less than the stratigraphic age, indicate severe annealing, which requires paleotemperatures of at least ~100°C for any reasonable geological timescale of heating (>~10 Ma). Note that this applies even when apatites contain tracks inherited from source areas. More moderate degrees of annealing can be detected by inspection of the single grain age data, as the most sensitive (fluorine-rich) grains will begin to give fission track ages significantly less than the stratigraphic age before the mean or pooled age has been reduced sufficiently to give a noticeable signal. Note that this aspect of the single grain age data can also be used for apatites which have tracks inherited from source areas. If signs of moderate annealing (from single grain age reduction) or severe annealing (from the mean or pooled age) are seen in samples which are from present temperatures at which the observed degree of annealing would not be expected, then this suggests that the sample has been subjected to elevated paleotemperatures at some time in the past.

Similarly, the present temperature from which a sample is taken, and the way this has been approached (as inferred from the preserved sedimentary section), forms a basic point of reference for track length data (as well as fission track age data). If observed track shortening cannot have been produced from the apparent burial to the present temperature, then this suggests higher paleotemperatures at some time in the past. Using the kinetic description of fission track annealing described in an earlier section, we can predict a value of mean length, l_p, that would be expected in each sample from the thermal history suggested by the burial history derived from the preserved stratigraphic section, and using the present thermal gradient, ie assuming there has been no uplift and erosion, and no changes in thermal gradient through time. These values of l_p are then compared with measured mean track lengths in assessing past variations in paleotemperature. Values of l_p for all samples analysed are shown in Table 1.

The influence of track lengths inherited from source areas can readily be allowed for, by comparison of the fission track age with the stratigraphic age and inspection of the length distribution. If l_p is less than the stratigraphic age then either the sample has been subjected to elevated paleotemperatures, sufficient to produce the observed degree of length reduction, or

else the sample contains a large proportion of tracks inherited from source areas. However in such a case, the sample should give a mean or pooled fission track age correspondingly older than the stratigraphic age, and the length distribution should contain a component of longer track lengths corresponding to the value of l_p. It is important in this regard that the length of a track depends primarily on the maximum temperature to which it has been subjected, whether in the source regions or after deposition in the sedimentary basin. Thus any lengths retaining a provenance signature will be towards the shorter end of the length distribution where track lengths will not have "equilibrated" with the prevailing temperature within the basin.

Timing of cooling from maximum paleotemperatures can be estimated from a number of lines of evidence. The most direct of these is "correction" of measured fission track ages for the observed degree of length reduction, which provides an estimate of the time over which tracks have been retained. Corrected ages, shown for each sample in Table 1 are calculated using the relationship between length reduction and the reduction in fission track age during annealing reported by Green (1988). In samples which have been totally annealed prior to cooling, and have undergone a relatively simple history since cooling, the corrected age should directly indicate the time of cooling. Note that any complexity in the thermal history leads to these "corrected ages" underestimating this parameter, but this procedure can often yield useful results. However, corrected ages can be very misleading, particularly in samples which have only been partially annealed.

Inspection of the distribution of single grain ages in partially annealed samples can also often yield useful information on the time of cooling, as the most easily annealed grains (those richest in fluorine) may have been totally annealed prior to cooling. The form of the track length distribution can also provide information, from the relative proportions of tracks with different lengths. Normally, all of these aspects of the data are employed in reaching a consistent thermal history interpretation.

References

Duddy, I.R., Green, P.F. and Laslett G.M. 1988, Thermal annealing of fission tracks in apatite 3. Variable temperature behaviour. *Chem. Geol. (Isot. Geosci. Sect)* , 73, 25-38.

Gleadow, A.J.W. and Duddy, I.R. 1981, A natural long-term track annealing experiment for apatite. *Nuclear Tracks*, 5, 169-174.

Gleadow, A.J.W., Duddy, I.R. and Lovering, J.F. 1983, Fission track analysis; a new tool for the evaluation of thermal histories and hydrocarbon potential. *APEA J.* 23, 93-102.

Gleadow, A.J.W., Duddy, I.R., Green, P.F. and Lovering, J.F. 1986, Confined fission track lengths in apatite - a diagnostic tool for thermal history analysis. *Contr. Min. Petr.*, 94, 405-415.

Green, P.F. 1988, The relationship between track shortening and fission track age reduction in apatite: Combined influences of inherent instability, annealing anisotropy, length bias and system calibration. *Earth Planet. Sci. Lett.*, 89, 335-352.

Green, P.F., Duddy, I.R., Gleadow, A.J.W., Tingate, P.R. and Laslett, G.M. 1986, Thermal annealing of fission tracks in apatite 1. A qualitative description. *Chem. Geol. (Isot. Geosci. Sect)* , 59, 237-253.

Green, P.F., Duddy, I.R., Gleadow, A.J.W. and Lovering, J.F. 1989a, Apatite Fission Track Analysis as a paleotemperature indicator for hydrocarbon exploration. *In:* Naeser, N.D. and McCulloh, T. (eds.) *Thermal history of sedimentary basins - methods and case histories*, Springer-Verlag, New York, 181-195.

Green, P.F., Duddy, I.R., Laslett, G.M., Hegarty, K.A., Gleadow, A.J.W. and Lovering, J.F. 1989b, Thermal annealing of fission tracks in apatite 4. Quantitative modelling techniques and extension to geological timescales. *Chem. Geol. (Isot. Geosci. Sect)*, (In Press)

Laslett, G.M., Green, P.F., Duddy, I.R. and Gleadow, A.J.W. 1987, Thermal annealing of fission tracks in apatite 2. A quantitative analysis. *Chem. Geol. (Isot. Geosci. Sect)*, 65, 1-13.

IKU SINTEF-GRUPPEN

APPENDIX A.9

THERMAL CONDUCTIVITY

by

Niels Balling
University of Aarhus, Denmark

A.9 THERMAL CONDUCTIVITY

Thermal conductivity has been calculated from well logs for well 7317/10-U-01 and measured on 39 core samples from wells 7317/10-U-01, 7316/06-U-02 and 7316/03-U-01 by Niels Balling, University of Aarhus, Denmark. The measured and calculated thermal conductivity values are plotted together with the sedimentology logs in Figures A.9.1, A.9.2 and A.9.3.

The measured thermal conductivity values in the homogeneous shaly and sandy siltstones in well 7317/10-U-01 show relatively stable values varying between 1.26 and 1.61 W/mK in vertical direction and between 1.52 and 1.91 W/mK in horizontal direction. The anisotropy coefficients are moderate with values varying from 1.10 to 1.28. The thermal conductivity values calculated from the well logs fit very well with the measured vertical values.

Well 7316/06-U-02 shows measured thermal conductivity values which seem to reflect the grain size distributions and structures of the regressive successions. The measurements show relatively high values with low anisotropy coefficients in the upper, most coarse grained parts of the successions, and lower values with higher anisotropy coefficients in the lower, more fine-grained parts of the successions. This is due to higher quartz-contents in the coarse parts of the successions (pure quartz has high thermal conductivity) and to increasing amounts of clay minerals with its thermal insulating properties relative to quartz, and to increasing anisotropy with increasing amounts of structural clay. The thermal conductivity values vary between 0.80 and 1.67 W/mK in vertical direction and between 1.09 and 1.85 W/mK in horizontal direction.

In well 7316/03-U-01 the measured thermal conductivity values vary mainly just below 2 W/mK with low anisotropy coefficients in the fine to medium grained sandstones. Lower values are measured in silty shale. The values vary between 1.10 and 1.96 W/mK in vertical direction and between 1.34 and 1.96 in horizontal direction. The anisotropy coefficients vary between 1.00 and 1.24 with a majority of the values close to 1.00.

The following is Niels Balling's report.

IKU SINTEF-GRUPPEN

THERMAL CONDUCTIVITY FOR THE BJØRNØYA WEST SAMPLES

Introduction

Thermal conductivity has been measured on 39 core samples from 3 localities (7317/10-U-01, 7316/06-U-02 and 7316/03-U-01). The measured cores have approximately cylindrical shape with typical lengths of 80-100 mm and typical "width" of 35-50 mm.

This report contains a description of the measuring technique, measuring conditions and the measuring results. Special emphasis is given to the measurements of any thermal conductivity anisotropy.

Measuring techniques

The measurements were taken by the needle probe method. The probes used have a length of 50 mm and an outer diameter of 1.5 mm. For all samples small holes were drilled with high speed drills for the insertion of the needle probes. The diameter of drills used is 1.5 mm, thus resulting in drill holes of only slightly larger diameter and generally of perfect size for the insertion of the measuring probes.

Measurements were carried out on water saturated/"near saturated" samples at room temperature (~20°C) and generally at slightly elevated pressure (~5-10 bar) to minimize effect of any minor secondary cracks. The samples were kept in water for at least 48 hours before measurements, resulting in practically water saturated conditions. Due to core conditions and the risk of disintegration, traditional water saturation procedure was not followed (saturation in water under vacuum). However, additional measurements on 5 samples (best quality samples) with traditional saturation after first measurements showed no significant differences (< 2-3%).

For each sample 4 single measurements were carried out; 2 measurements in two mutually perpendicular directions in the "top part" of the sample and 2 measurements in the "bottom part" of the sample. From these measurements conductivity anisotropy may be determined as well as local variations in conductivity.

From measurements with the needle placed along the core axis (vertical direction), the horizontal conductivity (kh) is measured, and from measurements with the needle placed in the perpendicular (horizontal) direction a weighted mean (km) of horizontal (kh) and vertical conductivity (kv) is measured. As $km = (kh \cdot kv)^{\frac{1}{2}}$ we obtain kv as km^2/kh.

During measurements all needle probes were currently tested in standard material of known conductivity. The needle probe technique used shows a conductivity repeatability generally within 1-3%. Depending on the quality of the core material, single conductivity measuring results normally show absolute accuracy better than 5%.

Results of measurements

Measuring results are summarized in Table A.9.1. For each sample horizontal conductivity (kh), vertical conductivity (kv), and the coefficient of conductivity anisotropy (A = kh/kv) are given.

Table A.9.1 contains sample mean values together with supplementary information. Here, the results of the "top" and "bottom" sets of measurements are included. The sample values are determined as mean values of these "top" and "bottom" sets of measuring results.

Also a sample quality code is given (Table A.9.1). Quality code 2 is assigned to samples where minor "cracks" may, to some extent, affect the measuring results. For the present data set such cracks are assumed to affect measuring results by no more than 10-15%. The effect of cracks may be a minor decrease in conductivity. When code 3 is used, sample quality is poor, and inaccuracy may be up to 25%.

For 9 sets of measurements (marked with (a) in Table A.9.1) original data sets showed indications of conductivity anisotropy coefficients less than 1. Inspection of core samples indicated that apparent reversed anisotropy may result from local conductivity variability or local minor cracks rather than well defined conductivity anisotropy. In all these cases conductivity values given are determined as mean values of measurements in the different directions (mean value of kh and km) resulting in no resolved conductivity anisotropy.

For each of the three localities, mean conductivity values are calculated for the actual samples together with standard deviation and standard error of the mean. These values are given mainly for statistical reasons and not to indicate lithologically representative station averages.

Generally "top" and "bottom" sets of measurements show good agreement, especially for the locality mean values, but also for single samples. Generally, conductivities agree with 0.1 to 0.3 W/mK and anisotropy with 0.10-0.15. For a few samples (8661 and 8666) conductivity differences of 0.3-0.4 are observed. Some anisotropy variability, especially for locality 7316/06-U-02, is observed. Here, about half the samples show anisotropy differences of ~0.2 to ~0.4. Locally, due to the character of the samples (some are rather porous and loose), some inaccuracy (of the order of 10-20%) may be present. However, as a whole the data set shows a high degree of internal consistency. Conductivity and conductivity anisotropy are generally well defined. We note that "locality mean values" for "top set" and "bottom set" of measurements show agreement within 0.01 to 0.05.

IKU SINTEF-GRUPPEN

Table A.9.1 Thermal conductivity (W/mK) of the 1989 Bjørnøya West samples.

Sample no.	Depth/ (m)	kh(k)	Sample kv(k)	A	kh(k)	Top kv(k)	A	kh(k)	Bottom kv(k)	A	Sample quality (b)
7317/10-U-01											
E 8650	143.94	1.59	1.26	1.26	1.61	1.26	1.27	1.56	1.26	1.24	2
E 8651	148.44	1.91	1.60	1.19	1.92	1.54	1.25	1.90	1.67	1.14	1
E 8562	158.00	1.52	1.20	1.26	1.51	1.26	1.20	1.52	1.15	1.33	2
E 8653	167.98	1.73	1.41	1.22	1.74	1.40	1.24	1.71	1.43	1.20	1
E 8654	176.81	1.84	1.52	1.21	1.84	1.60	1.15	1.84	1.43	1.29	1
E 8655	184.39	1.56	1.23	1.27	1.60	1.26	1.27	1.53	1.19	1.28	1
E 8656	195.52	1.76	1.38	1.28	1.83	1.41	1.29	1.69	1.34	1.26	1
E 8657	204.99	1.78	1.48	1.20	1.75	1.49	1.17	1.80	1.46	1.23	1
E 8658	212.75	1.66	1.34	1.24	1.69	1.37	1.23	1.64	1.31	1.25	1
E 8659	221.60	1.77	1.61	1.10	1.82	1.51	1.21	1.72	1.72	1.00	1
Mean value		1.71	1.40	1.22	1.13	1.41	1.23	1.69	1.40	1.22	
Stand. dev.		0.13	0.15	0.05	0.13	0.12	0.05	0.13	0.19	0.09	
St.err. of mean		0.04	0.05	0.02	0.04	0.04	0.01	0.04	0.06	0.03	
7316/06-U-02											
E 8660	81.65	1.70	1.58	1.07	1.66	1.59	1.04	1.74	1.57	1.10	2
E 8661	73.36	1.85	1.56	1.18	1.81	1.37	1.32	1.88	1.75	1.08	2
E 8662	88.67	1.49	1.00	1.49	1.45	0.97	1.50	1.53	1.04	1.48	2
E 8663	98.64	1.55	1.19	1.30	1.49	1.16	1.28	1.61	1.22	1.32	2
E 8664	109.09	1.88	1.67	1.13	1.93	1.84	1.05	1.84	1.51	1.22	2
E 8665	122.26	1.52	1.15	1.32	1.41	1.23	1.14	1.63	1.07	1.53	2
E 8666	131.59	1.52	1.29	1.18	1.57	1.11	1.41	1.46	1.46	1.00(a)	2
E 8667	142.91	1.62	1.02	1.59	1.61	1.11	1.45	1.64	0.94	1.75	2
E 8668	152.86	1.54	0.99	1.56	1.45	1.04	1.39	1.64	0.94	1.74	2
E 8669	163.13	1.48	0.80	1.86	1.54	0.80	1.91	1.42	0.79	1.80	2
E 8670	174.04	1.58	1.31	1.20	1.56	1.24	1.25	1.60	1.39	1.16	1
E 8671	181.08	1.59	0.96	1.67	1.57	0.98	1.60	1.62	0.93	1.73	2
E 8672	191.09	1.09	1.09	1.00(a)	1.09	1.09	1.00(a)	1.10	1.10	1.00(a)	3
Mean value		1.57	1.20	1.35	1.55	1.20	1.33	1.59	1.21	1.38	
Stand. dev.		0.19	0.27	0.26	0.20	0.27	0.26	0.20	0.30	0.31	
St.err. of mean		0.05	0.07	0.07	0.06	0.08	0.07	0.05	0.08	0.09	
7316/03-U-01											
E 8673	35.76	1.64	1.54	1.07	1.65	1.51	1.09	1.64	1.56	1.05	2
E 8674	49.51	1.44	1.41	1.02	1.45	1.39	1.04	1.43	1.43	1.00(a)	2
E 8675	58.61	1.96	1.96	1.00	2.02	2.03	1.00	1.89	1.89	1.00(a)	2
E 8676	66.22	1.75	1.70	1.03	1.79	1.79	1.00(a)	1.71	1.60	1.06	2
E 8677	75.12	1.34	1.23	1.09	1.33	1.19	1.12	1.35	1.27	1.06	1
E 8678	85.99	1.36	1.10	1.24	1.33	1.08	1.23	1.40	1.13	1.24	2
E 8679	90.56	1.74	1.59	1.09	1.69	1.61	1.05	1.79	1.58	1.13	2
E 8680	95.40	1.78	1.62	1.10	1.79	1.69	1.06	1.77	1.56	1.14	1
E 8681	106.00	1.87	1.87	1.00(a)	1.85	1.85	1.00(a)	1.90	1.90	1.00(a)	2
E 8682	106.56	1.80	1.79	1.01	1.73	1.71	1.02	1.87	1.86	1.00	2
E 8683	115.86	1.78	1.68	1.06	1.80	1.79	1.00	1.77	1.58	1.12	2
E 8684	127.48	1.74	1.59	1.09	1.70	1.66	1.02	1.77	1.53	1.16	2
E 8685	145.75	1.71	1.62	1.05	1.68	1.68	1.00	1.74	1.57	1.11	1
E 8686	154.49	1.81	1.63	1.11	1.79	1.61	1.11	1.84	1.64	1.12	1
E 8687	165.72	1.87	1.78	1.05	1.89	1.80	1.05	1.85	1.76	1.05	1
E 8688	174.46	1.69	1.68	1.01	1.72	1.69	1.02	1.67	1.67	1.00(a)	2
Mean value		1.71	1.61	1.06	1.70	1.63	1.05	1.71	1.60	1.08	
Stand. dev.		0.18	0.22	0.06	0.19	0.24	0.06	0.17	0.21	0.07	
St.err. of mean		0.04	0.05	0.02	0.05	0.06	0.02	0.04	0.05	0.02	

(a): Significant anisotropy not resolved.
(b): Sample quality code used: 1:good, 2:fair, 3:poor.

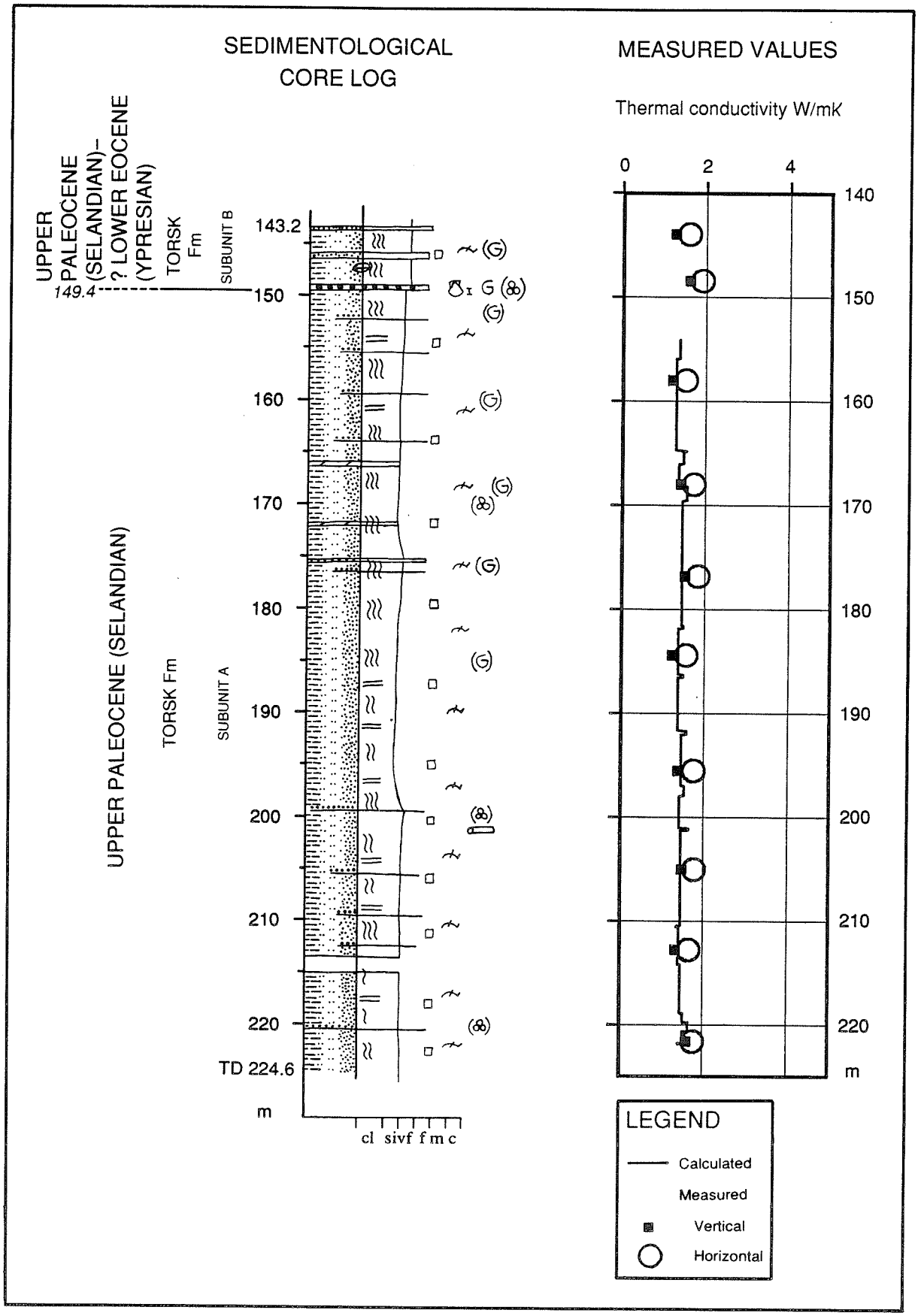


Figure A.9.1 *Measured and calculated thermal conductivity values and sedimentology log for well 7317/10-U-01.*

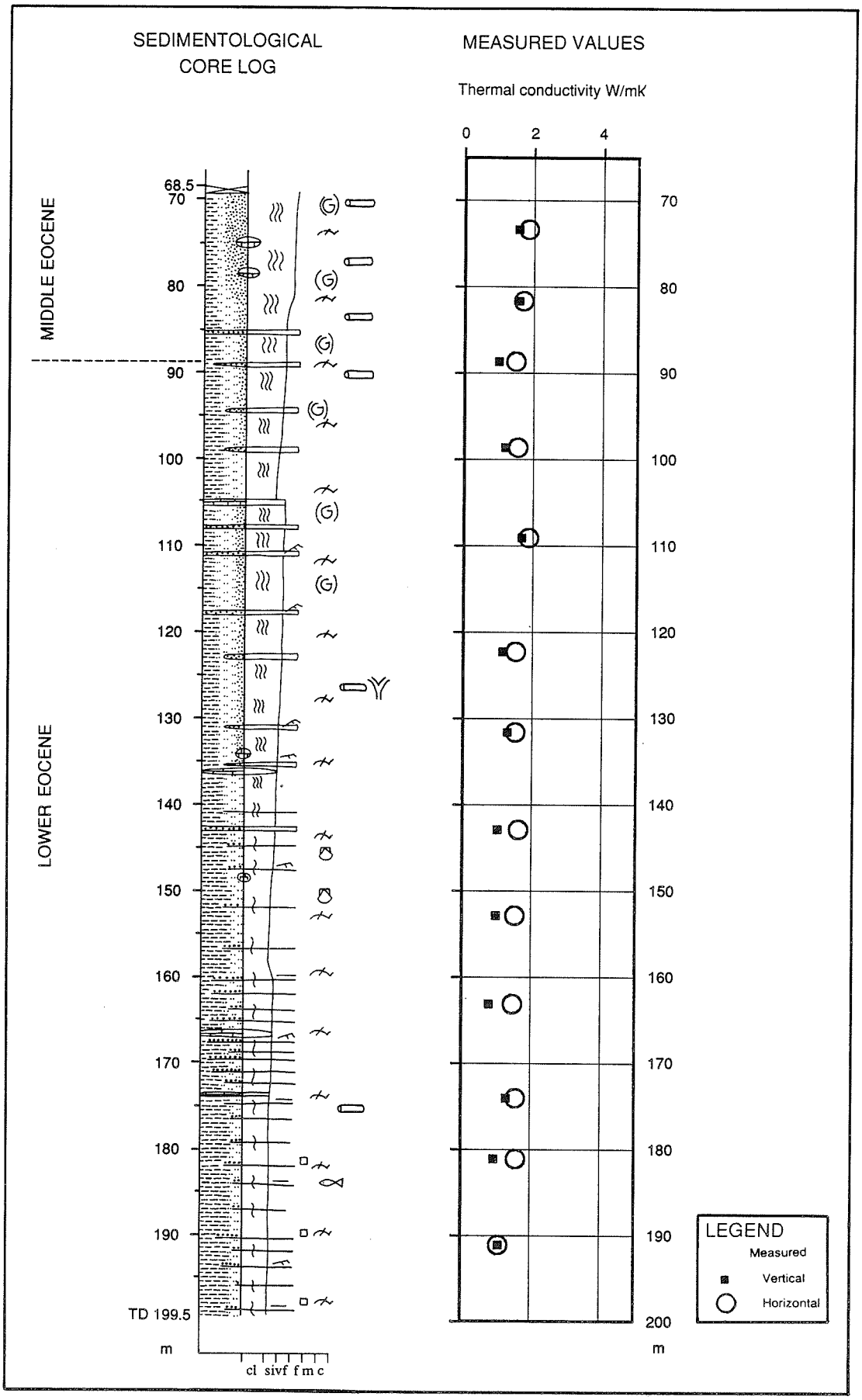


Figure A.9.2 *Measured thermal conductivity values and sedimentology log for well 7316/06-U-02.*

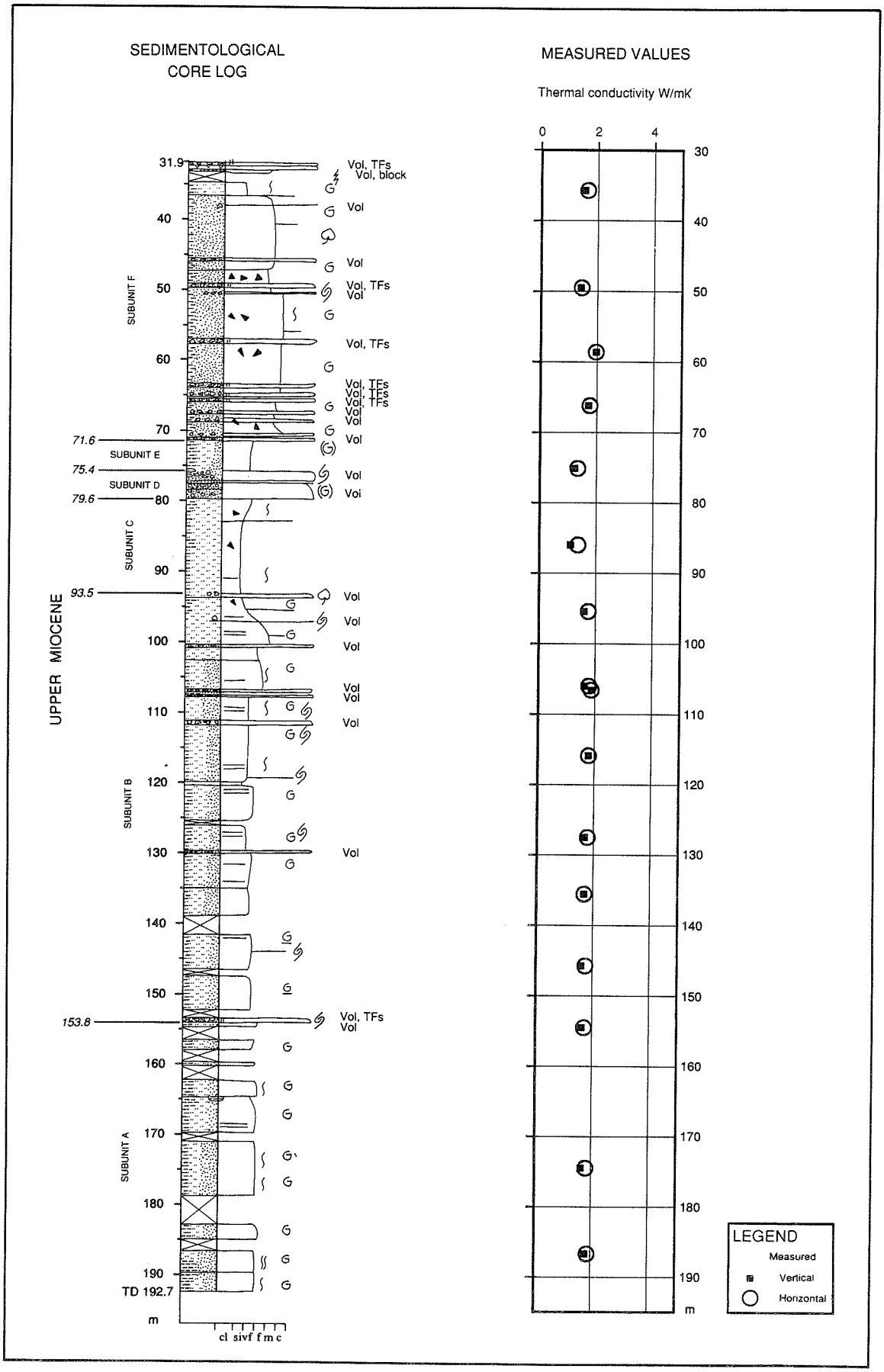


Figure A.9.3 *Measured thermal conductivity values and sedimentology log for well 7316/03-U-01.*

IKU SINTEF-GRUPPEN

APPENDIX A.10

DISCUSSION OF PETROPHYSICAL CORE MEASUREMENTS AND WIRELINE LOGS

IKU SINTEF-GRUPPEN

A.10 DISCUSSION OF PETROPHYSICAL CORE MEASUREMENTS AND WIRELINE LOGS

A.10.1 The logging operations

With aims to gain a maximum of information from the cores and the drillholes, an extensive program for core measurements and downhole logging was planned. Due to hole collapse in the overall poorly consolidated sediments, only a part of the logging program could be executed.

The logging operations was done by the logging section of BPB (British Plaster Board Instruments Ltd.) who perform API calibrated slim line logging. A full log suite for each well contained gamma, long spaced and short spaced sonic, bed resolution and long spaced density, neutron porosity and caliper. To ensure that some log data were collected, the plan was to log the wells in two runs, one inside the HR drill string and one in open hole after pulling the drill string. Only well 7317/10-U-01 was logged completely in open hole because the other wells collapsed when the drill string was pulled out. Table A.10.1 summarizes the operational data for the logging operations and Table A.10.2 the technical data of the sondes and logs.

The logging values were recorded both on analog and digital form. The logs are sent to the participants plotted on paper and as LIS format tapes. Please, note that the sonic logs on the tapes are recorded in µs/ft.

Whenever possible, horizonal sound velocity measurements and spectral gamma measurements on cores were done contemporaneously with the drilling operations in the laboratory on board, see Appendix A.5. These data were recorded on the survey data base. Laboratory and log sonic and gamma measurements are plotted side-by-side for each core and matched visually when avaliable, see figures in sections "Petrophysical logs and core measurements" of each core description chapter.

In addition, density was measured on core pieces from core 7316/06-U-02 as a basis together with laboratory measurements of horizontal sound velocity, to calculate an estimate for acoustic impedance (Figure 3.2.2). Acoustic impedance was also calculated for well 7317/10-U-01 (Figure 3.1.2).

Table A.10.1 Sondes run and operational comments.

Hole no.	Sondes run	Depths	Remarks
7317/10-U-01 Water depth 465 m	DD3, NN1 MS1	223-0 m 223-153 m	Logged in open hole to 153 m.
7316/06-U-02 Water depth 421 m	NN1	198-0 m	Logged inside HR string.
7316/06-U-01 Water depth 427 m	DD3, NN1	103-0 m	Logged inside HR string, and inside both HR and API strings from 94 m.
7316/03-U-01 Water depth 297 m	DD3, NN1	182-0 m	Logged inside HR string.

DD3 = Dual density, gamma ray, caliper

NN1 = Dual neutron (porosity), gamma ray

MS1 = Multichannel sonic

Table A.10.2 Technical data for BPB sondes and logs.

Log type	LIS tape name	Sonde name	Source/receiver spacing	Unit
Gamma ray	GRNP	NN1		API
Gamma ray	GRDE	DD3		API
Long spaced density	CODE	DD3	48 cm	g/cm^3
L.s. dens., uncompensated	LSDU	DD3	48 cm	SDU
Bed resolution density	BRDE	DD3	15 cm	g/cm^3
Neutron porosity	NPRS	NN1	45 cm	%
Neutron porosity	NLPS	NN1	45 cm	SNU
Caliper	CADE	DD3		inch
Long spaced sonic	SONL	MS1	60 cm	µs/ft
Short spaced sonic	SONS	MS1	20 cm	µs/ft

The neutron porosity log is plotted together with calculated total and effective porosity values based on Elphick's (1987) algorithms for well 7317/10-U-01 on Figure 3.1.5 and on the summary sheet for well 7317/10-U-01 in Appendix A.1.

Thermal conductivity values have been calculated from the log values with algorithms developed by Griffiths (1987), see Figure 3.1.5. This is discussed in Section A.10.3 below.

IKU SINTEF-GRUPPEN

A.10.2 Depth shift of logs

There were some deviations between drillers depth and loggers depth on the survey. A manual correction of log depth was done on board and all depths were referred to depth in core (drillers depth). Optimal depth shift was later tried obtained by finding the maximum correlation coefficient for laboratory measurements of gamma and the gamma log for depth shifts between -2.0 and 2.0 m in 10 cm steps, shown in Figures A.10.1 a-d. Due to homogeneous lithology in the separarte cores and, due to this, very low variance in the gamma log and laboratory measured data, the depth shift study showed very poor correlation coefficients (Figures A.10.1 a-d). This means that the variance of the gamma data due to lithology changes is smaller than the variance caused by measuring errors.

As a result, there was not possible to calculate any enhanced depth shifts for these wells.

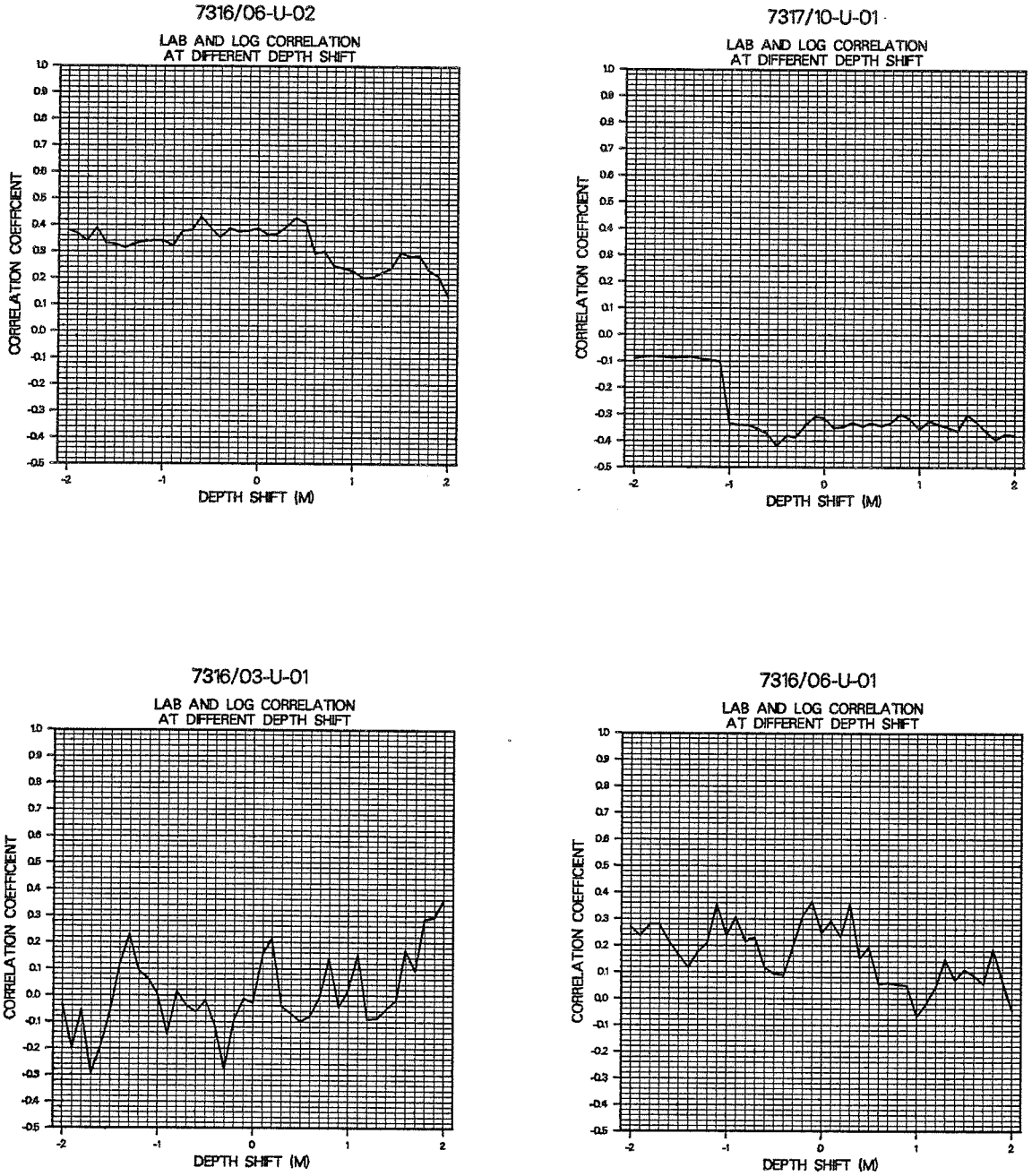


Figure A.10.1.a-d. *Optimal depth shift analyses for wells 7317/10-U-01, 7316/06-U-02, 7316/06-U-01 and 7316/03-U-01.*

A.10.3 Log measurements and calculations of porosity

The neutron porosity log is plotted together with calculated total and effective porosity based on Elphick's (1987) algorithms on Figure 3.1.5 and on the summary sheet for well 7317/10-U-01 in Appendix A.1.

Elphick's (1987) algorithm for calculation of effective porosity needs some mineral densities as input parameters, and 2.0 g/cm^3 was used as density of dry clay and 2.65 g/cm^3 as density of heavy minerals. Other density values may have changed the results. The gamma ray values are used as clay indicator, but the algorithms do not compensate for high gamma values caused by K-feldspar in arkosic sandstones, where K-feldspar is present. The algorithms interpret this as high clay contents and the result may be too high Vclay and too low effective porosity.

A.10.4 Gamma log inside drill string and in open hole

The gamma logs were not run both inside the HR drill string and in open hole in any of the wells. This means that there is not possible to establish a relationship between API gamma values measured inside the HR drill string and values from open hole logging based on this shallow drilling survey.

Instead, a formula from a previous shallow drilling operation, based on logging in more heterogenous lithology, was used for this purpose.

The result of these recalculations are show on the gamma logs from wells 7316/06-U-02, 7316/06-U-01 and 7316/03-U-01.

A.10.5 Log and laboratory measurements of natural gamma radiation

The gamma log values are displayed together with the laboratory measured gamma values for each core in figures in the core description chapters for visual and qualitative correlation. Both the weak trends and discrete values seem to correlate reasonably well.

Linear regression analyses of the lab measurements of total gamma radiation in counts/10 min vs. the values from the gamma log in API units, recalculated to open hole values when necessary, has been performed for the data from all the wells, and the data are plotted in Figure A.10.3. Deviations of sampling depth between the two measurement methods are maximum 5.0 cm. The result of this analysis is that the empirical linear formula for converting IKU laboratory measurements of total gamma radiation in counts/10 min (CM) to API units is:

$$API = 0.000279 * CM + 82.3$$

with a very poor correlation coefficient equal to -0.0329, which means that there is no correlation at all.

This lack of correlation is most probably caused by the fact that the statistical variations due to measurement errors totally overrides the variations due to lithological changes, which is caused by very homogeneous lithology. Another explanation could be that it was impossible to enhance the log depth shift, also due to homogeneous lithology, and that there may be a depth difference between the cores and the log values.

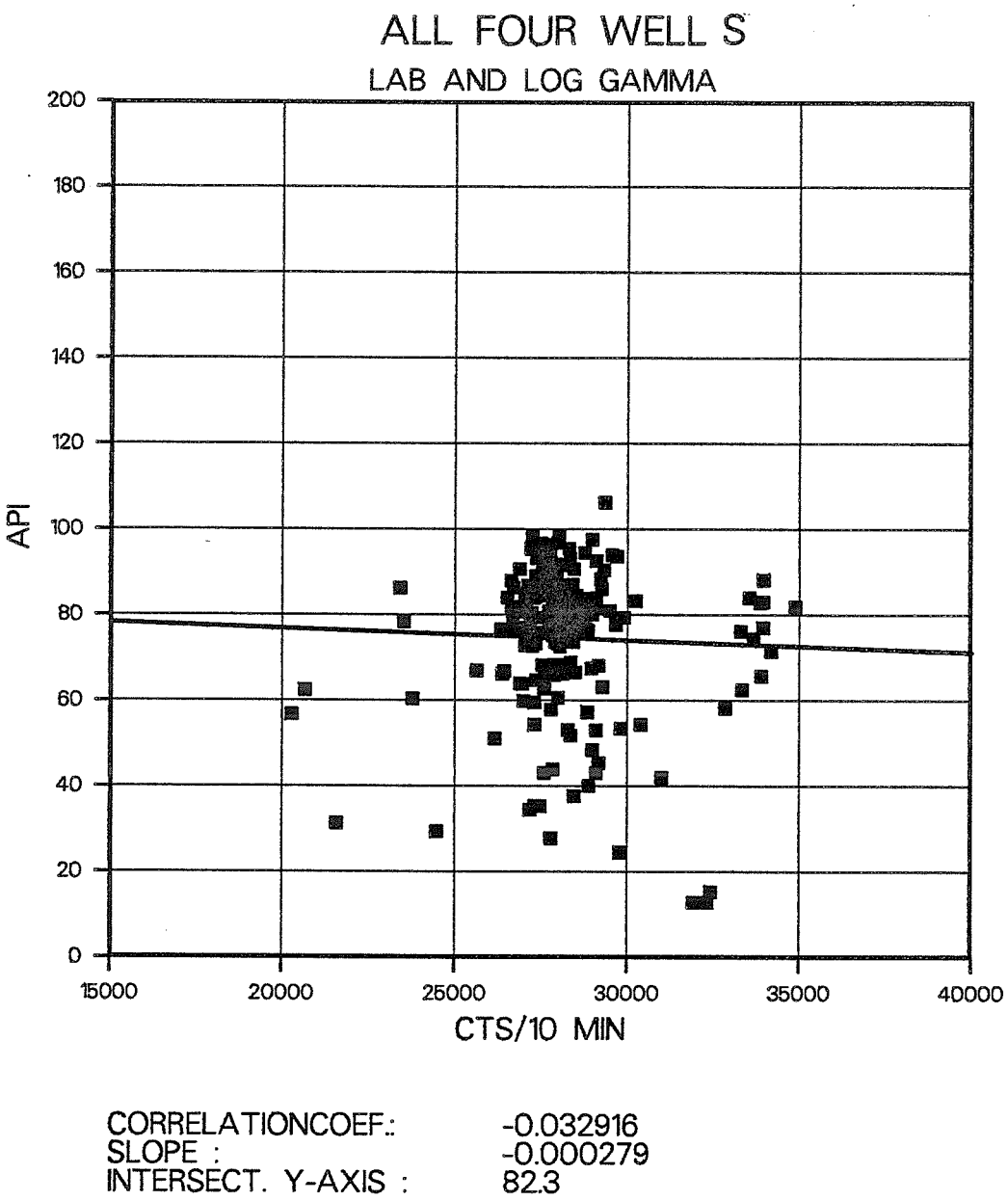


Figure A.10.2 *Crossplot of laboratory measurements of total gamma radiation (counts per. 10 minutes) and log values (API) for all the wells.*

IKU SINTEF-GRUPPEN

A.10.6 Log and laboratory measurements of sound velocity

The sound velocity values calculated from the long spaced sonic log are only available for well 7317/10-U-01 and are displayed together with the laboratory measurements of horizontal sound velocity on Figure 3.1.4 in Chapter 3.1 for visual and qualitative correlation. The trends and discrete values seem to correlate reasonably well.

Figure A.10.3 shows a crossplot of the values from the laboratory measurements of horizontal sound velocity vs. sound velocity calculated from the short spaced sonic log. The short spaced sonic log is used because even the source/reciever spacing for this log (20 cm, see Table A.10.2) is large compared to the diameter of the transducers of the Pundit (Appendix A.5). Deviations of sampling depth between the two measurement methods are maximum 5.0 cm. Figure A.10.3 shows again a very poor correlation between the laboratory and log values with a correlation coefficient equal to 0.1272.

This lack of correlation is also due to low variance in the data due to homogeneous lithology, as discussed in Section A.10.5.

A.10.7 Thermal conductivity

Thermal conductivity has been measured on several samples from three of the four cores. Based on the wireline logs, thermal conductivity has also been calculated from well 7317/10-U-01 which were logged in open hole. The laboratory measurements were performed by N. Balling at the University of Aarhus, Denmark, see Appendix A.9.

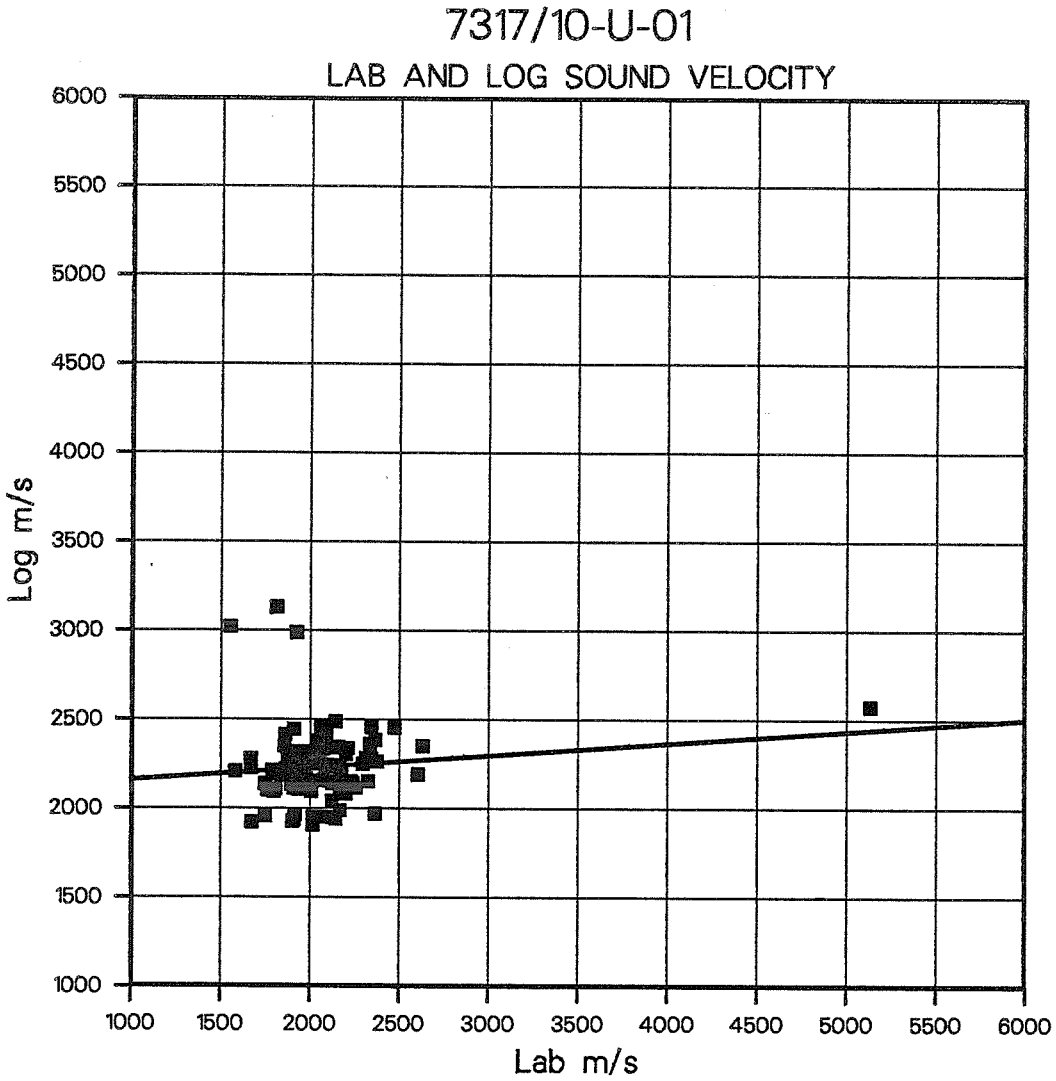


Figure A.10.3 *Crossplot of laboratory measurements of horizontal sound velocity and sound velocity calculated from the short spaced sonic logs for well 7317/10-U-01.*

A.10.8 Calculation of thermal conductivity

The thermal conductivity algorithm (Griffiths 1987) relates thermal conductivity to several log variables based on equations from Goss et al. (1975) modified by curves for variations with porosity (Balling et al., 1981) based on identification of sand, shale and carbonates. The algorithm does this identification with the M-N crossplot together with the gamma log. The porosity used is the calculated total porosity.

The calculated thermal conductivity values for well 7317/10-U-01 are plotted on Figure 3.1.5 and on the summary sheet for well 7317/10-U-01 in Appendix A.1.

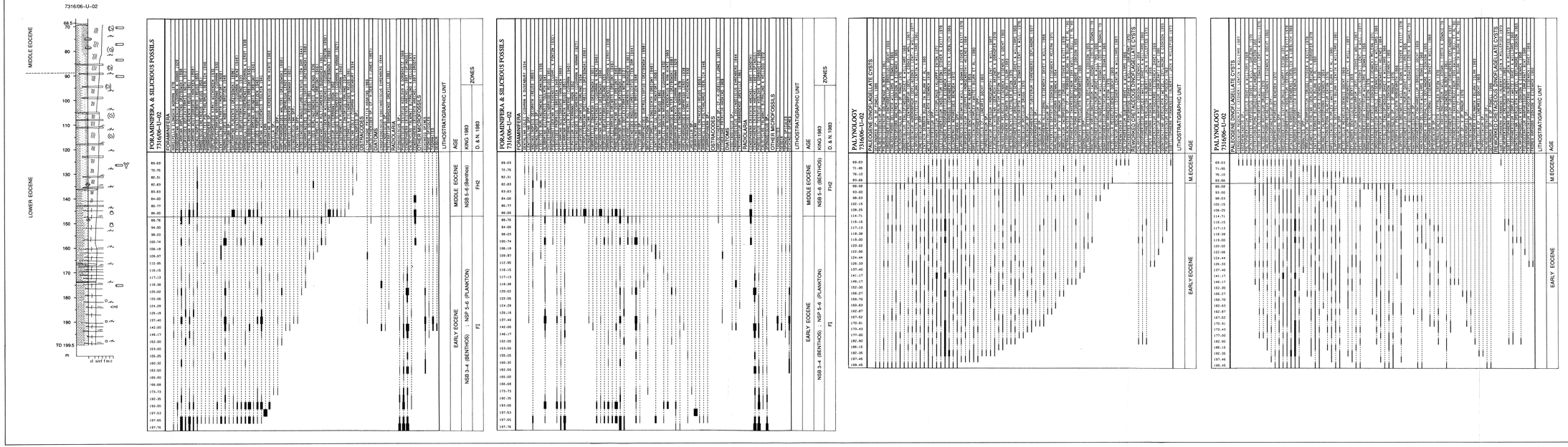
References

BALLING, N., KRISTIANSEN, J.I., BREINER, N., POULSEN, K.D., RASMUSSEN, R. and SAXOV, S., 1981: Geothermal measurements and Subsurface temperature modelling in Denmark. Department of Geology, Aarhus University: Geoskrifter, No. 16, 172 pp.

ELPHICK, R.Y., 1987: Neutron/Density/GR Interpretation in Shaley Sands. Geobyte 1987 Vol.2, No.2, pp 51-53.

GOSS, R., COMBS, J. and TIMUR, A., 1975: Prediction of thermal conductivity in rocks from other physical parameters and from standard geophysical well logs. SPWLA sixteenth annual logging symposium, june 4-7,1974, pp 1-21.

GRIFFITHS, C.M., 1987: COMPULOG software, 1987 update of NULITH module. IKU.



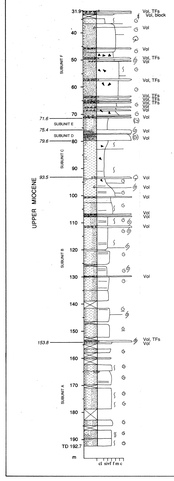
IKU SINTEF GROUP

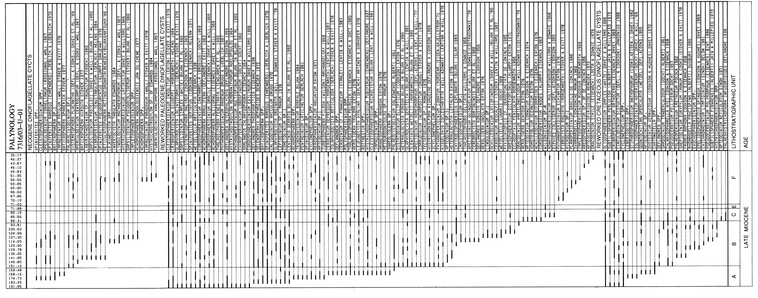
7316/06-U-02

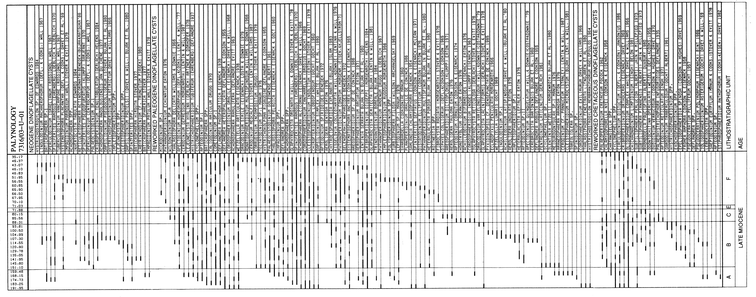
APPENDIX A.11.1
DISTRIBUTION CHARTS

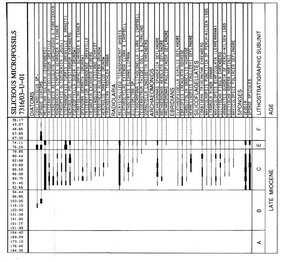
21.3465.00/02/90

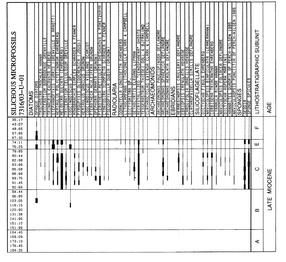
7316/03-U-01











IKU SINTEF GROUP

7316/03-U-01

APPENDIX A.11.2
DISTRIBUTION CHARTS

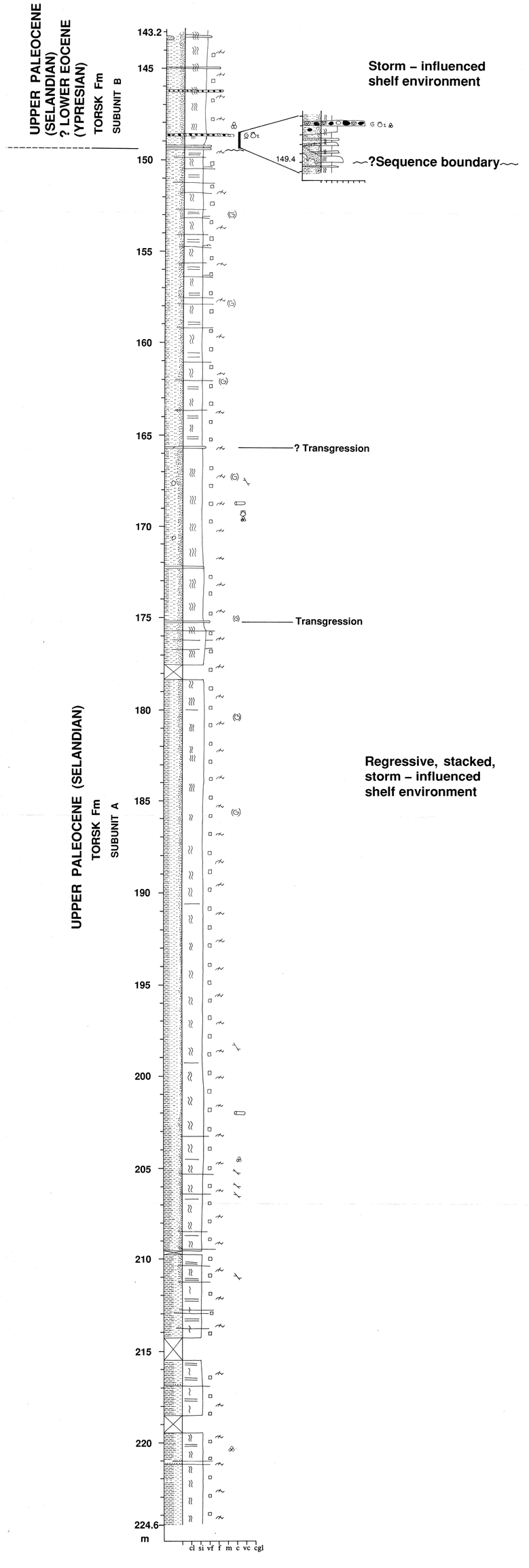
21.3465.00/02/90

IKU SINTEF GROUP

APPENDIX A.12.1
CORE LOG

21.3465.00/02/90

Scale 1:100 **7317/10-U-01**

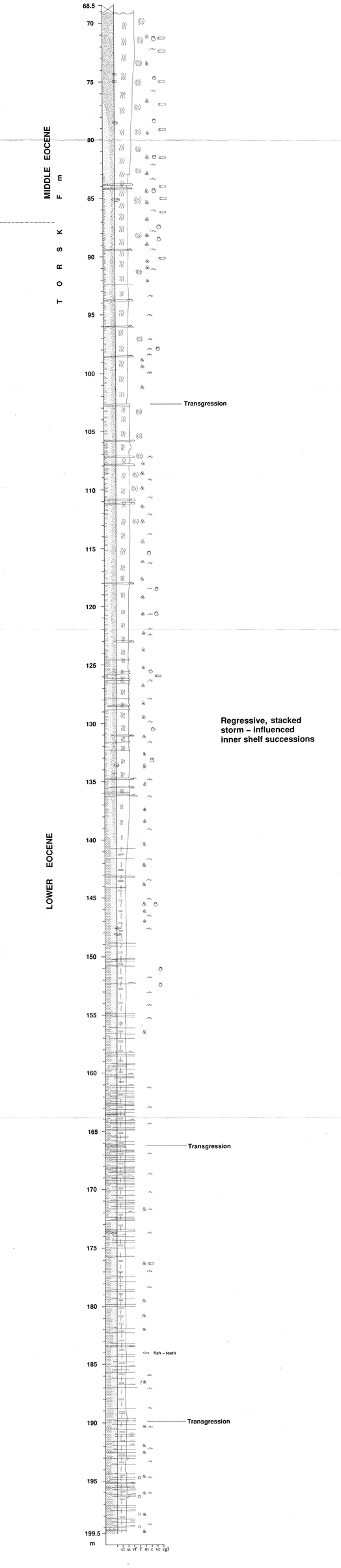


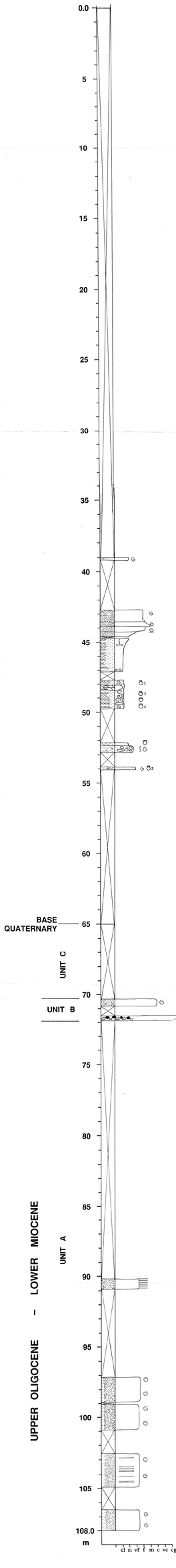
IKU SINTEF GROUP

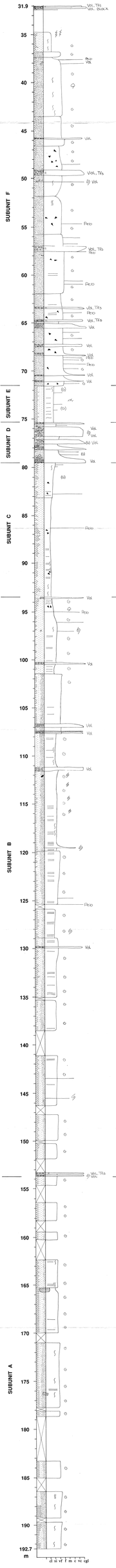
Scale 1:100 **7316/06-U-02**

APPENDIX A.12.2
CORE LOG

21.3465.00/02/90




0.0
5
10
15
20
25
30
35
40
45
50
55
60
BASE QUATERNARY
65
UNIT C
70
UNIT B
75
80
85
UNIT A
90
95
100
105
108.0
m
cl si vf f m c vc cgl
UPPER OLIGOCENE - LOWER MIOCENE
Cretaceous megablock in Quaternary till. Glauconitic sandstone overlies silty and marly shale. All represent shelf sediments.
Coarse, well rounded sand.
Polymict conglomerate.
Possibly forming a channel.
Immature very fine sandstone. Deposited in shelf break or upper slope environment, possibly by mass flows.



Fine to medium grained, glauconitic sandstone with volcanic debris beds. Deposited by debris flow and mass flow mechanisms in upper slope environment by resedimentation of Eocene shelf sediments.

Silty shale deposited by turbidity currents or possibly by hemipelagic deposition.

Fining upward beds with volcanic debris deposited by debris flows in slope setting.

Silty shale deposited by turbidity currents or possibly by hemipelagic sedimentation.

Very fine to fine-grained glauconitic immature sandstone deposited by debris flows and turbidity currents in slope settings.

Very fine-grained glauconitic immature sandstone deposited in slope channels and by turbidity currents in slope setting.

Shallow Drilling
Bjørnøya West 1989

Appendix volume 1

Field work
Analyses
Consultant reports
Core logs (1:100)

IKU
SINTEF GROUP